

International Geology Review

UNIVERSITY OF MARYLAND
LIBRARY
DEC 5 '62

Vol. 2, No. 10

October 1960

Partial Contents

	Page
PRELIMINARY STUDY OF THE MANGANESE DEPOSITS OF CHINA by Chao Chia-hsiang and Liu You-hsin	833
USE OF DIFFERENTIAL GAMMA SPECTROMETRY IN PETROLEUM GEOLOGY by G. A. Nedostup, F. N. Prokofiev, A. I. Kholin, and E. P. Tsitovich	867
SOME PROBLEMS IN THE CONSTRUCTION OF A BORE HOLE NEUTRON GENERATOR by E. A. Abb, V. M. Zaporozhets, R. I. Plotnikov, and L. A. Khutsishvili..	882
GEOLOGIC RECONNAISSANCE OF THE EASTERN PART OF THE MOUNTAINS IN QUEEN MAUD LAND, ANTARCTICA by M. G. Ravich, P. S. Voronov, L. V. Klimov, and D. S. Solovyev	897
REFERENCE SECTION	921

- complete table of contents inside -

published by the

AMERICAN GEOLOGICAL INSTITUTE



INTERNATIONAL GEOLOGY REVIEW

BOARD OF EDITORS

EARL INGERSON, *Senior Editor*
Univ. of Texas, Austin, Texas
THOMAS S. LOVERING
U.S. Geological Survey, Denver, Colo.
SIEMON W. MULLER
Stanford Univ., Stanford, Calif.
JAMES J. ROARK
Jersey Production Research Co., Tulsa, Okla.

AGI TRANSLATION COMMITTEE

EARL INGERSON, <i>Chm.</i>	JOHN K. HARTSOCK
EUGENE A. ALEXANDROV	HENRY HOTCHKISS
E. C. T. CHAO	KURT E. LOWE
JAMES W. CLARKE	BRIAN MASON
DEAN F. FRASCHE	JOHN RODGERS
ALEXANDER GAKNER	FRANK C. WHITMORE, JR.

STAFF

MARTIN RUSSELL, *Managing Editor*
THOMAS RAFTER, JR., *Manager,*
Translations Office
NELLIE F. BROWN, *Compositor Supervisor*

AMERICAN GEOLOGICAL INSTITUTE

R. C. MOORE, *President*
PAUL L. LYONS, *Past President*
IAN CAMPBELL, *Vice President*
D. H. DOW, *Secretary-Treasurer*
R. C. STEPHENSON, *Executive Director*

MEMBER SOCIETIES

AMERICAN ASSOCIATION OF PETROLEUM GEOLOGISTS
AMERICAN GEOPHYSICAL UNION
AMERICAN INSTITUTE OF MINING, METALLURGICAL
AND PETROLEUM ENGINEERS
ASSOCIATION OF AMERICAN STATE GEOLOGISTS
GEOCHEMICAL SOCIETY
GEOLOGICAL SOCIETY OF AMERICA
MINERALOGICAL SOCIETY OF AMERICA
NATIONAL ASSOCIATION OF GEOLOGY TEACHERS
PALEONTOLOGICAL SOCIETY
SEISMOLOGICAL SOCIETY OF AMERICA
SOCIETY OF ECONOMIC GEOLOGISTS
SOCIETY OF ECONOMIC PALEONTOLOGISTS AND
MINERALOGISTS
SOCIETY OF EXPLORATION GEOPHYSICISTS
SOCIETY OF VERTEBRATE PALEONTOLOGY

The American Geological Institute operates under the National Academy of Sciences. It is governed by an Executive Committee and a Board of Directors composed of two directors from each of the fourteen Member Societies.

International Geology Review is published monthly by the American Geological Institute with the assistance of an initiating grant from the National Science Foundation. The journal will report, in English, significant contributions to pure and applied research in the earth sciences which appear in foreign-language journals, especially those published in the U.S.S.R.

The editors of International Geology Review will give consideration to full English translations, condensations, and reviews submitted voluntarily for publication. Translators will be appropriately credited.

Readers are invited to direct to the editors their comments and discussions of articles published in the International Geology Review. Readers are encouraged also to submit suggestions as to published foreign literature considered worthy of translation and publication. Such suggestions should relate to materials of broad, general interest, rather than materials of limited reader interest.

Address editorial and subscription inquiries to

AGI TRANSLATIONS OFFICE
AMERICAN GEOLOGICAL INSTITUTE
2101 Constitution Avenue, N.W., Washington 25, D. C.

The basic subscription rate for International Geology Review is \$55 per year, 12 issues. A special subscription rate of \$15 per year is available to members of AGI Member Societies who are on the GeoTimes mailing list and who will pledge to restrict the journal to their personal use. The \$15 per year subscription rate is also available to educational institutions and personnel. Foreign postage: No additional charge to Canada and Mexico; to Pan American Union countries add \$0.50 per year; to all other foreign countries add \$1.00 per year. Single copy price \$5.00 (\$1.50 to subscribers qualifying for special rates). Second class postage paid at Washington, D. C.

International Geology Review

published monthly by the
AMERICAN GEOLOGICAL INSTITUTE

Vol. 2, No. 10

October 1960

CONTENTS

Page

IGR TRANSLITERATION OF RUSSIAN	ii
PRELIMINARY STUDY OF THE MANGANESE DEPOSITS OF CHINA, by Chao Chia-hsiang and Liu You-hsin, translated by E. C. T. Chao	833
GEOLOGICAL STRUCTURE OF THE SOUTH KHINGAN MANGANESE DEPOSIT AND ESSENTIAL COMPOSITION OF ITS ORES, by M. V. Chebotarev, translated by E. A. Alexandrov and Associates	851
USE OF DIFFERENTIAL GAMMA SPECTROMETRY IN PETROLEUM GEOLOGY, by G. A. Nedostup, F. N. Prokofiev, A. I. Kholin, and E. P. Tsitovich, translated by Henry Faul	867
THE SPECTRUM OF SCATTERED GAMMA RADIATION IN ROCK STRATA OF VARIOUS MINERALOGICAL COMPOSITIONS, by E. M. Fillippov, translated by Henry Faul	874
SOME PROBLEMS IN THE CONSTRUCTION OF A BORE HOLE NEUTRON GENERATOR, by E. A. Abb, V. M. Zaporozhets, R. I. Plotnikov and L. A. Khutsishvili, translated by Henry Faul	882
DETERMINATION OF COEFFICIENTS OF RADIOACTIVE EQUILIBRIUM AS A METHOD OF STUDY OF THE MIGRATION OF URANIUM, IONIUM, AND RADIUM, by V. I. Malyshev, translated by Mark Burgunker	888
GEOLOGIC RECONNAISSANCE OF THE EASTERN PART OF THE MOUNTAINS IN QUEEN MAUD LAND, ANTARCTICA, by M. G. Ravich, P. S. Voronov, L. V. Klimov and D. S. Solovyev, translated by Douglas Alverson	897
ON THE AGES OF METAMORPHISM IN THE JAPANESE ISLANDS, by Masao Minato, translated by Reiko Fusejima	901
ALKALIC ROCKS OF THE NEMURO PENINSULA WITH SPECIAL REFERENCE TO THEIR PILLOW LAVAS, by Kenzō Yagi, translated by Kinkiti Musya	912

REFERENCE SECTION

RUSSIAN AND EAST EUROPEAN GEOLOGIC ACCESSIONS OF THE LIBRARY OF CONGRESS, August 1960	921
--	-----

IGR transliteration of Russian

The AGI Translation Office has adopted the essential features of Cyrillic transliteration recommended by the U. S. Department of the Interior, Board on Geographic Names, Washington D. C.

However, the AGI Translation Office recommends the following modifications:

1. Ye initially, after vowels, and after *ъ, ь*
Customary usage calls for "ie" in many names, e. g., SOVIET KIEV, DNEPER, etc.; or "ye", e. g., BYELORUSSIA, where "e" follows consonants. "e" with dieresis in Russian should be given as "yo".
2. Omitted if preceding a "y", for example, Arkhangelsky (not "iy"; not "ii").
3. Generally omitted.

NOTE: Well-known place and personal names that have wide acceptance will be used. Some translations may include elements of previous German transliteration from the Russian; this occurs in IGR most commonly in maps and lists of references. The reader's attention is called to the following variations between German and English systems which may cause confusion when trying to check back to original Russian sources.

Alphabet	transliteration	
А	а	a
Б	б	b
В	в	v
Г	г	g
Д	д	d
Е	е	e, ye ⁽¹⁾
Ё	ё	ë, yë
Ж	ж	zh
З	з	z
И	и	i ⁽²⁾
Й	й	y
К	к	k
Л	л	l
М	м	m
Н	н	n
О	о	o
П	п	p
Р	р	r
С	с	s
Т	т	t
У	у	u
Ф	ф	f
Х	х	kh
Ц	ц	ts
Ч	ч	ch
Ш	ш	sh
Щ	щ	shch
Ъ	ъ	" ⁽³⁾
Ы	ы	y ⁽³⁾
Ь	ь	" ⁽³⁾
Э	э	e
Ю	ю	yu
Я	я	ya

German	English
w	v
s	z
ch	kh
tz	ts
tsch	ch
sch	sh
schtsch	shch
ja	ya
ju	yu

TENTATIVE CONTENTS FOR THE NOVEMBER ISSUE

THE PROBLEM OF THE ORIGIN OF CONTINENTAL GLACIATION, by L. B. Rukhin

RUTILE-BEARING ECLOGITES FROM THE SHUBINO VILLAGE DEPOSIT IN THE SOUTHERN URALS, by B. V. Chesnokov

CHARACTERISTIC FEATURES OF ORE DEPOSITS FOUND IN CONTACT-METAMORPHIC AUREOLES IN JAPAN, by Takeo Watanabe

ON PRINCIPAL RULES IN THE OCCURRENCE OF OIL AND GAS ACCUMULATIONS IN THE WORLD, by I. O. Brod

PRELIMINARY STUDY OF THE MANGANESE DEPOSITS OF CHINA¹

by

Chao Chia-hsiang and Liu You-hsin²

translated by E.C.T. Chao

ABSTRACT

Exogenic manganese deposits in China occur in rocks of Precambrian, Devonian, Carboniferous, Permian, and Quaternary age. The three major types found are sedimentary, gossan, and residual; the most important deposits are Precambrian and Paleozoic marine sedimentary. Most of the ores occur in association with a stratigraphic hiatus in siliceous-carbonate facies of nearshore or lagoonal environment. South China has the largest reserves and is the most promising area for future prospecting. -- M. Russell.

PREFACE

In recent years, because of the demands of economic development and construction, definitive work was carried out by Chinese geologists in the search for and study of manganese deposits. They not only have determined the required reserve for the first five-year plan but also obtained a great deal of new data with respect to

the geology of manganese deposits. Based on the present data, those of economic value are restricted to exogenic deposits. It should however be pointed out that very little work has as yet been done on endogenic manganese deposits.

This is a summary study of the known exogenic manganese deposits of industrial importance in China (fig. 1). Other exogenic and

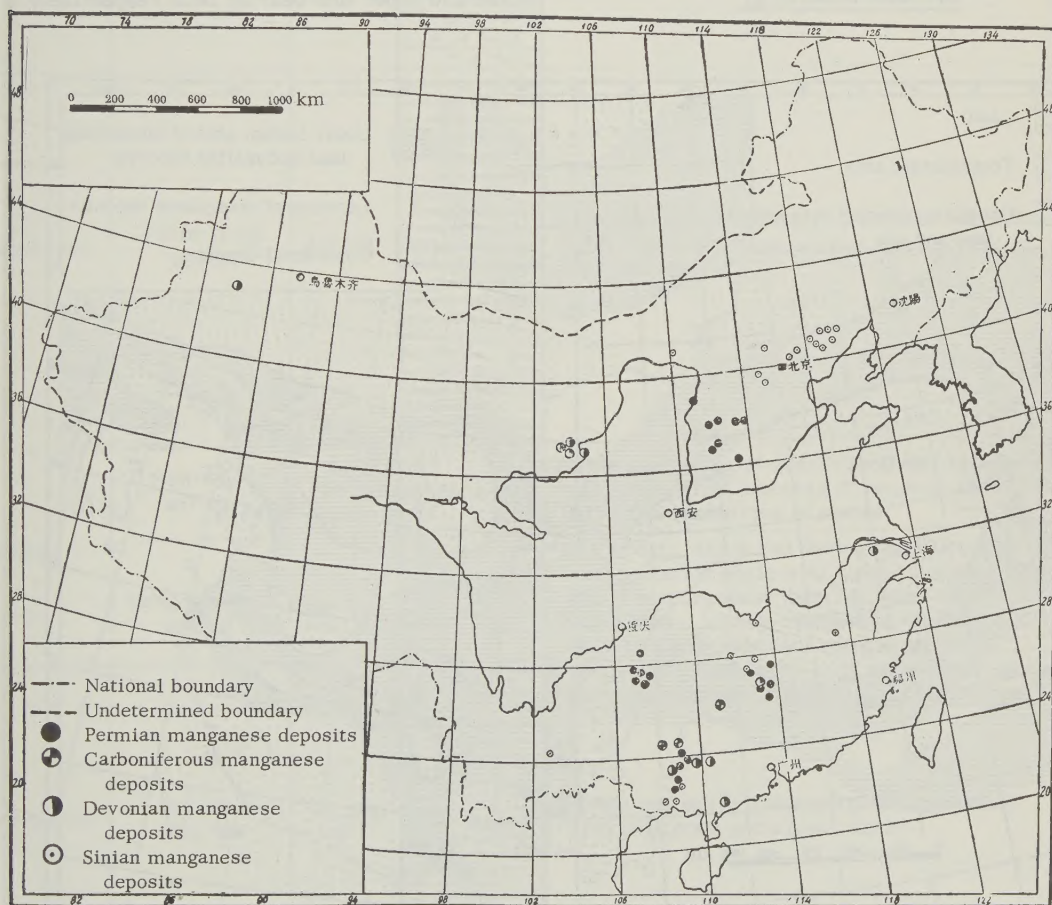


FIGURE 1. Distribution of important exogenic manganese deposits in China.

¹ Translated from Chung Kuo Wai Sheng Men K'uang Ti Ch'u Pu T'an T'ao [Preliminary study of the exogenic manganese deposits of China]; Ti Chih Hsueh Pao [Acta Geologica Sinica] v. 36, no. 4, p. 535-543, 1956.

² Ministry of Geology, People's Republic of China.

endogenic deposits are not considered owing to the lack of data. However, individual exogenic deposits of unknown industrial value are described here because of their geological importance. The purpose of this paper is to describe the environment, genesis, characteristics and the paleogeographic distribution of the manganese deposits on the basis of the type of deposit, country rock, mineralogy and stratigraphic position, and to develop criteria for future prospecting and exploration of such deposits.

This paper is based on the work of geologists dealing with manganese deposits in recent years, in addition to reporting the results of our investigations.

STRATIGRAPHY, DISTRIBUTION AND PALEOGEOGRAPHIC RELATIONSHIPS OF EXOGENIC MANGANESE DEPOSITS IN CHINA

Stratigraphic Position of Ore Deposits and their Mineralogy

Sinian Manganese Deposits (figs. 2, 3, 4, and 5)

Sinian manganese deposits occur in three stratigraphic horizons: the lowest at the base of the Lower Sinian. It overlies pre-Sinian beds (Pan-chi series or its equivalents) and underlies the Sinian tillite. Such deposits occur in southern China, for example, Hsiang-t'an of Hunan and Lo-p'ing of Kiangsi and Hsin-hsien of Kwangsi. The middle ore-bearing beds occur in the Kao-yu-chuang limestone of Upper Sinian age. They occur in the western and northern parts of Hopei but none have so far been found to be of economic value. The upper ore-bearing beds occur in the upper part of Hung-shui-chuang formation of Upper Sinian age. They are found north of the Yen-shan belt in northern China. The ore-bearing formation extends intermittently for about 200 km. [1]

The Hsiang-t'an deposit of Hunan, the Chih-sien deposit of Hopei and the Ch'ao-yang deposit of Liaoning which represents the lower, middle and upper ore-bearing beds respectively

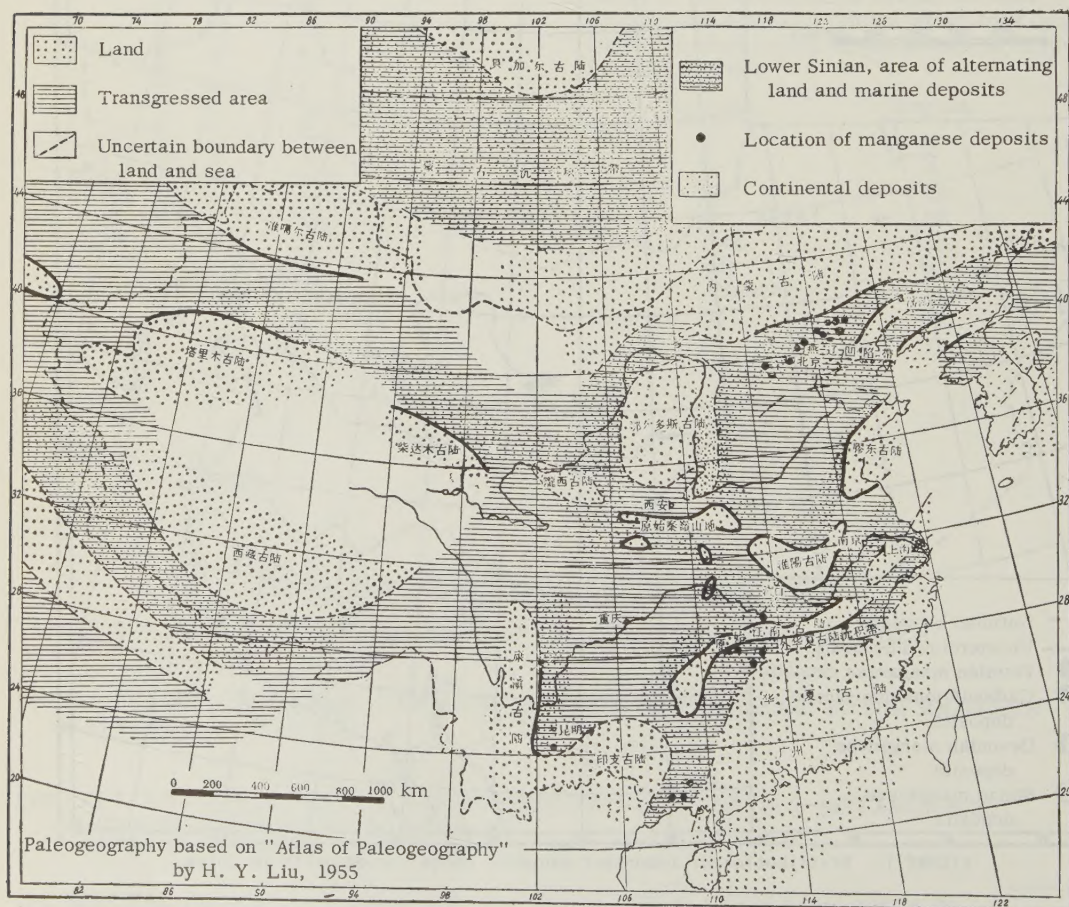


FIGURE 2. Sinian manganese deposits

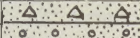


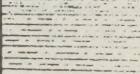
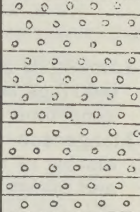
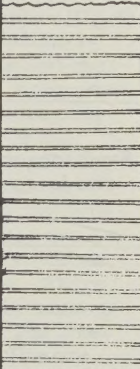
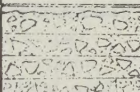

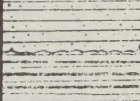
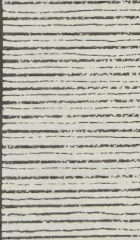
Geologic age	Stratigraphic horizon	Thickness in meters	Section	Lithologic description
Quaternary		5-10		Red clay and fragments of various rocks
Tertiary		30-50		Red sandstone and conglomerate
Devonian	Upper T'iao-ma-chien series	20		Pale yellowish green shale, with limestone nodules in the lower part
	Lower T'iao-ma-chien series	40-80		Purple sandy shale and shale
				Conglomerate with quartz pebbles cemented by sandy matrix
Cambrian	Ta-fu-p'ing series	60-100		Siliceous beds, frequently fractured and filled with limonitic material; one bed of chert in the lower part
Sinian	Nan-t'uo series	5-35		Tillite consisting of quartz sand and kaolinitic clay with small amounts of limonite derived from the weathering of pyrite
	Hung-chiang series	10-78		Upper part: Black and dark gray siliceous and carbonaceous shale with disseminated pyrite and thin manganese-bearing beds.
				Middle part: Mainly manganese-bearing beds. Gray to black carbonate manganese ore. Lower part: Dark gray to grayish white sandstone intercalated with lenticular limestone.
Pre-Sinian	Pan-ch'i series	> 1,500		Weakly regionally metamorphosed greenish gray siliceous and clayey shale

FIGURE 3. Columnar section of the marine Lower Sinian deposits of Hsiang-t'an, Hunan province

INTERNATIONAL GEOLOGY REVIEW




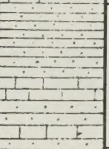
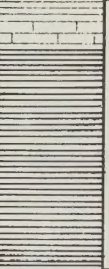
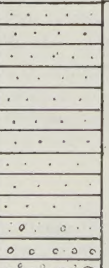
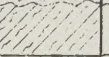
Geologic age	Stratigraphic horizon	Section	Thickness in meters	Lithologic description
Sinian	Wu-mi-shan formation		> 2,000	Banded cherty limestone.
	Yang-chuang formation		800	Pink sandstone and clayey limestone intercalated with clay beds.
	Kao-yu-chuang formation		1,900	Limestone and dolomite above the manganese-bearing beds and gray cherty limestone and sandstone below the manganese bearing beds. Manganese-bearing beds 50-120 m thick consisting of manganiferous and siliceous beds and manganese-bearing limestone.
	Ta-hung-yu formation		800	Sandstone with intercalated limestone with andesite lavas in the upper part.
	Chuan-ling-kou formation		1,300	Black shale with limestone in the upper part.
	Ch'ang-ch'eng formation		1,300	Quartzite and sandy conglomerate.
Archean				Gneisses.

FIGURE 4. Columnar section of the marine Upper Sinian manganese deposits of Chi-hsien, Hopei province

are described as follows:

Hsiang-t'an, Hunan: Lower Sinian manganese deposit of Hsiang-t'an, Hunan [2], occurs in the Hung-chiang series which unconformably overlies the Proterozoic Pan-chi series of slightly regionally metamorphosed greenish gray siliceous and clayey shale (fig. 3). It is also unconformably overlain by the Lower Sinian Nan-t'uotillite. The Hung-chiang series consists of dark gray to grayish white sandstone intercalated with lenses of limestone in the lower part and black to dark gray siliceous and carbonaceous shale with disseminations and seams of pyrite and thin beds of manganese ore in the upper part. The main ore-bearing bed occurs at the lower part of the ore-bearing section, consisting of black manganese carbonate. Those within 40 or 50 meters of the surface and under the water table were converted to oxidized ore. Analysis of the manganese carbonate ore shows Mn, 11-25 percent; SiO_2 , 17 percent; $\text{CaO} + \text{MgO}$, 9 percent; and loss on ignition, about 20-30 percent.

Chi-hsien, Hopei: The manganese deposits of Chi-hsien, Hopei [3] occur in the lower part of the Upper Sinian Kao-yu-chuang formation (fig. 4). The manganese-bearing beds are underlain by gray cherty limestone and sandy shale and overlain by limestone and dolomite. The manganese bearing section is 50 meters thick, increasing to 120 meters westward. It consists of calcareous and siliceous manganese ore and manganese-bearing limestone. The basal and the upper parts consist of manganese-bearing limestone. Above and below the manganese ore are yellowish-purple manganese-bearing siliceous rocks and manganese carbonate rocks. There are four beds of ore, the uppermost is more or less bedded and is more persistent. The other three are irregular and lenticular. The ore beds are thin. The dense part of the ore consists of needles of pyrolusite and blocky psilomelane to unknown depths. The ore contains about 28 percent Mn, and about 35 percent acid-insoluble residue.

Ch'ao-yang, Liaoning: The manganese deposit of Ch'ao-yang, Liaoning [5] occurs at the top of the Upper Sinian Hung-shui-chuang formation (fig. 5). The manganese-bearing section is underlain by gray cherty limestone and black shale and overlain unconformably by lower Cambrian basal conglomerate. This section is 20-30 meters thick and consists of liver-colored manganese-bearing dolomite, brownish black shale and interbedded siltstone. Chert layers occur in places in the shale. There are three manganese-bearing beds; the upper is irregular, the other two are more persistent, consisting of small lenses. The ore grades both vertically and laterally from carbonate manganese ore to oxidized manganese ore. The carbonate manganese ore and the primary oxide manganese ore are blocky and massive, oolitic

or pisolitic in texture, the former being lighter in color. The secondary oxidized ore is loosely compacted and contains yellow clay. The ore is high in iron and contains iron and manganese minerals. The carbonate manganese ore consists of manganoan calcite and some ferroan rhodochrosite. The tenor of the ore: Mn 15-18 percent; Fe, 10-15 percent; SiO_2 , 17-23 percent; and $\text{CaO} + \text{MgO}$, 8-15 percent. The primary manganese ore consists essentially of manganite, its tenor is: Mn, 20-30 percent; Fe, 12-18 percent; and SiO_2 , 22-27 percent.

Devonian Manganese Deposits (figs. 6 and 7)

Northern China was uplifted and became land during Devonian so that marine Devonian manganese deposits occur only in the shallow seas of southern China and in the geosyncline of Ch'i-lien-shan in the northwest. The known deposit in southern China occurs on the southern slope of Yao-shan of Kwangsi province [6]. Ore occurs in two stratigraphic horizons: One located in the basal part of the Upper Devonian Liu-chiang series above the erosional surface of the Middle Devonian Tung-kang-ling limestone. The ore is bedded. The other horizon consists of several seams of manganese ore occurring in the middle of the Liu-chiang series. Of the latter, the topmost seam is more persistent in ore bed; the others are all lenticular. The strata above and below the ore-bearing horizons consist of purplish brown platy sandy shale interbedded with layers of black chert and some manganese-bearing limestone. The ore consists of soft manganese oxide occurring in botryoidal or boxwork type of secondary structure. The manganese minerals are chiefly psilomelane and pyrolusite, locally accompanied by p'ien-meng-suan-k'uang.³ The thickness of the ore at the basal part of the Liu-chiang series ranges from 0.5 to 10 meters. The ore contains 35-40 percent Mn, 6-7 percent Fe and 15-19 percent SiO_2 . The ore occurring in the middle part of the Liu-chiang series is of poorer quality. It contains about 20 percent Mn, 9 percent Fe, and 30 percent SiO_2 . This type of deposit was formed as a result of the extensive oxidation of the manganese-bearing rocks which lie near the surface.

The manganese deposit of the Ch'i-lien-shan geosyncline [7] occurs in the highly calcareous metamorphosed volcanic rocks in the upper part of the Devonian Pai-yin-chang member. The rocks above and below the ore horizon consist of andesite porphyries, chert, siliceous phyllites and manganese-bearing marble, etc. The ore bodies are lenticular, several hundred meters

³A monoclinic manganate? A mineral term which cannot be translated from available dictionaries.--E.C.T.C.


Geologic age	Stratigraphic horizon	Section	Thickness in meters	Lithologic description
QUATERNARY	Q		-	Alluvium.
	Cr ₃			Andesitic pyroclastics.
MESOZOIC	Cr ₂			Acid volcanic series, thickness unknown. Chiefly quartz-trachyte, trachyte, rhyolite and tuff with small amounts of tuffaceous shale; abundant silicified wood.
	Cr ₁			Sandy shale, thickness unknown.
CAMBRIAN	Cm ₁₅		19-78	Uppermost part of the Cambrian section consists of the upper edgewise limestone conglomerate member. Lower part consists of dark purple sandstone and sandy shale; its middle part contains edgewise limestone conglomerate and its upper part is represented by bluish gray, thick-bedded limestone with abundant chert.
	Cm ₁₄		9-25	Upper oölitic limestone, bluish gray color.
	Cm ₁₃		13.5-41	Lower edgewise limestone conglomerate member. In ascending order: purple sandstone, sandy shale intercalated with yellow crystalline limestone, and yellow, red or bluish edgewise conglomeratic limestone.
	Cm ₁₂		12-17	Middle oölitic limestone, gray color, in relatively thin beds.
	Cm ₁₁		47-62	Light gray cherty limestone; the chert is nodular and more abundant in the upper part.
	Cm ₁₀		8-10	Upper alternating shale bed; light yellow and greenish gray shale with dark purple shale in the upper part.
	Cm ₉		30-38	Lower oölitic limestone; upper part light gray limestone, lower part gray and yellowish gray oölitic clayey limestone.
	Cm ₈		6-7	Lower shale bed; upper part yellow shale, and the lower part dark purple sandy shale.
	Cm ₇		48-72	Pisolithic limestone; lower part consists of yellowish gray clayey limestone interbedded with shale; the upper part consists of thick-bedded crystalline limestone with pisolithic texture near the top.

FIGURE 5. Columnar section of the marine Upper Sinian manganese deposits of Chao-yang, Liaoning province (Continued on next page)

Geologic age	Stratigraphic horizon	Section	Thickness in meters	Lithologic description
C A M B R I A N (Concluded)	Cm ₆		80-100	Upper brown shale series; lithologically same as Cm ₄ ; middle part with a 2 m-thick limestone.
	Cm ₅		7-14	Black limestone, black to dark gray; lower part with undulating bedding surface; occasionally red places are silicified, so rocks are of variable hardness.
	Cm ₄		10-19	Middle brown shale; same as Cm ₂ , 1 m of green shale at the top.
	Cm ₃		3-7	White limestone, thin-bedded with chert; joints well developed. Generally 4 m thick.
	Cm ₂		7-19	Lower brown shale; grades into the conglomerate below. The two vary alternately in thickness. One thin bed of limestone near base.
	Cm ₁		3-14	Basal conglomerate unconformable with underlying beds. Lithology varies greatly. Essentially red clayey conglomerate with pebbles mostly of limestone, 5-10 cm in diameter.
S I A N	Sn ₅			
	Sn ₄		20-30	Manganese-bearing series; mainly shale, brownish, in part greenish brown. Basal part is layer of bright red shale in contact with Sn ₃ . There are 3 manganese-bearing horizons in this series: the one above the bright red shale near the base is the lower bed; 4-6 m above this is the middle ore bed; and 8-12 m above the middle ore bed is the upper ore bed.
	Sn ₃		22-45	Banded limestone. Lower part grades into Sn ₂ . Middle parts are banded limestone (alternating black and white bands). Bands undulate with its axis at an angle with the general strike. The upper part becomes thick-bedded with small amount of chert. One bed 5-15 cm thick of grayish white quartzite near the top.
	Sn ₂		50-80	Black papery shale, exposed around the mineralized area, conformable above and below. The lower parts are yellow and gray sandy slate and grayish black shale. Middle part is brownish gray siliceous shale intercalated with dark gray thin-bedded sand limestone and limestone.
S	Sn ₁		150	Light gray chert-bearing limestone. Lighter color in upper part with chert increasing towards lower part; bedding undulating; the cherty lower part has banded structure.

FIGURE 5. Columnar section of the marine Upper Sinian manganese deposits of Chao-yang, Liaoning province (Concluded)

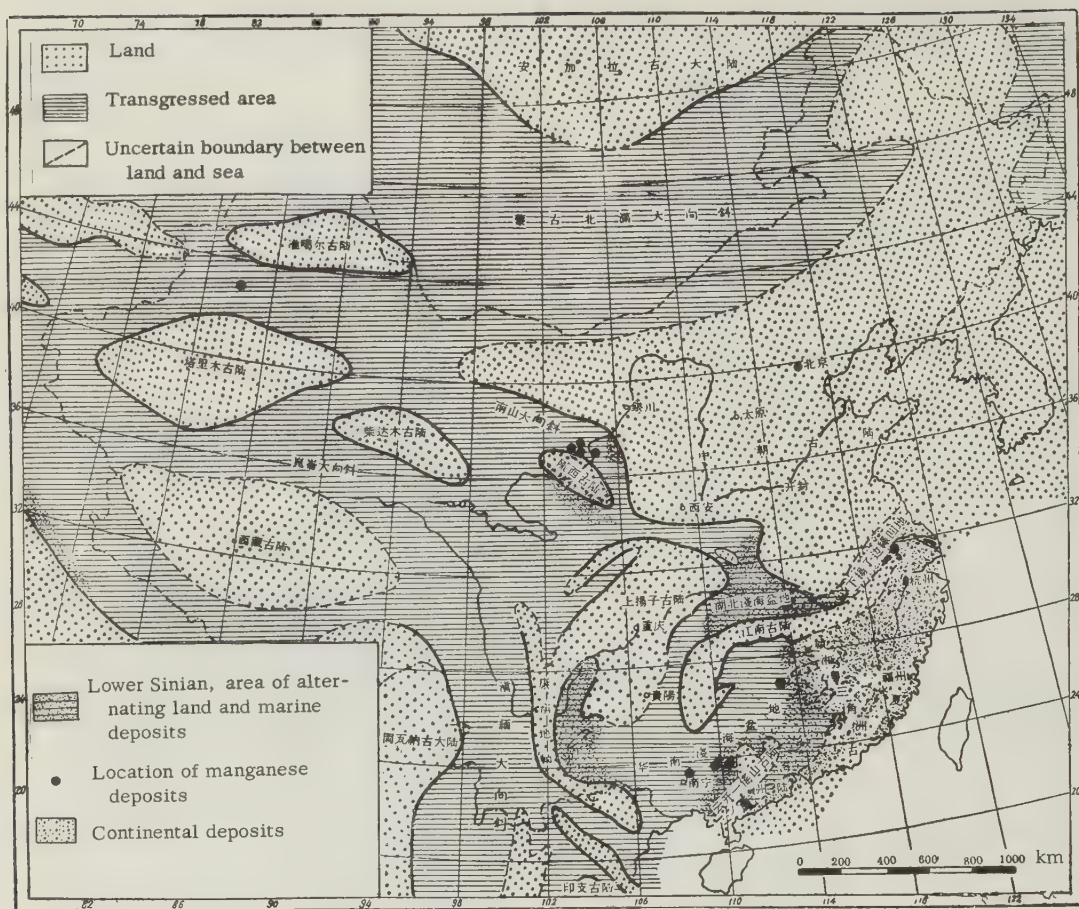


FIGURE 6. Devonian manganese deposits

long and 3-10 meters thick. The ore-bearing belt extends for more than 1 kilometer in length. The ore is high in silica and in places consists of manganese-bearing chert. The manganese minerals consist of pyrolusite, psilomelane and P'ien-meng-suan-k'uang with small amounts of magnetite and goethite. The ore contains 20-30 percent Mn. Based on its geologic occurrence, this type of deposit occurs as a marginal deposit of the geosyncline. Both the source of manganese and silica could have been derived from the volcanic rocks of the submarine volcanic extrusion.

Carboniferous Manganese Deposits (figs. 8 and 9)

A carboniferous manganese deposit was discovered in 1955 in northern Kwangsi province of southern China. [8] The stratigraphic horizon is probably Middle Carboniferous. Study is still in progress. The most recent data show that the carbonate ore consists essentially of manganiferous calcite with small amounts of rhodochrosite. Oxidized and partially oxidized secondary ore occurs near the surface. Rocks

above and below the ore consist of clayey and siliceous limestone interbedded with chert and manganese-bearing and carbonaceous limestone. The limestones are in part oölitic or pisolitic. There are four seams each 0.3-0.6 m thick. The maximum thickness is 1.5 m. The ore-bearing zone is 10 m thick. The carbonate ore contains 15-25 percent Mn, about 13 percent SiO_2 , 12-14 percent CaO and about 25 percent loss on ignition.

Upper Permian Manganese Deposits (figs. 10 and 11)

In Permian time, most of China south of Tsingling was under the Yangtze Sea. The northern part was uplifted and constituted a part of the Sino-Korean massif. During Upper Permian time the sea of southern China became shallow so that along the margin of the landmass numerous coal basins were formed where alternating marine and continental sediments were deposited. As sea transgressed again, marine manganese deposits were laid down in such areas as mentioned above. Contemporaneously in the continental coal basins of northern




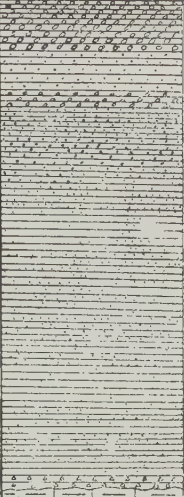
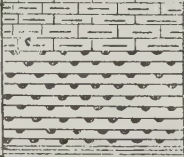


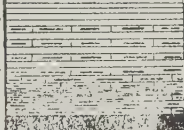
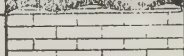
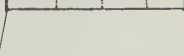
Geologic age	Stratigraphic horizon	Section	Thickness in meters	Lithologic description
QUATERNARY	Alluvium		2-10	<p>Fragmental chert, siliceous shale, soil and recent river gravel, sand and clay.</p> <p>Mostly residual soil over rocks of the middle Liu-chiang series, yellowish brown or brownish red. Loose part commonly contains manganese fragments; residual and talus accumulated enriched manganese layer below red clay.</p> <p>Red sandstone gravel, clay, and sand with few manganese fragments. Loose, no bedding.</p>
	Red clay		2-12	
	Gravel		3- 8	
TRIASSIC	Red-bed series		220+	<p>Upper part consists of conglomerate, locally with red sandstone. The middle and lower part consists of purplish red dense massive fine-grained sandstone with some intercalated conglomerate. Basal part consists of conglomerate with limestone and chert pebbles.</p>
			70±	Upper part is pale yellowish gray thick-bedded chert. Lower part is light yellowish green and light purplish red mamillary chert nodules and thin-bedded siliceous shale.
			54.5	<p>Dark purplish red and brownish yellow shale for 10 m, over soft friable manganese bed resulting from weathering of manganese-bearing limestone. Liver-brown or black, locally with fragments of pyrolusite and psilomelane. In turn underlain by brownish yellow thin bedded weathered siliceous shale or thin beds of light gray to gray limestone. Lower part is alternating beds of lenticular limestone or wavy siliceous shale and chert, often manganese-bearing and locally with thin manganese beds but generally of no industrial value.</p>
			24	
UPPER DEVONIAN	Liu-chiang series		80+	Coarse sandy chert underlain by alternating thin-bedded chert and siliceous shales in turn over bluish gray chert with yellow clay and manganese iron concretions. Followed downward by laminated dark brown manganese-bearing limestone and its weathered product. Northward grades into a siliceous facies. Basal part is thin-bedded manganiferous siliceous shale intercalated with purplish gray chalcedonic chert, separated from underlying rocks by an ammonite bed.
			20+	<p>Upper part is alternating beds of variegated platy, siliceous shale and gray chert. Shale has concentric color rings, is closely jointed and breaks into rhombic fragments by weathering. Lower part consists of light grayish black thin-bedded banded chert. Basal part is thick manganese ore.</p> <p>Yellowish green clayey shale over thick grayish black limestone and clayey limestone. Uncertain whether the contact between the Tung-kang-ling limestone and liu-chiang series is an unconformity.</p>
MIDDLE DEVONIAN	Tung-kang-ling limestone		20+	

FIGURE 7. Columnar section of the Gossan type of the Upper Devonian manganese deposits of Kwangsi province

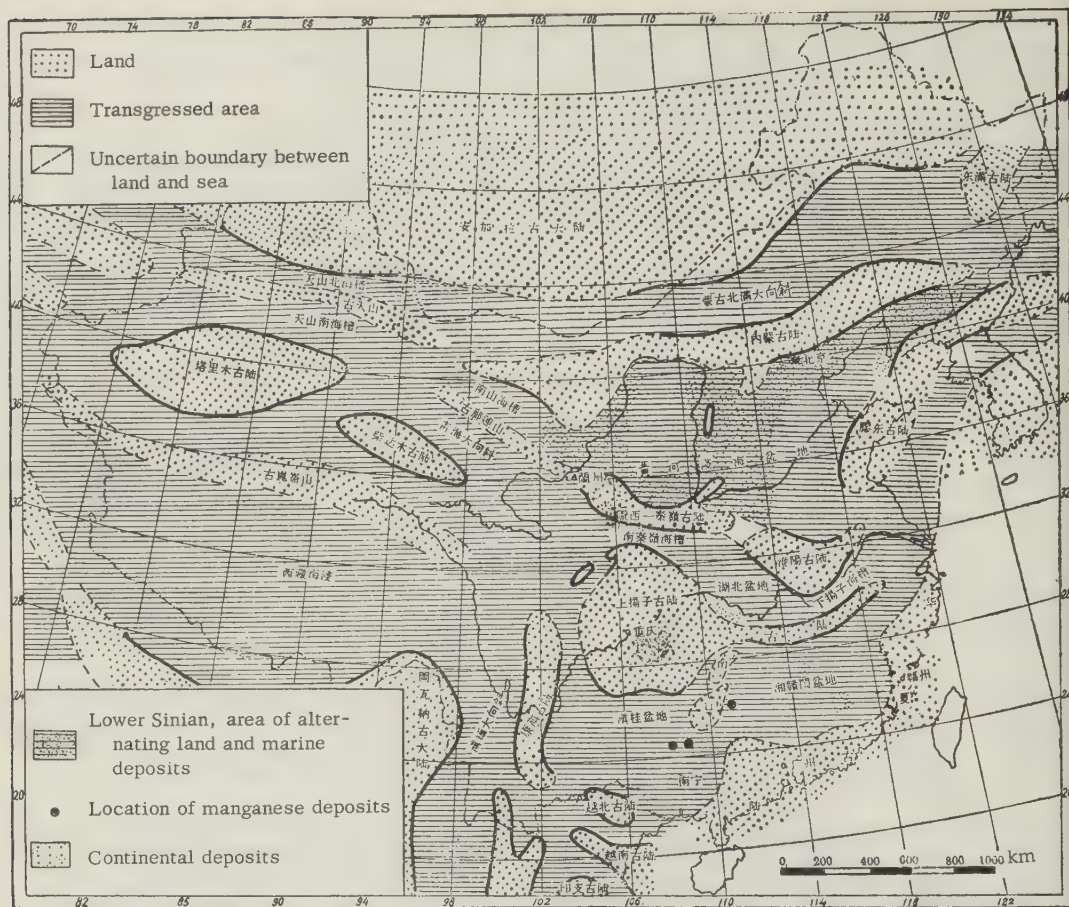


FIGURE 8. Carboniferous manganese deposits

China, iron-manganese deposits of probably lacustrine origin, high in phosphorus, were deposited. This latter type of manganese deposit occurs in the middle of the Shih-ho-tze series, widely distributed in Shansi province [9]. The country rocks above and below the ore-bearing beds consist of sandstone and sandy shale intercalated with clay shales. The ore bodies are lenticular and small and consist of oxide ore. Both the thickness and the tenor of ore vary greatly. The ore contains about 10 percent Mn, 23 percent Fe, 25 percent SiO_2 and 0.3-0.6 percent P. The silica occurs largely as opal.

The marine Permian manganese deposits of southern China are typically developed in the central part of Kweichow [10]. The ore-bearing horizon occurs at the disconformity between the top of the Lower Permian Pai-ni-t'ang formation and the base of the Upper Permian Lo-ping coal series. The Pai-ni-t'ang formation consists essentially of pyritiferous grayish black chert-bearing siliceous limestone which overlies the Yang-hsin limestone. The ore bodies are intercalated in the grayish black clay shale which underlies the coal series with siliceous limestone. The ore-bearing bed is persistent

and about 2 meters thick. Beds both above and below the ore contain pyrite crystals and concretions. Ore near the surface consists of psilomelane, pyrolusite and p'ien-meng-suan-k'uang and is botryoidal or in boxwork filled with blocky or powdery manganese oxide. The ore contains from 10 percent to more than 30 percent Mn, 5-20 percent Fe, and 8 percent to more than 20 percent SiO_2 . Because the depth of the oxidized zone is reflected by topography, the oxidation must be of recent age. The ore that occurs at depths of 20-30 meters below the surface consists mainly of manganoan calcite with rhodochrosite-bearing light gray carbonate rocks and some primary sedimentary pyrite crystals. This ore contains 17-23 percent Mn and 5-12 percent CaO.

Quaternary Manganese Deposits

In Kwangsi and Kwangtung province of southern China, where there are primary manganese deposits as described above, there often are accumulated manganese rubble or gravel ores intercalated in the Quaternary red clay. Several such deposits are known to be of good quality and industrial value. The ore is

Geologic age		Formation and series	Symbol	Thickness in meters	Section	Lithologic description
Cenozoic	Quaternary	Alluvium	Q			Grayish yellow, grayish brown and reddish yellow clay
	C A R B O N I F E R O U S	Mao-k'ou limestone	P ₁ ² n ₁	600		Grayish white, gray and bluish gray or brownish limestones, occasionally oölitic; becomes white after weathering.
Chi-hsia limestone		P ₁ ¹ C	300		Black or blackish brown limestone, the former is fine-grained, brittle and contains calcite veinlets the latter is thick-bedded, coarse-grained, brittle, and weathers into grayish white color.	
Upper Carboniferous	Ma-p'ing limestone	C ₃ M	400		Light gray or grayish white, brittle, dense thick-bedded limestone inter-bedded with nodular and banded chert.	
Middle Carboniferous	Huang-lung limestone	C ₂ h	275		Grayish white or gray thick-bedded crystalline coarse limestone, locally containing chert nodules; weathers into yellowish white color.	
Manganese bearing series		C ₂ L	300		Blackish gray thick-bedded limestone, locally oölitic underlain by alternating black thin-bedded limestone and chert; weathers grayish yellow. Carbonate manganese ore is interbedded in this this series.	
Lower Carboniferous	Yen-tzu series	C ₁ Y	110		Gray fine-grained limestone weathers into thin beds and is intercalated with thin carbonaceous shale.	
DEVONIAN	Upper Devonian	Liu-chiang series	D ₃ L	170		Gray limestone, lenticular limestone and bluish gray clayey limestone.
Middle Devonian	Tung-kang-ling series	D ₂ T	150		Thin-bedded limestone, brittle intercalated with chert and bluish gray and black thick-bedded limestone with chert nodules.	

FIGURE 9. Columnar section of the Middle Carboniferous marine manganese deposits of Kwangsi province

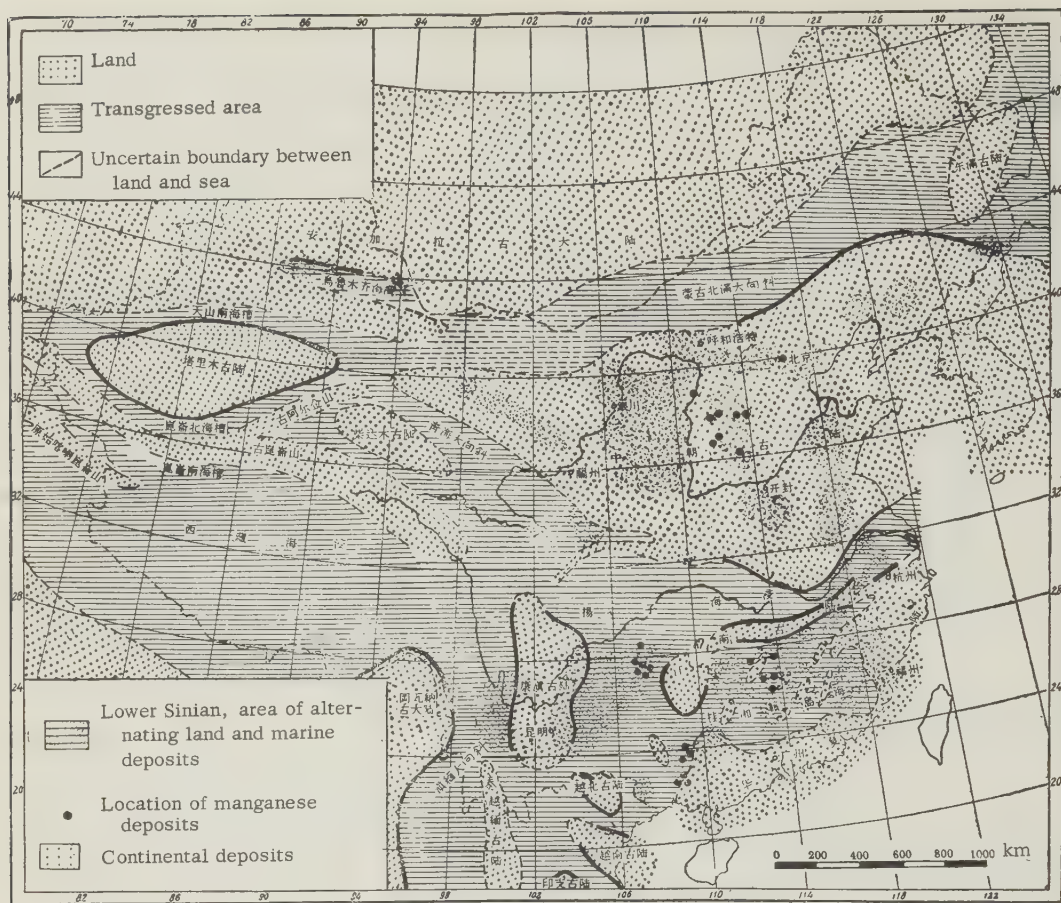


FIGURE 10. Permian manganese deposits

essentially a gossan-type formed by the weathering of manganese-bearing beds. Such gossans commonly were broken up by weathering and re-deposited as residual ore. Some of the ore was probably derived from fragments of manganese-bearing beds from which the manganese was concentrated with gravel by secondary enrichment. The rubble ore consists of manganese-oxide with more than 30 percent Mn, 10-25 percent SiO_2 , and is very low in P. The highest tenor of ore exceeds 36 percent. Some of the ore gravels are subangular, suggesting transportation for short distances. A few of this type of deposit overlie primary manganese deposits.

Paleogeographic Distribution and Genetic Characteristics of the Ore Deposits

Genetic Characteristics

From the geology of the typical deposits described above, their characteristic sedimentary features are: 1) The ore usually occurs at a stratigraphic hiatus. 2) The associated country rocks are primarily fine-grained

detrital fragmentary rocks and siliceous limestone or other siliceous rocks. 3) The ore is often associated with black shale or carbonaceous shale and contains pyrite. The Upper Permian manganese ore which occurs below the Lo-ping Coal series is most typical. 4) At only a few deposits does the country rock above and below contain glauconite.

The following discussion on the conditions of formation of exogenic manganese deposits is based on facts already described; discussion of this kind have been published by Hou Te-feng [12], and Yeh Lien-tsun [13].

Stratigraphic hiatus: One of the important conditions is a sedimentary hiatus. The average abundance of manganese in the earth's crust is but 0.1 percent [14]. Sediments with relatively high concentration of manganese which might serve as source beds are rarely observed beneath known manganese deposits. Therefore, the origin of exogenic manganese deposits requires a long period of weathering and erosion during a break in sedimentation. With prolonged weathering, manganese was first removed














Geologic age	Stratigraphic horizon	Thickness in meters	Section	Lithologic description
CRETACEOUS	Tsun-i formation			Purplish red clayey shale intercalated with platy red fine-grained sandstone, with grayish green conglomerate and shale in the basal part. Secondary kaolinite stringers occur perpendicular to the bedding.
JURASSIC	Shi-ma-t'an sandstone	248		Dark red, brownish yellow, grayish white and grayish green coarse-grained sandstone. Mostly platy and consists essentially of quartz with some feldspar and mica. Cementing material is essentially iron, occasionally by clay or siliceous material. It is disconformable on Triassic.
TRIASSIC	Shih-tzu-shan limestone	304		Reddish yellow conglomerate at the top. The middle upper part consists of gray, yellowish gray and red thick-bedded limestone. The lower part consists of dense limestone, brittle. Where stylolytic surfaces were developed the weathered surface is gray or grayish white.
	Sung-tzu-k'an formation	26.7		Gray massive limestone, intercalated with thin-bedded calcareous shale and yellow hard mudstone.
		89		Upper part consists of earthy brown massive hard mudstone and shale with intercalated thin-bedded clayey limestone. Lower part consists of gray thin-bedded clayey limestone intercalated with brown shale.
		42		Earthy brown, yellowish green and purple shale with intercalated brown hard mudstones.
		87.6		Earthy gray thin-bedded clayey limestone intercalated with brownish yellow shale.
		76.2		Upper part consists of brown and purplish gray clayey limestone. Middle part: gray calcareous shale and clayey limestone. Lower part: gray thick-bedded clayey limestone.
		36.6		Ironstained gray, purplish gray and dark gray thick-bedded limestone near the top. The lower part is conglomeratic, dary gray, and red conglomerate intercalated with a layer of dark red thick-bedded limestone.
	Mao-tsao-pu limestone	306.2		Grayish purple, earthy brown and red thick-bedded limestone; much of which is stained red; vugs of calcite occur in the earthy brown limestone. Stylolytes were developed in the grayish purple limestone.
		47-28		Gray, and dark gray thin-bedded limestone with massive limestone in the middle part.
	Chiu-chi-t'an series	130		Purple shale intercalated with thin-bedded hard mudstone and thick-bedded shale.
		118.8		Purple shale intercalated with thin-bedded hard mudstone and thick-bedded shale.

FIGURE 11. Columnar section of the marine Upper Permian manganese deposits of Kweichow province (Continued on next page)

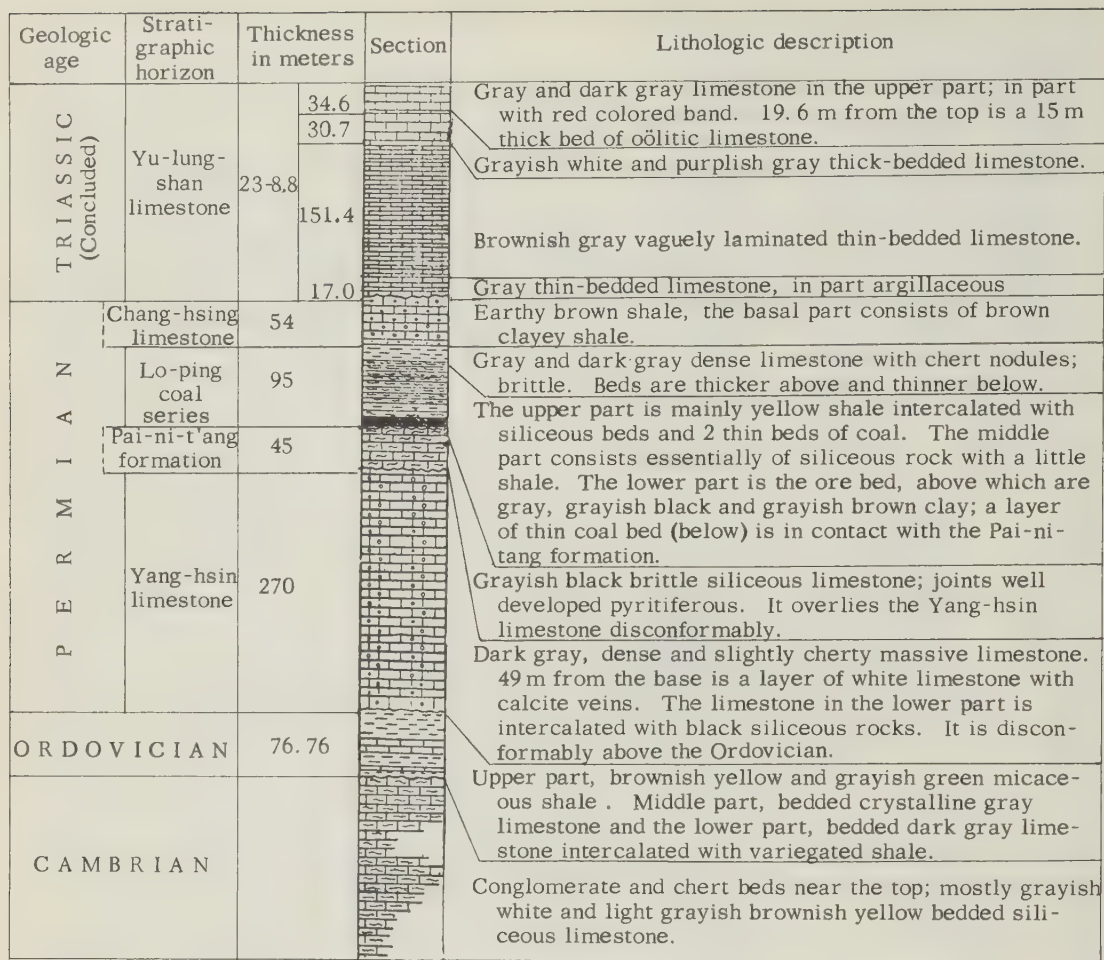


FIGURE 11. Columnar section of the marine Upper Permian manganese deposits of Kweichow province (Concluded)

from the silicate minerals of rocks which contain trace quantities of manganese to form a manganese-type of gossan. The manganese was then leached from the gossan, transported and redeposited and concentrated in ore horizons. Thus the sedimentation hiatus is an important prerequisite for the formation of exogenic manganese deposit. The manganese deposits of southern China as described above and the manganese-bearing bed above the pre-Sinian unconformity at Hai-chou of Kiangsu are characteristic examples of this type. In addition this also explains why most of the manganese deposits were laid down in a transgressive sequence.

Depositional environment: The environments for the deposition of exogenic manganese deposits are those of near shore or marginal sea or lagoonal areas. From the paleogeographic maps of each period of manganese deposition (figs. 2, 6, 8, 10), it is evident that with few exceptions the manganese deposits of various periods were distributed in a border area

between the marine basin and the old landmass. There were a few cases where the deposition was farther away from shore but the site was still within a lagoonal shallow sea. This is fully reflected from the lithology of the country rock of the manganese deposits, mainly of fine-grained fragmental clastic rocks, siliceous limestone and dolomite. The fine-grained fragmental rocks are mostly the suspended and colloidal sediments, which are deposited mostly in the marginal areas of the sea at depths of 0-200 meters. [16] The dolomitic limestone is also a shallow-sea deposit. Furthermore, this interpretation is enhanced by the fact that the Lo-ping coal series overlies Upper Permian manganese-bearing beds. In addition, in the ore-bearing rocks and the country rocks, oölitic texture and the presence of glauconite (which occurs at depths of about 200 meters in the sea) are evident characteristics of near-shore deposits.

Topographic environment: During the deposition of an exogenic manganese deposit the near-

shore old landform should have a mature topography. Pieh-chieh-he-chin [18] [transliteration of a Russian author] pointed out that the origin of the marine manganese deposit is related to the colloidal chemistry of silica in shallow water. Manganese was dissolved in colloidal form, brought to the sea, and deposited, so that the manganese ore commonly contains opal and other siliceous material. The examples described above are consistent with this phenomenon. We can therefore postulate that the dispersed manganese and abundant silica of the bed rocks occur in one stage in a colloidal solution which is only possible if this occurs in the slowly moving, shallow, meandering water of a region of mature topography.

Climatic environment: Moist and temperate climate is a necessary condition for the formation of exogenic manganese deposits. The source of manganese of exogenic manganese deposits must have gone through a stage where the manganese was released from manganese-bearing minerals by chemical weathering under an essentially moist and temperate climate in an area of mature landforms. Under such conditions, large numbers of organisms (including plant and bacteria) flourished and perished, forming large quantities of organic acid, humic acid and hydrogen sulfide which decomposed manganese-bearing silicates and other minerals forming carbonates or colloidal solution of manganese and iron. At the same time, leaching also gives rise to a silica-rich colloidal solution, which accounts for the common association of silica in manganese ore. Under such a predominantly reducing condition we find pyrite commonly associated with carbonate manganese ore and its common association with pyritiferous black shale, carbonaceous shale or coal-bearing sediments.

The above discussion of the characteristics pertaining to the origin of manganese ore was based on the stratigraphy of the ore-bearing bed, its ore mineralogy and rock facies. Other factors important to the problem of the formation of exogenic manganese ore, such as the chemistry of marine water and the activities of manganese-loving bacteria are not discussed in this paper.

Paleogeography

Sinian (fig. 2): The manganese deposits of Lower Sinian in southern China such as those of Hsiang-t'an and Lo-ping occurred in a shallow sea of a strait outside of the sedimentation belt of the Cathaysia. The area to its north is the old landmass of Chiangnan and the area to its south is Cathaysia. The region along Ch'in-hsien and Fang-ch'eng of Kwangtung province corresponds to the southern extension of the sedimentation belt, east of which is the Cathaysia and west of it the Indo-China landmass. The manganese location near Kuming

is situated in the marginal sea of the Si kang-Yunnan landmass. As a whole, they are all coastal deposits of shallow seas. The old landmass mentioned above consists of the Proterozoic Pen-chi series of slate, phyllite, and quartzite or its equivalents (such as the Shuang-ch'iao series and the Kun-yang series) which probably supplied the source of manganese.

The various Upper Sinian manganese deposits (southern part of Liaoning, northern Hopei and along the east flank of T'ai-hang-shan) of northern China are located in the Yen-Liao trough, along the shallow marginal belt. The Inner Mongolia landmass and the Ordos massif are located to the north and to the west with outcrops of Archean metamorphic rocks which are ideally the source rocks of manganese.

Of the deposits mentioned above, except Kuming, Ch'in-hsien and Fang-ch'eng of Kwangtung and the northern and western part of Hopei, the manganese ore consists essentially of manganoan calcite type of carbonate manganese ore. This is new information obtained during exploration for manganese ore in recent years. It provided a lead for future prospecting of this type of new deposits in such stratigraphic horizons along the margins of the old landmass. Such deposits were postulated to occur west of the area of Ch'ao-yang in Liaoning province.⁴ Manganese-bearing beds have been found in many places in the Upper Sinian Kao-yu-chuang limestone in northern China. With this as a guide, it should be possible to find more commercial deposits. In southern China, one should not only pay attention to the marginal belt of the Cathaysian old landmass for possible occurrence of such ore but also search the areas of the northwestern marginal areas of the Proto-Chiangnan landmass. In Kwangtung and Kwangsi, exploration should be guided by known stratigraphy for possible large carbonate-type manganese deposits.

Devonian (fig. 6): Devonian manganese deposits occur along the margin of the shallow sea basin in southern China, for example, the (manganese) producing area at the "Yun-kai-Yao-shan landmass" which is located to the south of Cathaysia. The latter was separated from Cathaysia by the "Kwangchou strait" (a lagoonal sea). The producing area at An-jen of Hunan [19] was located in the triangular area between Kiangsi, Hunan and Kwangtung province, in the bay area between Chiangnan and Cathaysia. The source of the manganese of the above mentioned localities could be the Pan-chi series or its equivalents exposed near the surface of the old landmass. For this reason, potential manganese deposits may be located in the southeastern part of Hunan and in the "Kwang-chou Strait" area mentioned above. A similar sedimentation

⁴Since the writing of this paper, localities of carbonate manganese ore have been found in this region.--Auth.

environment occurs to the east of the Sikang-Yunnan Axis.

In northwestern China, the source of the manganese of sedimentary manganese deposits could be the volcanic rocks of the Nan-shan series. Although at present the study of this type of environment has not been completed, it does constitute a condition which may serve as a new guide to ore-prospecting in the Ch'i-lien-shan geosynclinal belt.

Carboniferous (fig. 8): The exogenic manganese deposits of Middle Carboniferous age were located in the shallow sea area southwest of Chiangnan. The lithologic facies of this type of deposit is characterized by limestone. The ore mineral is manganoan calcite. It represents the carbonate type of sedimentary facies formed in a moderately deep sea along the marginal land area, and constitutes the clue for the search of this type of manganese deposit along the southwestern marginal areas of Chiangnan. In addition, proceeding northward from known localities towards the old landmass, there is the possibility of finding the primary oxide type of ore at an equivalent stratigraphic horizon.

Upper Permian (fig. 10): Besides the Upper Permian marine manganese ore of Kweichow, manganese-bearing beds occur at equivalent stratigraphic horizons in the central part of Kwangsi and southern part of Hunan provinces. Based on paleogeography, the Kweichow localities are located in the lagoonal sea between Chiangnan and the coal basins of Yunnan and Kweichow. The environment was excellent for the formation of manganese deposits so that it was not accidental that the deposits of this area are so extensive. In Kwangsi, because of the lack of such favorable environment, although the distribution of manganese-bearing beds are quite widespread, the future prospect is poor. Nevertheless, the possible occurrence of gossan type of manganese deposits should be kept in mind. The island area of Kiangsi and Hunan have similar sedimentological environment as those of Kweichow. On the north and south, are islands adjoining Chiangnan and Cathaysia. Moreover, coal basins occur in central and southern Hunan; therefore, the central and southern Hunan area are the most promising prospecting area for this type of manganese ore.

In north China, during the Upper Permian time, the northern China basin was formed along the southwestern foothills of the T'ai-hang range. Continental deposits of the Shih-ho-tzu series were deposited. Sparse lacustrine iron-manganese deposits occur in this region. Because of its origin, these deposits are small, high in iron and low in manganese. Their distribution is, however, quite extensive. From the regional point of view of the manganese resources, although the chance of finding large deposits of this type is poor, the continued

search for this type of widely scattered iron-manganese deposits in the Upper Permian northern China basin still has its significance.

Quaternary: The Quaternary manganese deposits of China which are deposits of residual weathering, are the main type of deposits of industrial value. They are also a particular type of the exogenic manganese deposits of China. Their distribution is restricted by climatic conditions to occurrences in the many rainy subtropical zones where primary manganese-bearing sediments are abundant such as in Kwangsi and Kwangtung province. Within the last three years several deposits of industrial value have been found. Such accumulative type manganese deposits were formed by recent chemical weathering and erosion in numerous small basins of the extensive karst area. It is likely that the discovery of this type of deposits will continue in the quaternary basins of Kwangsi and Kwangtung.

THE GENETIC TYPES OF KNOWN EXOGENIC MANGANESE DEPOSITS OF CHINA

Tentatively the various important exogenic manganese deposits of China can be genetically classified into three types.

Sedimentary Deposits

Based on the known deposits there are two types of sedimentary deposits, marine and lacustrine.

Marine Sedimentary Deposits

This type includes the Sinian, Devonian [of all China] and the Carboniferous and Permian beds of southern China. These can further be divided into the individual primary manganese oxide and manganese carbonate mixed type of ore (Ch'ao-yang of Liaoning) and the majority of rather pure manganese carbonate type. Most of the deposits consist of secondary oxides or partially oxidized ore which occur, to various extent, near the surface. The depths of oxidation, about 20-50 meters is in general determined by topography and the depth of the water table. The oxidized portion is only a minor part of the reserve. The larger deposits of this type are the Sinian deposits of Hsiang-t'an of Hunan and Ch'ao-yang of Liaoning, the Middle Carboniferous deposit of northern Kwangsi and the Upper Permian deposit of central Kweichow.

Lacustrine Sedimentary Deposits

This type refers to the iron-manganese deposits of the Upper Permian Shih-ho-tze series of Shansi. The deposits are small. The ore-bearing zones vary greatly in thickness and quality. Most of them are of poor quality and

little industrial value.

Gossan-type Manganese Deposits

These are the high-grade secondary oxidized ores derived from nearly completely oxidized primary manganese carbonate ore and manganese-bearing sediments. The former type is illustrated by the manganese deposits of Hsiang-t'an of Hunan where the lower limit of the gossan was the water table. The latter is represented by the Upper Devonian manganese deposit of central Kwangsi, medium in size and of fairly good quality. Although the Lower Sinian manganese deposits of Chin-hsien of Kwangtung are small, the manganese content of the ore is high.

Residual Ore

This is the result of weathering. The ore consists of weathered fragments from manganese gossan which accumulated in the surface soil or have been locally transported for short distances. This type possibly also includes manganese-bearing gravel which occur in the red clay where the manganese was concentrated by desiccation enrichment. The rubble ore in the red clay contains manganese oxide with more than 30 percent Mn and low in S, and P. This type of ore has a known pattern of distribution. It is easy to mine and concentrate. It constitutes ores of special industrial value of southern China and is therefore classified as a particular type.

From the above description it is clear that the most important exogenic manganese deposits of China are the marine deposits. The quarternary accumulative type of deposits are next in importance.

CONCLUSIONS

The known exogenic manganese deposits of China occur in many stratigraphic horizons. They are distributed in both north and south China, but are more abundant in the south. Except for the Quaternary and Upper Permian deposits of northern China, all deposited in shallow marine seas and originated under mild and moist climates favorable to the formation of coal. Most of the deposits occur above a depositional hiatus which represents the beginning of a marine transgression.

There are three types of major known exogenic manganese deposits in China: the sedimentary type, the gossan type and the residual-accumulative type. The third is a particular type which has industrial importance.

With regards to the mineral composition, the majority of the marine Paleozoic manganese deposits belong to the carbonate facies. It is possible however, that due to the small present

coverage, manganese deposits of the primary oxide facies have not yet been found. The Tertiary exogenic manganese deposits of Soviet Russia show distinct regular variation of facies [19, 20]. Is it possible that this type of regular variation would not apply to the marine Paleozoic manganese deposits? This is an important problem worthy of further study.

Exogenic manganese deposits occur in relatively few stratigraphic horizons in northern China. This is primarily because northern China has been essentially a landmass since Ordovician time, and therefore lacked the opportunity of the formation of marine manganese deposits except for brief periods during Permian-Carboniferous time when locally alternating marine and continental sediments were deposited. The outlook concerning the Upper Sinian carbonate manganese ore in northern China is favorable. In addition, Devonian exogenic manganese deposits have been found in northwestern China, which is a lead to future search in the northwest. The present data indicates that the most promising future for new deposits lies in southern China.

The preliminary geological study of the exogenic manganese deposits of China shows that because of the lack of such studies in the past regarding the manganese deposits, there was no adequate knowledge regarding the outlook for manganese deposits. The limited effort in the prospecting and study of recent years sufficiently proves that the exogenic manganese deposits of China are widely distributed stratigraphically and areally and the outlook is good. Chinese geologists should continue the survey and study with unlimited faith in order to meet the growing demand for manganese.

REFERENCES

- 1-11. VARIOUS GENERAL SURVEY REPORTS OF MANGANESE DEPOSITS: Ministry of Geology; Ministry of heavy industry, 1953-1956.
12. Hou, T. F., T'SUNG TI-TS'EN KUAN-TIEN TUI CHUNG-KUO MENG T'IEH TENG K'UANG-CH'AN TI SHUN-CHAO TI-KUNG CHI-TIEN I-CHIEN [SUGGESTIONS, BASED ON THE STRATIGRAPHIC POINT OF VIEW, CONCERNING THE IRON AND MANGANESE DEPOSITS OF CHINA]: Ti-chih Hsueh-Pao [Acta Geologica Sinica], v. 33, no. 1, 1953.
13. Yeh, L. T., CHUNG-KUO MENG-K'UANG T'AN-SUO KUNG-TSO CHUNG TI CHI-KE CHI-PEN WEN-T'I [SOME BASIC PROBLEMS CONCERNING THE PROSPECTING WORK OF CHINESE MANGANESE DEPOSITS]: Ti-chih Hsueh-pao [Acta Geologica Sinica], v. 33, no. 4, 1953.

INTERNATIONAL GEOLOGY REVIEW

14. Sa-wu-k'e-fu [Saukoff], TI-CH'IU HUA-HSUEH [GEOCHEMISTRY].
[SU-LIEN TI MENG-K'UANG [THE MANGANESE DEPOSITS OF SOVIET RUSSIA]
15. Ministry of Geology. GEOLOGICAL REPORT OF THE MANGANESE DEPOSIT OF HAI-CHOU OF KIANGSU, 1955.
16. Rankama, K., and Sahama, Th. G., [GEOCHEMISTRY], 1949.
17. Ssu-t'e-la-ho-fu [Strahoff ?] TI-SHIH HSÜEH YUEN-LI [THE PRINCIPLES OF HISTORICAL GEOLOGY].
18. Pieh-chieh-he-chin [Bechehokin ?]
19. Tien, C. C., and Hsu, T. 'Y., HU-NAN-SHENG AN-JEN-HSIEN-CH'ENG PEI-CHIAO MENG-K'UANG, HU-NAN MENG-KUANG CHIH [THE MANGANESE DEPOSITS IN THE NORTHERN SUBURB OF AN-JEN IN HUNAN PROVINCE, FROM "THE MANGANESE DEPOSITS OF HUNAN PROVINCE."], 1935.
20. A-wa-li-an-ni [Awaliani ?] MENG [MANGANESE].

GEOLOGICAL STRUCTURE OF THE SOUTH KHINGAN MANGANESE DEPOSIT AND ESSENTIAL COMPOSITION OF ITS ORES¹

by

M.V. Chebotarev

translated by E.A. Alexandrov and Assoc.

ABSTRACT

The South Khingán manganese deposits are geologically a part of the Malyy Khingán manganese-iron ore district. The geological sequence of the region consists of Precambrian and Lower Cambrian sedimentary, sedimentary metamorphic, extrusive and intrusive rocks. The lower series are exposed in anticlines intruded by granites. The manganese ores are confined to the base of the ferruginous quartzite ore horizon, which is located in the middle part of the Lower Cambrian ore-bearing series. The latter lies transgressively but without apparent unconformity, on the eroded surface of Upper Sinian dolomites. The manganese ores are paragenetically associated with banded ferruginous quartzites and siliceous-argillaceous slates which contain variable amounts of dolomite of chemical or clastic origin. The banded ore structure is characterized by rhythmic interbedding of ore and barren bands from 0.10 to 10 cm thick. The essential ore-body minerals are braunite, hematite, hausmannite, magnetite, rhodochrosite, chalcedony, quartz, clay minerals and dolomite. The major minerals forming the ore bands are braunite, hausmannite, and rhodochrosite. Barren material is composed of other minerals. Mineralogically the following ore types are distinguished: braunite and its varieties (hausmannite-braunite and braunite hematite), hausmannite-rhodochrosite, and siliceous rhodochrosite. In origin and mode of occurrence the Lower Cambrian Malyy Khingán manganese ores are similar to the marine Devonian manganese ores of central Kazakhstan. The manganese ores and overlying banded ferruginous quartzites are similar to the manganese ores and jaspilites of the Morro do Urukum in Brazil. -- M. Russell.

REGIONAL GEOLOGICAL SETTING

The Lower Cambrian manganese and iron ores are developed in a region within the boundaries of the Amur region of Malyy Khingán, which is bordered on the south by the Amur River and on the north, west and east by the Pompeyevka, Manchzhurka and Samara rivers, respectively.

The geological sequence of the region consists of sedimentary, sedimentary-metamorphic, extrusive and intrusive rocks. The sedimentary-metamorphic rocks form the so-called Khingán complex, consisting, from bottom to top, of the Soyuznoye, Ditura, Igincha, Murandava, ore-bearing and Londoko series. The complex is about 6,000 meters thick. Its first four members are Precambrian, while the ore-bearing and Londoko series are Lower Cambrian. The series are composed of rocks in various stages of metamorphism, and range from argillites, with negligible development of sericite, to highly metamorphosed slates and marbles.

The lower Soyuznoye series is exposed in anticlines intruded by granites. It is sub-

divided into two subseries: the lower series, about 500-700 m thick, consists mainly of quartz-mica graphitic schists. Quartz-feldspar-mica, quartz-amphibole, amphibole, quartz-tourmaline, quartz-mica-sillimanite schists, quartzitic and other schists are of subordinate importance. All of them commonly contain garnet. Migmatites, and injection gneisses are found in the zones of contact with granites. Further away from the granite contacts, within the subseries, occur metamorphosed carbonaceous-argillaceous schists, alevrolites and sandstones. The upper subseries is 1,500-2,000 m thick, and consists mainly of crystalline limestones with graphite flakes, thin quartzite beds, quartz-tourmaline, quartz-graphite, amphibolite and mica schists. The Soyuznoye series is conformably overlain by the Ditura series, which is about 800-1,000 m thick and consists of limestones with subordinate layers of sericite, calcite-sericite, carbonaceous-siliceous, and carbonaceous schists and siltstones. There is no distinct boundary between the Soyuznoye and Ditura series.

The Ditura series is overlain by the Igincha series which is 1,000-2,000 m thick. It consists of green-gray sericite, quartz-sericite, quartz-chlorite, cherty-argillaceous schists, siltstones and sandstones.

In the upper parts of the Khingán complex lies the 500-800 m thick Murandava series. This series is divided lithologically into three horizons (from bottom to top): 1) massive, crypto-crystalline dolomites, to a greater part

¹ Translated from *Geologicheskoye stroeniye yuzhno-khinganskogo margantsevo go mestorozhdeniya i veshchestvenny sostav v go rud; Sovetskaya Geologiya*, no. 8, p. 114-136, 1958.

cherty, with lenses of magnesite; 2) cherty, cherty-argillaceous, carbonaceous-argillaceous slates, slaty and laminated dolomites, in places intraformational breccia occur; 3) massive, light gray dolomites. The magnesite deposits are associated with Murandava dolomites. The formation of the Murandava series was followed by an interruption in sedimentation and erosion. Therefore the overlying ore-bearing series overlaps transgressively the Murandava series and contains material eroded from the latter in the form of dolomite and schist fragments. Lithologically the series is subdivided into a lower horizon, an ore horizon and an upper horizon. The lower horizon is about 50 to 100 m thick, and consists of cherty, argillaceous, carbonaceous slates, arenaceous dolomites, and breccias. The ore horizon, 25 to 35 m thick, is subdivided into two layers; a manganese layer which is up to eight meters thick, and an iron ore layer, which is 20 to 25 m thick. The horizon overlying the ore formation is 100-130 m thick, and consists of carbonaceous-argillaceous and argillaceous slates with lenses of limestone and dolomite.

The Londoko series is 600-800 m thick, covers conformably the ore-bearing series, and consists of a lower horizon, dark-gray bituminous limestones, and an upper horizon consisting of siliceous slates.

The formation of the Khingan complex was completed during three major cycles of sedimentation. Deposits of each cycle consist of arenaceous slates and carbonates. The first cycle includes arenaceous slates of the lower Soyuznoye sub-series and limestones of the upper Soyuznoye sub-series and Ditura series; the second is represented by arenaceous slaty sediments of the Igincha and by dolomites of the Murandava series; the third cycle consists of arenaceous slaty sediments of the ore-bearing series and limestones of the Londoko series. Every cycle is characterized by its geochemical peculiarities. Sediments of the first cycle contain, in their lower part, economic concentrations of carbon (graphitic slates). In the upper part vanadium, nickel, and other elements, not in economic concentration, are found. The second cycle is characterized by the constant presence of titanium in its lower part, and economic concentration of magnesium as magnesite in the upper part. And, finally, the lower part of the third sedimentary cycle consists of economic concentrations of manganese and iron.

The formation of the Londoko series marked the end of a major stage of geological development of the region. All sedimentary formations were strongly folded and intruded by equigranular biotite granites. Later igneous activity was renewed with the formation of massive porphyritic biotite granites, later followed by leucocratic tourmaline granites. The previously described sedimentary formations, that

have been subjected to various degrees of regional and contact metamorphism and intrusion of granites, are overlain by Upper Cretaceous sediments which are preserved in small areas along the Pompeyevka, Plotnichikha and Khlebnaya rivers. These formations consist of broadly folded arkosic sandstones, tuffaceous in their upper part, which contain plant detritus, gravel, and conglomerates. Basalt flows are found along the Tertiary-Quaternary boundary in the southeastern part of the region. The basalt flows are 90-110 m thick. Recent sediments are represented by shingle, sand and clays of alluvial origin, up to 60 m thick, and by thin (1-3 meters) diluvial deposits on mountain slopes. Structurally the South Khingan deposit represents a synclinal zone which is developed within the boundaries of the Khingan-Bureya anticlinorium, or, on a larger scale, it is part of the Khingan-Bureya median massif (according to the definition of some Soviet and Chinese geologists). This synclinal zone was named the Samara synclinorium. There are five structural complexes in the region (fig. 1): 1) Lower Proterozoic folded gneisses; 2) Upper Proterozoic-Lower Paleozoic folded Khingan sedimentary-metamorphic complex; 3) Lower Paleozoic intrusive complex; 4) Upper Cretaceous folded sedimentary-tuffaceous complex; 5) Cenozoic (mainly Quaternary) sedimentary-extrusive rock complex.

ORE OCCURRENCE AND STRUCTURE OF THE ORE-BEARING SERIES

The South Khingan manganese and iron ore deposit represent sparsely distributed ore sectors, distributed over 450 square kilometers.

The ore field (fig. 2) is located in the central zone of the Samara synclinorium in the form of narrow band between 6 and 8 kilometers wide, and extending north-south for 60 kilometers along the Bolshaya Samara River and its tributaries, the Stolbukha and Starichikha rivers.

Three ore formations can be followed through in the perimeter of the ore field, each 200-300 m thick, and separated by two to five kilometers from each other. The ore formations are called: Western, Central and Eastern. Each ore layer is in its turn cut by faults into a series of ore sectors (large and small structural blocks, see fig. 2).

The bulk of the manganese ore reserves are located in the southwestern corner of the ore field, within the limits of Poperechnyy, Serpukhovskiy and Stolbukha sectors (see fig. 2).

The greater and best manganese deposits are located in the Poperechnyy sector, located 15 kilometers from the Soyuznoye landing on the Amur River (fig. 3). The manganese deposits in the remaining part of the ore field are

not of industrial importance except for small separate sectors (Gematitovy Ust-Starichikha).

The ore-bearing series is 150-250 m thick. A characteristic feature for this series is the thin rhythmic Flysch type intercalation of beds of different lithological composition. Clastic rocks are well developed in the western ore formation, where they are represented by sedimentary breccias and sandstones; in the central

and eastern ore formations argillaceous slates are dominant, while coarsely fragmented beds, such as sandstones, have a subordinate role. Various types of ore alternate at even shorter intervals within the limits of a single sector (fig. 4).

Horizon Underlying the Ore Horizon

This horizon consists mainly of greenish-gray siliceous-argillaceous slates. In the upper part of the horizon, in many cases, are developed siliceous-argillaceous reddish-brown slates directly underlying the ore horizon. In the western formation where the high quality ores are located, the horizon underlying the ore horizon is divided into lower and upper layers. The lower layer is dominantly slaty, but its lowest part (three to five meters thick) consists of black carbonaceous-argillaceous slate. Basically the layer consists of argillaceous-dolomitic breccia with carbonaceous-argillaceous and siliceous-argillaceous slates. The rocks are usually black or dark gray. The total thickness of the layer is 20-25 m. The upper layer, immediately underlying the manganese ore, consists predominantly of carbonates. It is predominantly made of dolomitic

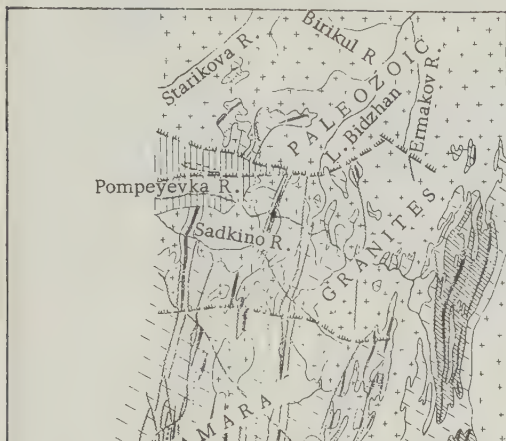

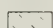
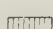
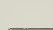
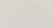
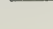
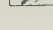
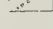


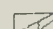
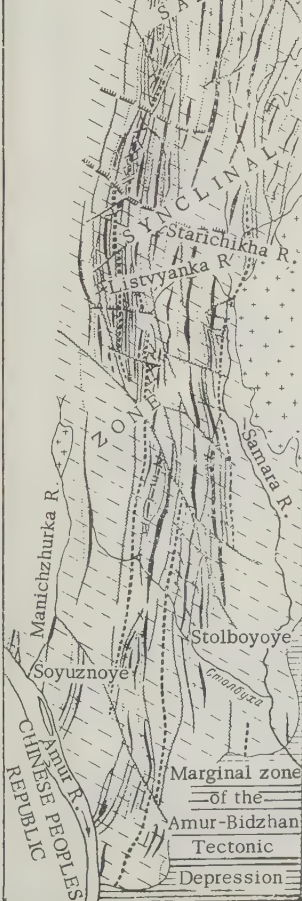


FIGURE 1. Tectonic map of the South Khingan deposit

0 2 4 6 8 km

-  - Lower Proterozoic folded complex
-  - Cambrian-upper Proterozoic folded complex
-  - Upper Cretaceous folded complex
-  - Quaternary horizontal complex
-  - Lower Paleozoic intrusive complex, Fold axes:
-  - Axes of major and secondary anticlines
-  - Axes of major synclines
-  - Axes of minor synclines
-  - Axis of superimposed basin
-  - Pre-Cenozoic faults
-  - Cenozoic faults



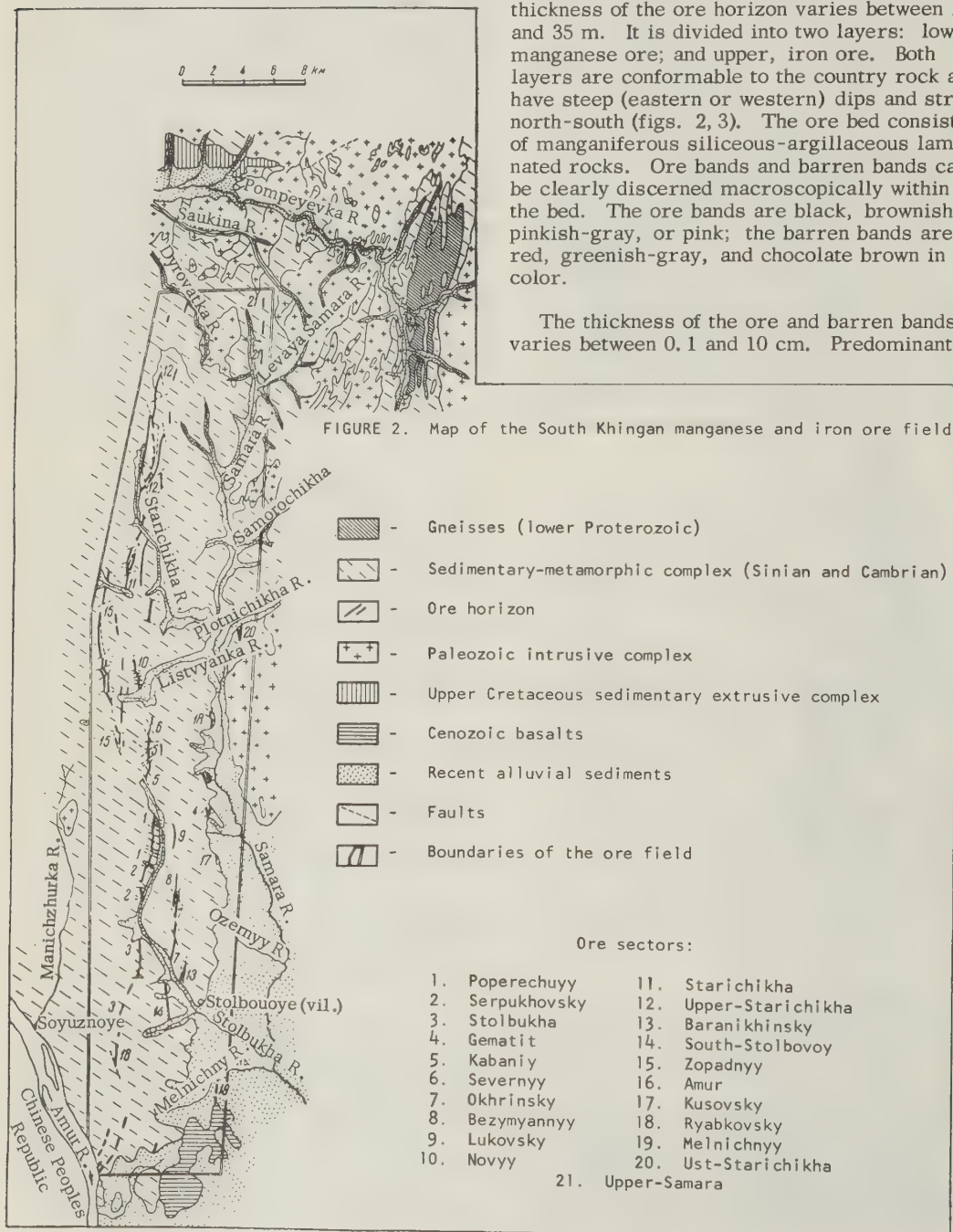
sandstone and dolomitic breccia (the cement and fragments are dolomitic), partially of intraformational origin. This intraformational breccia indicates local erosion during the time of deposition of the underlying [?] ore horizon. Pelitic, [Tr.: Consists of particles <0.01 mm], often argillaceous dolomites (dolomitic marls) and siliceous-argillaceous slates, forming bands 2 to 10 cm thick, play a subordinate role. Rhodochrosite occurs in slates in the upper

part of the layer. The thickness of the layer varies from one to twelve meters, and is on the average five to six meters thick. The rocks in the upper layer are light gray with a greenish tinge.

The Ore Horizon

This horizon is made of deposits of chemical origin and terrigenous sediments. The total thickness of the ore horizon varies between 25 and 35 m. It is divided into two layers: lower, manganese ore; and upper, iron ore. Both layers are conformable to the country rock and have steep (eastern or western) dips and strike north-south (figs. 2, 3). The ore bed consists of manganiferous siliceous-argillaceous laminated rocks. Ore bands and barren bands can be clearly discerned macroscopically within the bed. The ore bands are black, brownish, pinkish-gray, or pink; the barren bands are red, greenish-gray, and chocolate brown in color.

The thickness of the ore and barren bands varies between 0.1 and 10 cm. Predominantly



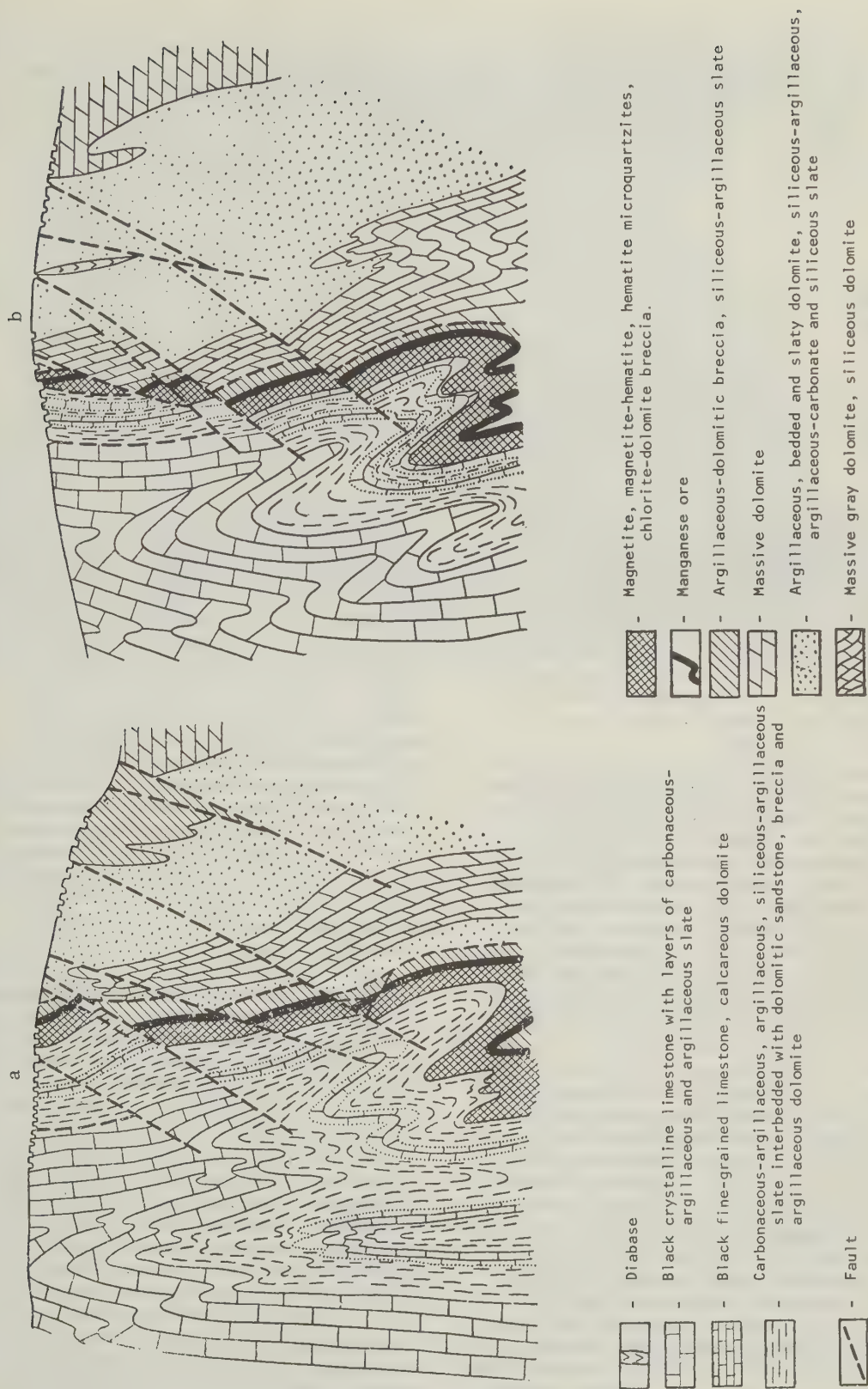


FIGURE 3. Cross sections of the Poperechmy sector in the South Khingan deposit.

a- Section across the northern part of the sector

b- Section across the southern part of the sector

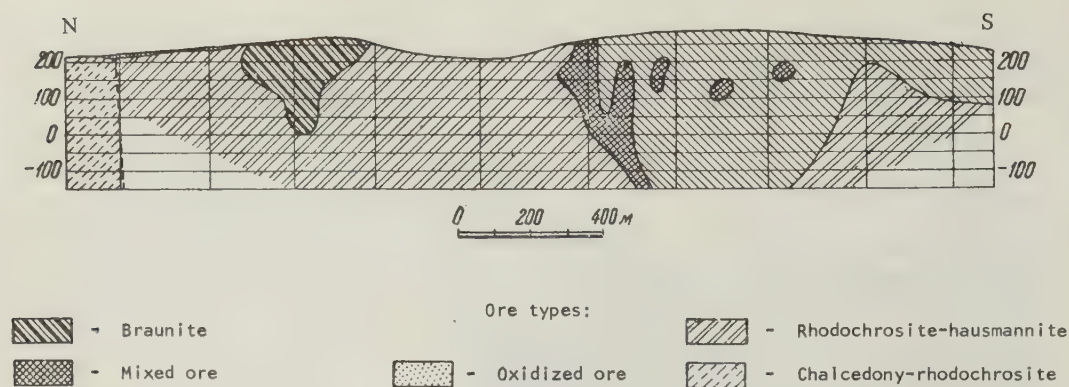


FIGURE 4. Scheme of the distribution of various ore types in the limits of the Poperechnyy sector (vertical elevation)

the bands are 1 cm thick. The ore bands as well as the barren bands are usually high in fragmentary material. At the base of the major manganese ore bed there is a layer of siliceous-rhodochrosite rock (carbonate ore) 1 m thick. This layer is in places separated from the main manganese ore bed by 1 m of dolomitic sandstone. In some cases, a layer of braunite-hematite ore is encountered in the hanging wall of the manganese ore bed, which represents the transition stage between manganese and iron ore.

Mineralogically the following principal types of manganese ores are identified, characterizing in themselves also separate facies: braunite ores and their variations (hausmannite-braunite and braunite-hematite) characterizing the oxidation facies. The hausmannite rhodochrosite ores characterize the transitional oxidation-carbonate facies, and the siliceous rhodochrosite ores represent the reducing facies. Finally, in the oxidation zone there are pyrolusite-psilomelane ores formed as the result of oxidation and hydration of the above mentioned three ore types.

The braunite ores (fig. 5) are confined to the western, coastal strip of the ore bearing series. They form the southern part of the ore in the Poperechnyy sector along a distance of 1, 100 m and also the most northern end of the ore deposit in the Serpukhov sector. Separate blocks of the braunite ores occur in the northern part of the Poperechnyy sector and the southern part of the Serpukhov sector, among the oxide-carbonate ores, which indicate the unstable facial conditions of sedimentation. The ores can be traced from 200 to 400 m down dip. The oxide ores are replaced gradually, to the south and north down dip and along strike, by hausmannite-rhodochrosite ores, the latter being traced in the northern direction for 1, 2 km forming

the northern flank of the Poperechnyy sector, changing further north into proto-oxide carbonate ore facies. To the south, the hausmannite-rhodochrosite ores are traced along the strike for seven kilometers, making the southern part of the Serpukhov sector and the northern half of the Stolbukha sector. Further to the south they are replaced by carbonate ores. The latter wedge out completely in the Amur sector. The transition of various ore types is gradual (down dip as well as along strike of the ore body). The gradual change of braunite into hausmannite-rhodochrosite ores usually takes place within a distance of 50 to 100 m and in places less. These transitional zones are characterized in their columnar sections by the presence of braunite and hausmannite-rhodochrosite ore bands. Braunite ores are usually localized in the roof of the ore bed. But in other cases, both ore types are interbedded with each other without a particular regularity, forming areas of mixed ore.

To the east, across the strike, the hausmannite-rhodochrosite ores are replaced by manganese siliceous-argillaceous slates. The latter are developed within the limits of the central ore-bearing area in the sectors of Kabaniy, Severnyy, Okhrinsky, Bezmyannoye, Lukovsky, etc. They form a bed up to six meters thick consisting of slaty banded rocks of reddish-brown color forming a background for darker bands, representing bands enriched by ore minerals such as braunite, hausmannite, and hematite. The greater part of the mentioned ore minerals as well as rhodochrosite and magnetite are dispersed in the slaty rocks, and do not form separate bands. The manganese content in these rocks is 8-12 percent.

The siliceous-carbonate manganese ores have no economic value and occur within the Zapadnyy, upper-Starichikha, and Stolbukha

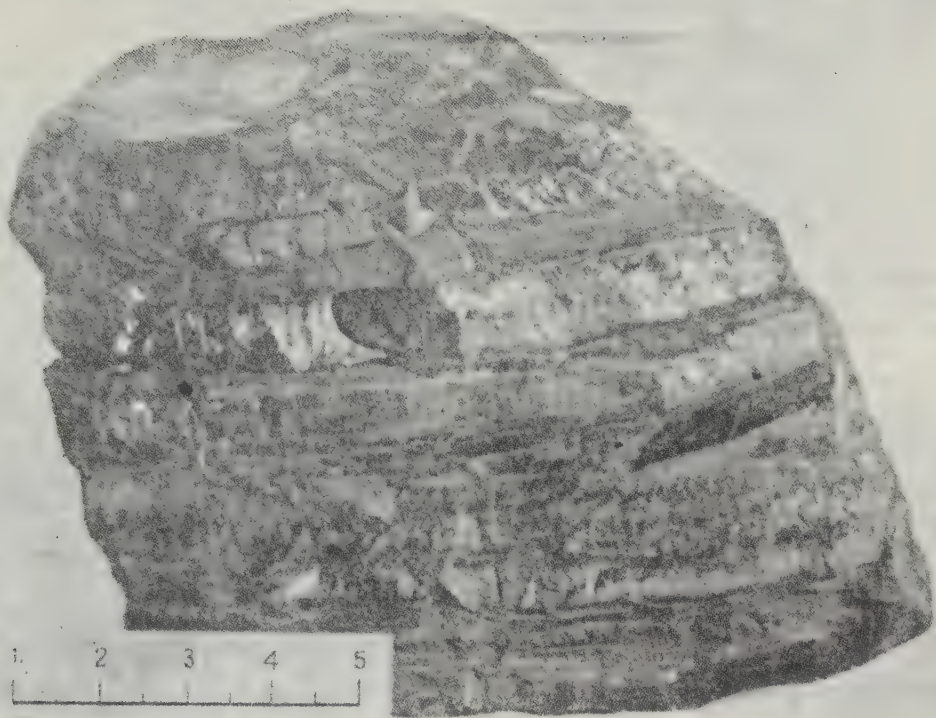


FIGURE 5. Banded braunite ore

sectors. They also are part of the companion bed located at the foot of the main manganese ore bed in the Poperechnyy sector. The oxidized ores have a limited distribution in the area of the deposit, and are encountered in the near-surface part of the manganese ore bed at a depth not exceeding 20 m.

The iron-ore bed consists of ferruginous quartzites, sedimentary chlorite-dolomite breccia and siliceous-argillaceous slates. The ferruginous quartzites represent banded rocks, rhythmities according to N. S. Shatsky, [4], consisting of intercalating ore bands and barren bands, with average thicknesses of 1 to 2 cm. From the point of view of texture, the ferruginous quartzites are similar to manganese ores. Mineralogically, the ferruginous quartzites are represented by hematite, hematite-magnetite and magnetite-quartzite. The hematite quartzites are predominant. They are developed in the central and eastern ore-bearing formations. The magnetite and hematite-magnetite quartzites are developed only in the western (probably in the coastal) formation. The barren bands of the iron ore beds consist mainly of chalcidony and microcrystalline quartz having a red tinge due to dissemination of fine particles of hematite. The barren bands of the ferruginous quartzites in the western ore formation in places consist of dolomites of fine chlorite-dolomite breccia. Within this formation, there are also lenses

and bands of chlorite-dolomite breccia and siliceous-argillaceous slates. The chlorite-dolomite breccia represents a massive greenish-gray rock. The slates are also green. Within the boundaries of the western sector, on its northern flank, chlorite-dolomite breccia and siliceous argillaceous slates dominate in the ore-bearing horizon. Ferruginous quartzites in this area form lenses and thin bands among slates and breccia. In 1955, Yu. A. Khodak found, for the first time, dessication cracks in ferruginous microquartzites of the Bidzhan deposit (northern ore sector), indicating shallow water conditions and interruptions in sedimentation during formation of the ore horizon.

The ore horizon is covered by a horizon, 100-150 m thick, consisting mainly of argillaceous carbonate rocks with a considerable amount of carbonaceous material, due to which this horizon is in most cases dark gray or black. This horizon is composed mainly of carbonaceous-argillaceous, argillaceous, siliceous-argillaceous slates, closely associated by mutual transitions with carbonaceous dolomites, calcareous dolomites, calcareous and dolomitic marlites. Within the limits of the Okhrinsky sector there are intraformational breccias that were locally deposited in the horizon underlying the ore horizon. The horizon

overlying the ore horizon is conformably covered by the Londoko limestone series.

Size and Shape of Ore Bodies

The ore bodies occur as layered, steeply dipping beds, elongated north-south (see fig. 3). Along the strike their sides are usually bounded by faults, and occasionally they wedge out due to a change in facies. They are from 0.5 to 8 m thick, from 300 to 2,400 m long, and extend at least 350 m down-dip. At 350 m there are still no signs of wedging out. Within the limits of the ore sectors, numerous faults separate the ore bodies into large and small blocks with relative throws that range from 2 or 5 m up to tens of meters (see fig. 3).

All ore bodies are conformable to the country rock.

MANGANESE ORE TYPES AND THEIR COMPOSITION²

The ores of the South-Khingian deposit are classified genetically and mineralogically in the following way:

- A. Primary ores (regionally metamorphosed) oxides.
 1. Braunite
 2. Hausmannite-braunite
 3. Braunite-hematite oxide-carbonate ores
 4. Hausmannite-rhodochrosite carbonate ores
 5. Siliceous-rhodochrosite
- B. Secondary ores (oxidized)
 6. Pyrolusite-psilomelane ores

Primary Ores

Oxides

Braunite is the most common ore oxide. Hausmannite-braunite and braunite-hematite ores have a relatively limited development.

1. Braunite ores. These ores are economically the most important. They represent about half of the proven economic deposits, and are developed in areas of southern Poperechnoye and northern Serpukhovo, that belong to the western ore-bearing formation. The braunite ores are from 1 to 8 m thick. Along the strike and dip they are replaced by oxide-carbonates and carbonate ores.

They are dark, hard, banded rocks (fig. 6), composed of interlayered ore (black) and barren (red) bands.

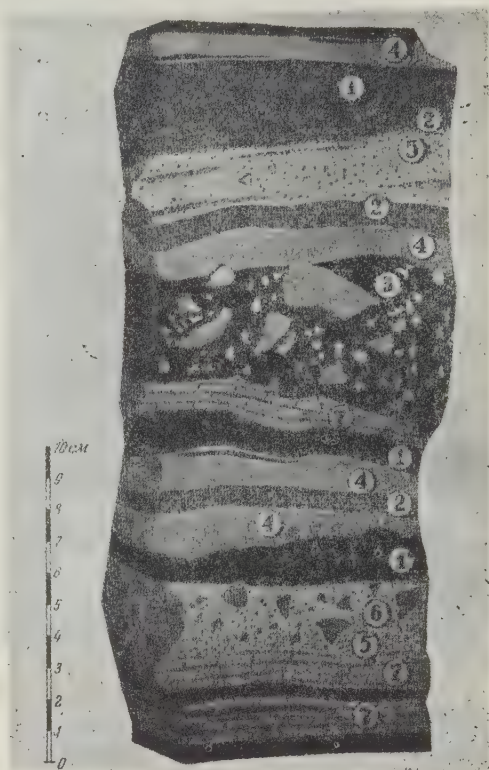


FIGURE 6. Braunite ore from Poperechnyy sector. Drawing of ore block.

- 1) Braunite, chalcedony-hausmannite bands;
- 2) Braunite, with dolomite fragments (ore bearing sandstone); 3) Dolomite-braunite-breccia (dolomite) is of light color; 4) Siliceous-argillaceous, red-jasper like band; 5,6) Breccia-like dolomite sandstone with siliceous-argillaceous cement; 7) Dolomite band, composed of fine-grained dolomite.

Barren bands are dominant. The ore bands vary from 0.1 to 7 cm thick, with predominant thickness of 1-2 cm. The barren bands are somewhat thicker, varying between 1 and 20 cm but usually 2-3 cm. The total thickness of ore bands represents 25-40 percent of the bed. The ore bands have sharp rectilinear margins and, because of their black color, stand out from the red barren component. Usually their thickness is uniform, but in places they wedge out and form lenses, tongues, boundinage and thick ore bands. The ore bands have a metallic luster with a bluish tinge, and a characteristic step-like fracture caused by transverse microfractures found only in the ore bands. They contain about 85-90 percent fine-grained braunite and 5-10 percent chalcedony,

² The iron ores of Malyy Khingan have been already described in numerous publications and are therefore not considered here.

quartz fragments and dolomite. Nonmetallic minerals are distributed evenly among the fine-grained braunite or form microscopic bands within bands. The size of the dolomite fragments ranges from 0.1 to 20 or 30 mm in diameter. With the increase in amount and size of fragments the braunite bands are sometimes replaced by sandstones and varieties of breccia cemented by braunite. The texture of ore bands are massive and consist of xenomorphic grains. Braunite forms massive fine-grained aggregates of cubic or octahedral appearance. The size of individual grains is 0.006-0.009 mm in diameter. Well-shaped braunite crystals of 0.25 mm are relatively rare, in the fine-grained braunite mass.

The chemical composition of braunite layers is given in Table 1. The layers are characterized by a high manganese and a low iron content, with a constant presence of 10 percent silica and 0.1 percent phosphorous.

The barren bands contain predominantly siliceous-argillaceous bands, enriched in various degree by dolomite. Dolomitic, siliceous-dolomitic, argillaceous, argillaceous-dolomitic, arenaceous-dolomitic and siliceous-hematite bands are of subordinate importance. All the bands merge with one another.

The siliceous-argillaceous bands are jasperoid and are bright red. They are composed of chalcedony and argillaceous minerals and up to 15 percent hematite dust. Because of this, they could have been justifiably called "ferruginous bands."

Clastic dolomite and dolomite of chemical origin also occur in varying amounts. Fine-grained braunite, hausmannite and rhodochrosite occur in subordinate amounts in the siliceous-argillaceous and other barren bands. The latter become brownish, with an increase in braunite and hausmannite content.

The dolomite and siliceous-dolomite bands are lighter-colored, fine-grained in texture, and are cemented respectively with dolomite or a mixture of dolomite and chalcedony. Fine-grained hematite, argillaceous minerals, hausmannite and magnetite occur in small amounts in these bands. Phlogopite, chlorite and tremolite are newly-formed minerals. Separate barren bands contain many dolomite fragments. Bands of this type are characterized by dolomitic sandstones or dolomite breccias. Largely argillaceous bands are usually brown and are rare.

The siliceous-hematite bands resemble typical jasper, and have no significance in the structure of the ore bed; they are confined to the hanging wall in the transitional interval between manganese and iron ores.

A brief description of the major minerals forming the barren bands follows.

Chalcedony is the most substantial compound of barren bands and occurs most often in the siliceous-argillaceous and siliceous argillaceous-carbonate bands. In association with opal, it forms a weakly polarized, nearly isotropic mass, often containing carbonate accumulations probably formed contemporaneously with the chalcedony.

Opal is closely associated with chalcedony and in places with chlorite. Opal is found in the chalcedony-rhodochrosite bands. In the chalcedony bands it occurs as either continuous or discontinuous residual accumulations.

Hematite is the most common of the iron minerals in the ores. It occurs as dispersed impregnation which evenly and densely saturates the siliceous-argillaceous-carbonate mass, thus giving it a bright red color. Separate hematite scales are rarely 0.003 mm across and usually are much smaller. Their size increases at the contacts of barren and braunite bands. In places hematite lamellae form lens-like or layered accumulations.

In the upper parts of the manganese bed, near the margin of the iron-ore bed, the amount of hematite gradually increases in the barren bands and forms separate monominerallic hematite layers.

Considerable amounts of clay minerals occur in the ores. They have not been studied. They occur in a fine-grained mixture with chalcedony and fine-grained dolomite. Magnesium-manganese hydrated micas possibly occur among the argillaceous minerals (taking into account the composition of the country rocks). Some sericite occurs in the argillaceous material and forms aggregates of micro flakes and rosette accumulations parallel to the bedding.

Quartz occurs mainly as fragments, veinlets, and in places fine-grained accumulations in the barren bands. The fragments range in size from 0.01 to 0.2 mm and have a weakly rounded shape. In the fine-grained aggregates quartz is closely associated with hematite.

Dolomite occurs as dolomite of chemical origin, clastic dolomite, and dolomite of terrigenous origin. Dolomite of chemical origin occurs as cryptocrystalline fine-grained masses in a fine mixture with chalcedony and other non-metallic minerals. Dolomite is commonly associated with clay minerals. Pelitic dolomite forms separate dolomite layers, usually strongly permeated with hematite dust, which gives them a bright red color. Clastic dolomite is more widely developed. It occurs in considerable amounts in the ore and barren horizons. The rock fragments range widely from .01 mm

INTERNATIONAL GEOLOGY REVIEW

TABLE 1. Chemical composition of manganese ores¹

No.	Type of ores and location of assay		SiO ₂	TiO ₂	Al ₂ O ₃	Fe	Mn	MgO	CaO	BaO
1	Poperechny sector	Braunite	26.45	0.50	5.62	9.02	21.55	4.34	5.47	0.20
2		Braunite-hematite	30.42	n.i.	4.58	15.03	13.90	5.61	5.84	n.i.
3		Hausmannite-rhodochrosite	23.82	0.37	4.59	8.47	20.62	4.62	5.15	0.20
4		Siliceous-rhodochrosite	43.04	0.64	8.94	6.24	17.47	1.67	1.01	n.i.
5		Oxidized pyrolusite psilomelane	28.08	0.68	6.98	16.32	24.45	1.29	1.56	n.i.
6	Banded ore and barren rock	Braunite	10.05	n.i. ²	0.94	1.27	55.15	1.17	1.97	0.44
7		Siliceous-argillaceous-carbonates, enriched with braunite and hematite	48.8	-	12.01	8.40	9.61	3.73	4.81	0.12
8		Siliceous-argillaceous-carbonates, enriched with hematite	52.27	n.i.	12.48	5.57	0.62	5.07	6.92	0.06
9		Siliceous-hematite enriched with braunite	44.17	n.i.	4.58	16.80	8.62	1.28	2.71	n.i.
10		Siliceous-argillaceous enriched with braunite	59.13	n.i.	15.60	9.74	1.08	0.39	0.48	n.i.
11		Siliceous-carbonates enriched with rhodochrosite and hematite	58.42	n.i.	2.61	5.85	9.92	4.62	6.63	n.i.
12		Siliceous-hausmannite in hausmannite-braunite ore	22.35	0.23	3.41	7.11	44.65	0.85	1.00	n.i.
13		Rhodochrosite	2.11	0.08	0.27	0.79	43.42	1.62	3.31	n.i.
14		Hausmannite-rhodochrosite, enriched with silica	9.0	0.25	5.55	10.16	28.43	3.12	3.87	n.i.
		Hausmannite-rhodochrosite, enriched with chalcedony	12.35	-	6.48	6.48	26.87	4.09	5.21	n.i.

TABLE 1. Chemical composition of manganese ores¹ (Concluded)

No.	Type of ores and location of assay		Na ₂ O	K ₂ O	P	S	Co	Ni	H ₂ O	CO ₂
1	Poperechny sector	Braunite	0.95	0.86	0.06	0.05	0.06	0.10	0.98	10.0
2		Braunite-hematite	n.i.	n.i.	0.08	n.i.	n.i.	n.i.	0.30	11.49
3		Hausmannite-rhodochrosite	1.05	0.61	0.07	0.05	0.05	0.10	0.66	20.75
4		Siliceous-rhodochrosite	0.30	1.72	0.10	n.i.	n.i.	n.i.	2.72	13.50
5		Oxidized pyrolusite psilomelane	0.84	0.30	0.14	0.00	0.05	n.i.	6.71	5.96
6	Banded ore and barren rock	Braunite	n.i.	n.i.	0.10	0.13	n.i.	n.i.	n.i.	3.60
7		Siliceous-argillaceous-carbonates, enriched with braunite and hematite	n.i.	n.i.	0.04	0.00	n.i.	n.i.	n.i.	n.i.
8		Siliceous-argillaceous-carbonates, enriched with hematite	n.i.	n.i.	0.04	0.06	0.00	n.i.	n.i.	n.i.
9		Siliceous-hematite enriched with braunite	n.i.	n.i.	0.06	0.01	0.02	n.i.	0.76	2.60
10		Siliceous-argillaceous enriched with braunite	n.i.	n.i.	n.i.	n.i.	0.04	n.i.	n.i.	1.87
11		Siliceous-carbonates enriched with rhodochrosite and hematite	n.i.	n.i.	0.02	0.08	0.00	n.i.	2.25	4.60
12		Siliceous-hausmannite in hausmannite-braunite ore	n.i.	n.i.	0.02	n.i.	n.i.	0.05	0.17	2.15
13		Rhodochrosite	n.i.	n.i.	0.02	0.06	0.04	n.i.	0.24	35.45
14		Hausmannite-rhodochrosite, enriched with silica	n.i.	n.i.	0.23	n.i.	0.02	0.09	0.64	27.08
		Hausmannite-rhodochrosite, enriched with chalcedony	n.i.	n.i.	0.04	n.i.	0.01	0.03	0.09	28.60

¹ The composition of various components is expressed as an average from many tens of analyses.

² n.i. = not identified.

to 10 cm in cross section.

Besides the previously mentioned minerals, the barren bands contain small amounts of actinolite, tremolite, clinozoisite, talc, biotite,

phlogopite, graphite, tourmaline and barite. Pyroxene and feldspar are found in the clastic material. The chemical composition of some barren bands is given in Table 1 (samples 6-10).

The barren siliceous bands have a high iron content according to this table, while manganese varies from 0.62-9.94 percent. It appears that iron silica in ores is associated mainly with barren bands, which always contain much hematite. Thus the ore consists of bands enriched with manganese and bands enriched with iron.

The chemical composition of the braunite ores is given in Table 1 (assay 1).

Spectral analysis has shown the presence of vanadium from tenths to hundredths of one percent, copper, zinc in hundredths and thousandths of one percent. Lead, zirconium, arsenic and gallium are rarer and occur in thousandths of one percent in the ores.

Hausmannite-braunite ores: Braunite is also associated with hausmannite in subordinate amounts of limited occurrence. The ores are banded, with successive bands of braunite along with hausmannite, hausmannite-braunite and siliceous-hausmannite. The hausmannite layers are of various shades of red-brown in contrast with the black braunite layers. The red-brown color of the hausmannite layers is probably due to hausmannite dust. Pure fine-grained hausmannite bands are very rare. In the hausmannite-braunite ore layers, fine-grained hausmannite is usually subordinate in amount to braunite, and is closely intergrown with the latter.

The siliceous-hausmannite layers differ from the rest by their greatly hardness and conchoidal fracture. Hausmannite occurs either as fine dust which is unevenly distributed in the chalcedony, or as discontinuous, irregular, fine-grained wavy bands with distinct margins. Hausmannite grains range from 0.001 to 0.2 mm across. The content of the major components in the siliceous-hausmannite band is given in the Table 1 (assay 11).

The presence of alumina and iron in the siliceous-hausmannite bands indicates the presence of clay and iron bearing minerals. The nature of additional minerals cannot be determined microscopically because of the cryptocrystalline structure of the latter.

The gross composition and external appearance of barren bands in the hausmannite-braunite ores does not differ much from the barren bands in the braunite ores. The hausmannite-braunite ores are also similar chemically to the braunite ores.

Braunite-hematite ores: The braunite-hematite ores contain more iron than manganese. Hematite and braunite form independent ore bands. The iron content of barren bands is greater than that of the braunite ores. Bands in braunite-hematite ores are usually thinner

than in braunite ores, and the barren bands in turn show microscopic banding. The composition of braunite-hematite ores is given in Table 1 (assay 2).

The braunite-hematite ore differs from the braunite ores by higher content of silica, iron, phosphorus, and by lower manganese content.

Oxide-carbonate Ores

Hausmannite-rhodochrosite ores. From 35 to 40 percent of all proven ores belong to the oxide-carbonate hausmannite-rhodochrosite ores. They occur separately and are closely associated with braunite ores. Localized sectors of hausmannite-rhodochrosite ores extend up to several kilometers. Oxide-carbonate ores are mainly developed in the limits of Poperechnyy, Serpukhovo and Stolbukha sectors.

Texturally and superficially the hausmannite-rhodochrosite ores are analogous to the braunite ores and differ from them only in composition and color, being blackish-brown and without a metallic lustre; their powder effervesces in hydrochloric acid. Hausmannite and rhodochrosite are the principal minerals in these layers. Braunite, magnetite, jacobite, mushketovite [8], oligonite (mangano-siderite), siderite, chlorite, tremolite, rhodonite, tephroite, and bementite occur in subordinate amounts. Occasionally, pyrite, chalcopyrite, limonite, and millerite are found. Bornite and marcasite are very rare. Ore bands in which the hausmannite content decreases sharply and rhodochrosite increases, have a dirty pink color with black magnetite or jacobite at the contacts with barren bands. Chalcedony occurs everywhere in considerable amounts in the ore layers, in addition to rhodochrosite and hausmannite. Hausmannite-rhodochrosite ores are magnetic.

Hausmannite is closely intergrown with rhodochrosite, and both form ore bands. In places, the former reaches 70 percent of the total band content.

It is also found in carbonates, as separate grains and clusters, with irregular curving margins. Hausmannite forms small cubic granular inclusions, 0.005 to 0.008 mm in cross section in the barren hausmannite-rhodochrosite bands.

Magnetite forms veins in the carbonate layers. It also occurs as disseminated grains and lenses. The grains have variable shape. Finer grains are irregular while the coarser ones are cubic. Their size varies from 0.01 to 0.07 mm in cross section. Under the microscope magnetite has a red and brownish color which is probably due to manganese (manganous-magnetite).

Manganese carbonates commonly occur as cryptocrystalline bodies and, to a lesser degree, as minute grains dispersed in the barren rock. Their microscopic identification is therefore rendered more difficult. Rhodochrosite and manganosiderite have been identified chemically and with x-rays among manganese carbonates.

Rhodochrosite is the major ore-forming mineral in the carbonate and oxide-carbonate facies. It occurs as uniform fine-grained mass, in close association with other minerals and as small grains, disseminated in the barren siliceous-argillaceous and opal-chalcedony rock. In carbonate ores, rhodochrosite occurs in variable amounts as fine associations with chalcedony and opal, often forming spherulites, pseudo-oolites and unidentified coagulated precipitates. These manganese carbonate precipitates are rather evenly distributed in the opal-chalcedony rock and represent the initial concentration of carbonate that has coagulated together with silica.

In massive bodies, rhodochrosite forms very fine-grained aggregates difficult to identify under the microscope. Their crystalline structure can be determined from the polarization of the aggregates. Pyrite, marcasite, chalcedony, opal and sometimes chlorite are paragenetically associated with rhodochrosite. A chemical analysis of the homogeneous cryptocrystalline rhodochrosite bodies is given in Table 1 (assay 12).

The presence of magnesium and calcium in the rhodochrosite bands is apparently due to isomorphic inclusion of these elements in rhodochrosite. The insufficient amount of CO_2 is possibly attributed to presence of small amounts of silicates or oxides of manganese.

Manganosiderite (oligonite) was mentioned first by P. F. Andruschenko, intergrown with other minerals in weakly manganiferous siliceous-argillaceous-carbonaceous slates. It usually appears as rhombohedral grains, 0.005-0.05 mm in cross section, generally disseminated in barren siliceous-argillaceous rocks. Occasionally it forms clusters 0.1 mm in cross section. In the oxidation zone manganosiderite is replaced by iron and manganese hydroxides.

The chemical composition of hausmannite-rhodochrosite ore bands, high in silica, is given in Table 1 (assay 13-14).

These layers usually contain considerable amounts of silica, iron, clay, and oxides of calcium and magnesium, representing 40 percent of the whole band.

The barren bands in those ores are similar in appearance, and in mineralogical and chem-

ical composition to the barren layers in the braunite ore.

The chemical composition of hausmannite-rhodochrosite ores is given in Table 1 (assay 3). Chemically they are similar to braunite ores. The major difference between the braunite and rhodochrosite-hausmannite ores is that, in the latter, manganese occurs not only as an oxide (hausmannite), but also as a carbonate (rhodochrosite), and therefore the volatile content of the ore increases on the average by 10 percent.

Carbonate Ores

Siliceous-rhodochrosite ores: The major manganese mineral in these ores is rhodochrosite. Sulfides are everywhere present in small amounts (pyrite, chalcopyrite, linneite, millerite, bornite) as well as magnetite. Non-metallic minerals in decreasing order are chalcedony, clay minerals, chlorite and dolomite. This ore can be called chalcedony-rhodochrosite ore.

In the area of the deposits, siliceous-carbonate ores have a limited distribution (in the Poperechnyy, Stolbukha, and Zapadnyy sectors). On the Poperechnyy sector, siliceous-rhodochrosite ores form a bed 1 m thick, along the bottom of the oxides and oxide-carbonate ores, or is separated from them by a bed of dolomitic sandstone 1 m thick. The ore bed wedges out after the first hundred meters, or is replaced by oxide-carbonate ores.

The siliceous-carbonate ore is stratified and dense, like the other ore types, but differs from them by its greenish-gray color. The colors are successively arrayed in bands of greenish-gray, brownish-gray, pinkish-gray, and dark gray. The ore bands are 0.3 to 2 cm thick. A characteristic feature of the siliceous-carbonate ores is their constant association with sulfides in the form of small grains or veinlets.

Usually, the brownish light-gray and pinkish-gray bands are entirely composed of cryptocrystalline rhodochrosite. The crystalline structure of the latter is apparent from the polarization of the aggregates. Chlorite and opal are present, in insignificant amounts, filling the interstices between the rhodochrosite aggregates. The structure of these interstices is cryptocrystalline, fine-grained, concretionary, and more rarely, spherulitic, and oolitic. Their manganese content is up to 43.42 percent, iron 0.79 percent, silica 2.11 percent, and phosphorus 0.12 percent.

Bands with a brown tinge are composed of 30 to 60 percent very fine-grained rhodochrosite and of 40 to 70 percent chalcedony and opal, chlorite, ferruginous concretions, clay minerals, sulfides, fragments of dolomite and

quartz. The manganese content in these bands is 26-27 percent, iron 5-7 percent, silica 30-35 percent, phosphorus 0.1 percent. In certain cases the bands have many dolomitic fragments.

The dark-gray and greenish-gray bands are siliceous-argillaceous material with weak polarization. Some siliceous-argillaceous bands contain a significant amount of fine chlorite flakes and magnetite powder. Chlorite and chlorite-opal bands are seldom found. The siliceous-argillaceous bands are composed of up to 18 percent iron and 1-2 percent manganese. The rhodochrosite and chalcedony bands are subordinate to the siliceous-argillaceous bands, the latter making 70-80 percent of the total ore volume.

The content of major components in siliceous-rhodochrosite ores is given in Table 1 (assay 4).

Ores of the Oxidized Zone (secondary)

Pyrolusite-psilomelane Ores

The oxidized ores are uncommon in the deposit and make about 3 percent of the total ores. They form the near-surface part of the ore beds to a depth of about 5-10 m. They do not penetrate deeper than 25-30 m from the surface.

These ores differ mineralogically from the above mentioned bedded primary ores. Their major minerals, manganese and iron hydroxides, were formed by the oxidation and hydration of manganese minerals and primary ores.

The barren parts were also subjected to alteration, which consisted mainly of leaching of carbonates, manganese enrichment, etc. A certain enrichment in manganese is observed due to the partial leaching and washing away of nonmetallic material. The ore texture and structure has been altered, the primary banding destroyed, and the ores become of concretionary, nodular, botryoidal, and stalactitic structure. The physical state of ores has been altered in the oxidation zone. Basically these ores remain rather hard, whereas the barren material becomes claylike, due to weathering. The major oxidized ores (psilomelane, pyrolusite and limonite) form massive secretions in the form of colloidal, radial veinlets, concretions, crusts and films. The nonmetallic part has been strongly colored by manganese and iron hydroxides, giving a false appearance of strong mineralization. In sectors where primary structure has been somewhat preserved the barren bands are nearly totally replaced by psilomelane and pyrolusite. The following minerals were identified microscopically in oxidized ores: (in decreasing order) psilomelane, hydrogoethite, pyrolusite and vernadite (by oxidation of manganese carbonate). Rel-

ict minerals are braunite, hematite, magnetite and rhodochrosite. The nonmetallic minerals are chalcedony, clay minerals, dolomite and calcite.

Psilomelane: is the dominant manganese mineral of the near-surface oxidized parts of ore beds. It is found sporadically, at greater depths, in fault zones. Usually it forms thin veinlets, 0.02-1.0 mm thick, which randomly criss-cross the numerous ore types. The accumulation of such veinlets produces characteristic network structures. Small inclusions of irregular shape, 0.001-0.4 mm in cross section, are also found. Veins and inclusions are often found in the same sectors. Psilomelane also forms accumulations, small irregular masses, 0.2-5 mm or more across. In such secretions pyrolusite lines small geodes, as well as accumulations of nonmetallic matter. Psilomelane is commonly found in the form of colloidal, rhythmically zoned botryoidal structures on the walls of geodes and fractures. Usually the colloform accumulations are closely associated with iron hydroxides and non-metallic minerals. Continuous psilomelane ore bands are formed as replacements of primary braunite, hausmannite-carbonate and rhodochrosite layers. Powdered psilomelane varieties are very rarely found. Crusts, coatings, and dendrites of psilomelane are well developed on the walls of fractures and bedding surfaces. Pseudomorphs of iron hydroxides and manganese hydroxides are found after small bands of manganese carbonate. The exogenetic formation of psilomelane is accompanied by a fine pigmentation of the nonmetallic part of the manganese hydroxide, giving a false impression of strong mineralization.

Pyrolusite occurs in the oxidized ores in limited amounts in close association with psilomelane. It forms radial and grainy aggregates in the central portions of psilomelane veinlets. Sometimes it forms large elongated flaky crystals with a characteristic transverse striation. Amorphous powdery varieties of pyrolusite are found along with crystalline ones.

Powdered brownish-yellow varieties of manganese hydroxides are found in some cases replacing manganese carbonates, which possibly represent accumulations of the hydrous dioxide, the manganous vernadite.

Iron hydroxides everywhere occur in close association with manganese hydroxides.

Goethite often occurs with manganese hydroxides. It forms radial, needle-like crystal growths in the nonmetallic material. Colloidal goethite is found in fractures filled with psilomelane. In places it forms crusts on rhombohedral carbonate grains.

Hydrogoethite is formed together with goethite

in the oxidized ores, in stalactitic and kidney-shaped forms on walls of geodes and on thin psilomelane veinlets. In places it forms pseudomorphs after pyrite and carbonate rhombohedra. The chemical composition of the oxidized ores is presented in Table 1 (assay 4).

The characteristic feature of the chemical composition of the oxidized ores is their higher content of manganese (average 24 percent) and water (6-7 percent), and their lower content of CO₂, calcium and magnesium carbonates, relative to the content of the same component in the primary ores.

Semioxidized Ores

Like the oxidized pyrolusite-psilomelane ores, the semioxidized ores have a limited distribution and are localized in the upper part of the manganiferous bed. Mineralogically, texturally and structurally they represent intermediate varieties between the primary and oxidized ores. These ores are dense despite the fact that lamination (fractures between the bands) is widely developed in them. On impact, they break into plates along the bedding planes. The banding is still preserved, in spite of considerable obliteration due to oxidation processes. Their mineral composition depends on the mineral composition of the primary ores. Besides the newly formed minerals, the primary minerals are present in various amounts.

The secondary alterations in semioxidized ores are shown by veinlets, films, and coatings formed by psilomelane and iron hydroxides. The ore bands are partially or totally replaced by psilomelane, which masks the shape and contacts between the ore and barren bands. Chemically and technologically, the semioxidized ores are similar to the primary ores.

Thus, the ores of different mineralogical composition in the South Khingan deposit are similar to each other from the chemical point of view.

SOME REMARKS ON ORE GENESIS

The manganese ores are of sedimentary origin, considerably altered by metamorphic processes. Their sedimentary origin is indicated by the bedded nature of the ores, conformity with the country rocks, and restriction to a certain stratigraphic horizon. The metamorphic effects are indicated by the complex of minerals in ores and country rocks. The deposition of the ore-bearing series occurred during the initial transgressive stage, and was confined to the beginning of the last cycles of sedimentation in the district. The shallow water and littoral nature of the rocks enclosing the manganese ores, the existence of local contemporary erosion (intraformational breccia) and even temporary dessication (mud

cracks in the ore horizon) indicate that the formation of manganese ores occurred near the coast, and shallows, and in quiet closed bays (thin banding of rocks and slight rounding of fragments). Lithologic studies of the ore-bearing series of the South Khingan deposit indicate that coarse sediments developed in the western part of the deposit, such as sedimentary breccia, sandstone, and siltstones, while the eastern part is dominated by fine argillaceous and chemical carbonate sediments. This regularity is characteristic for Malyy Khingan, and allows the assertion that the coast line of the sedimentary ore basin was located to the west of the present location of the ore-bearing series. The proximity of the shoreline to the western zones is confirmed by the abrupt facies changes, which are characteristic of coastal zones (see fig. 4). Besides, in the central and eastern ore zones the facies are more stable, indicating their greater distance from the shore.

Thus, the most intensive ore deposition in the Amur River sector of Malyy Khingan took place near the coast and decreased seawards. This corresponds to the general principles which have been determined by A. G. Betekhtin [2] for a group of manganese deposits.

The manganese bedded ore consists of alternating bands considerably enriched with manganese and slightly enriched in iron, indicating the existence of two different facies, differing in nature and separated in time, i.e., the ferruginous and the manganiferous facies. Also, while the manganese content is, in this particular case, 200-250 times greater than its clarke, iron is only 2-3 times more than its clarke. Therefore conditions were more favorable to the concentration of manganese. Later, conditions changed in favor of iron, increasing to 7-8 times its clarke (during the formation of the ferruginous bed). At this time manganese deposition was almost entirely completed. The facies conditions of iron and manganese deposition were similar.

Therefore the deposition of manganese ore in Malyy Khingan was closely associated with and preceded that of iron. This is possibly due to the greater mobility of manganese on the continent where it was derived. Due to its mobility it could have been brought from the continent earlier than iron.

Weathering of sedimentary and igneous rocks of the Amur-Zeya swell in the Sinian platform to the west of the ore deposit, could have formed the source of the manganese, iron and silica. There is no evidence of igneous activity either in the deposits or in adjacent areas, with which one could link the origin of manganese, iron and silica during this geological period.

The minerals forming the ore horizon can be

divided into three groups.

1. Primary sedimentary or those formed during the diagenesis of primary sediments which were not subjected to any serious further changes, except the recrystallization of carbonates.

This group can be subdivided into two subgroups:

a) minerals forming the clastic material (quartz, dolomite, feldspar, calcite, pyroxene, etc.)

b) minerals of a chemical-biogenetic origin (rhodochrosite, oligonite, dolomite, clay minerals, chalcedony, opal, carbonaceous matter, etc.)

2. Minerals formed as the result of regional metamorphism: braunite, hausmannite, hematite, magnetite, sericite, chlorite, rhodonite, bustamite, tephroite, tremolite, actinolite, tourmaline, biotite, etc.

3. Minerals formed during weathering of ores in the oxidation zone: psilomelane, pyrolusite, martite, hydrogoethite, limonite, vernadite, etc.

The presence of those mineral associations indicates that the deposit is of sedimentary-metamorphic origin. The primary ore sediments were probably represented by iron and manganese hydroxides and carbonates that were dehydrated and recrystallized during regional metamorphism, and resulted in formation of braunite, hematite, hausmannite, magnetite, rhodochrosite, and oligonite (manganosiderite).

It is necessary to indicate that the Cambrian manganese ores of Malyy Khingan are genetically and structurally similar to the Devonian manganese ores of Central Kazakhstan. The manganese ores and the overlying banded ferruginous quartzite are also similar to the manganese ores and jaspilites of the Morro do Urukum in Brazil, considered to be Cambrian-Ordovician by Brazilian geologists [4].

TECHNOLOGY AND PRACTICAL VALUE OF THE MANGANESE ORES

The South Khingan manganese ores are low-grade, highly siliceous and high in iron. However, they are low in phosphorus. For every 1 percent manganese there is 0.003-0.005 percent phosphorus. The best ores are braunite and hausmannite-rhodochrosite, making the major part of all proven deposits.

In accordance with technical requirements for manganese ores, the ores from Poperechnyy, Serpukhov and Stolbukha sectors are of the

3rd grade, suitable as an alloying addition to the charge, and when necessary the smelting of spiegeleisen and silicon spiegeleisen. After treatment the ores yield a better product. The banded nature of the ores creates favorable conditions for their effective beneficiation. Experiments made by Uralsmekhanobr with the beneficiation of manganese ores, showed possibilities for obtaining concentrates used in the manufacture of ferromanganese. The institute developed three methods of ore treatment.

1. Separation of ores of the 2.5 to 2 mm fraction in heavy media with successive magnetic separation in the strong 2 mm field, and washing of the products of gravitational separation.

2. Magnetic separation in strong field of all the ore crushed up to 2 mm.

3. Roasting and magnetic separation of the ore crushed to 0.6 mm or less.

These methods make it possible to obtain all types of manganese concentrates, depending on the quality and grades of ore, and beginning from grade III, containing 30-35 percent manganese, and ending with grade IA containing more than 50 percent manganese. The latter is used for smelting standard ferromanganese. The manganese ore of South Khingan produces a strong agglomerate for metallurgical use.

The good results obtained during the treatment of the manganese ores and their abundance in Malyy Khingan thus constitutes material which can satisfy the metallurgical needs of the area east of Lake Biakal, particularly since, up to now, there have been no other known large manganese deposits in that territory.

CONCLUSIONS

As a result of studies on the manganese ores of South Khingan, the following conclusions can be made.

1) The manganese ores are confined to the base of the ferruginous quartzite ore horizon, which is located in the middle part of the Lower Cambrian ore-bearing series. The latter lies transgressively, but without an apparent discordance, on the eroded surface of dolomites of the Mirandava series of the Upper Sinian.

2) The manganese ores are paragenetically associated with banded ferruginous quartzites and siliceous-argillaceous slates, which contain variable amounts of dolomite of chemical origin and of terrigenous dolomite.

3) Structurally, the manganese ores are similar to the widespread banded ferruginous quartzites (jaspilites). The banded ore structure is due to the rhythmic succession of ore and barren bands that are on average 1 cm

in thickness.

4) The essential mineral components of ore bodies are: braunite, hematite, hausmannite, magnetite, rhodochrosite, chalcedony, quartz, clay minerals and dolomite. The major minerals forming the ore bands are: braunite, hausmannite, and rhodochrosite. Barren material is composed of the other minerals.

5) Mineralogically, the following ore types are distinguished: braunite and its varieties (hausmannite-braunite and braunite-hematite); hausmannite-rhodochrosite and siliceous rhodochrosite. These minerals characterize definite facies. Braunite ores characterize the oxide facies, hausmannite-rhodochrosite characterize the oxide-carbonate facies, and the siliceous-rhodochrosite ores characterize the protoxide-carbonate facies. Pyrolusite psilomelane ores are found in the oxidized zone, formed by the oxidation and hydration of the above three types.

6) The South Khingan deposit is characterized by the abrupt change in ore facies and their gradation into each other in the transitive zones. The outlines of facies margins are complex.

7) The formation of manganese ores began soon after transgression, and preceded the formation of iron ores. Deposition took place in the coastal, shallow part of the shelf under quiet conditions.

8) The coast line of the ancient Lower Cambrian basin-bay, where manganese ores were deposited, was located somewhere to the west of the western zone.

9) The economic manganese ores are concentrated along the coastal line, in a limited 10 km strip, in the sectors of Poperechnyy, Serpukhovskiy and Stolbukha (see fig. 2). This indicates that the influx of manganese from the continent took place via one channel.

10) In iron ores there is only one oxide facies in which magnetite and hematite facies are identified. The magnetite facies is confined to the coastal and shallow water part of the basin, while the hematite is restricted to the deeper and central part.

In a western direction, slate and breccias appear within the iron horizon, closer to the coast line. They nearly totally displace the

ferruginous-microquartzites. Also in the western sector there is a wedge-out of the iron quartzite facies.

11) The economic reserves of manganese ores in the South Khingan deposit consist of layered braunite and hausmannite-rhodochrosite ore varieties amounting to about nine million tons. To the present time in Malyy Khingan, one other deposit, the Bidzhan, has been explored. It is located about 80 km north of the South Khingan deposit and its reserves are about four million tons of ore.

The ore reserves in both deposits total about 13 million tons. This amount of ore and the possibility of obtaining ferromanganese products from them permits classification of the Malyy Khingan deposit as one of the major economic ore regions in the Amur basin. This is supported by economic deposits in Malyy Khingan of iron, magnesite, graphite, flux materials and other minerals that are necessary for the creation of a large metallurgical industry.

REFERENCES

1. Andruschchenko, P. F., MINERALOGIYA MARGANTSEVKH RUD POLUNOCHNOGO MESTOROZHDENIYA [MINERALOGY OF MANGANESE ORES OF POLUNOCHNOYE DEPOSIT]: Trudy I. N. G. issue 150, Seriya Rudnykh Mestorozhdenii [Ore Deposit Series], (no. 16) Akad. Nauk, SSSR, 1954.
2. Betekhtin, A. G., PROMSHLENIYE MARGANSTSEVYE I RUD SSSR [INDUSTRIAL MANGANESE ORES OF THE U. S. S. R.]: Akad. Nauk, SSSR, 1946.
3. Goretsky, Yu. K., OB VSLOVIYAKH FORMIROVANIYA I NEKOTORKH ZAKONOMERNOSTYAKH V RAZMESHCHENII OSADOCHNKH I OSADOCHNO-METAMORFIZOVANIKH MESTOROZHDENII [CONDITIONS OF FORMATION AND SOME PECULIARITIES IN THE DISTRIBUTION OF SEDIMENTARY AND SEDIMENTARY-METAMORPHIC ORE DEPOSITS]: Akad. Nauk, SSSR, Geological Series, no. 1, 1954.
4. Shatsky, N. S., O MARGANTSEVONOSNKH FORMATSIYAKH I O METALLOGENII MARGANTSA [THE MANGANESE BEARING FORMATIONS AND METALLOGENY OF MANGANESE]: Akad. Nauk, SSSR, Geological series, no. 4, 1954.

USE OF DIFFERENTIAL GAMMA SPECTROMETRY IN PETROLEUM GEOLOGY¹

by

G.A. Nedostup, F.N. Prokofiev, A.I. Kholin and E.P. Tsitovich

translated by Henry Faul

ABSTRACT

Spectral analysis of gamma radiation arising from entrapment of neutrons by the nuclei of elements in rocks is one of the most favorable areas for development of radiometry of wells. The presence of sharp maxima in the spectra of the principal rock-forming elements (Si, Ca, H, Cl, and others) presents the possibility not only of a qualitative but also of a quantitative estimate of their content in the rocks. Laboratory investigations were carried out to evaluate this method. A 1-meter by 1-meter by 1.3-meter model was filled with sand, which was first saturated with fresh water and then with water comparable to formation water. The results were presented on a graph. The curves of a secondary gamma radiation for both water types have peaks characteristic of hydrogen, silicon and chlorine. This method appears to be particularly useful for determination of the composition of the liquid in reservoir rocks.

A schematic diagram of the borehole instrument is given, and the function of the various components is described. The instrument was tested in the Tuymazy oil field. The secondary gamma spectra of water-bearing sand, oil-bearing sand, and of cement-filled caves were measured. The results agree essentially with those obtained with the model. The potential of this method is estimated as very high, particularly for determination of the nature of the fluids in the rock. -- J. W. Clarke, *Geophysical Abstracts*, 180.

INTRODUCTION

Spectral analysis of the gamma radiation that is produced in capture of neutrons by nuclei of [the elements that compose] a rock, is one of the most promising endeavors in the exploration of oil wells by nuclear methods. The presence of sharp maxima in the [neutron-capture gamma-ray] spectra of the major rock-forming elements (Si, Ca, H, Cl, and others) permits us to anticipate not only the possibility of qualitative determination of these elements, but also the possibility of their quantitative estimation (of these elements). These procedures would permit the solution of a basic problem in logging geophysics - the clear identification of the rock traversed by the bore hole.

The unusual complexity of the solution of the basic problem is evident. The principal difficulty in the individual identification of the rock-forming elements by the analysis of secondary gamma-ray spectra is caused by the superposition of the spectra of many elements. Another difficulty arises from the fact that the radiation must first pass through the rock before it is detected in the hole. The result is a leveling of the spectrum of the measured radiation with an increase in the intensity on the low-energy end.

In order to clarify the suitability of secondary gamma-ray spectrometry for the study of drill holes, laboratory experiments were first undertaken and later followed by investigations in the field.

LABORATORY EXPERIMENTS

To confirm the effectiveness of differential gamma-ray spectrometry in the laboratory, experiments with a model were undertaken. The dimensions of the model (1 x 1 x 1.3 meters), made of sand with a porosity of 40 percent, were sufficient to consider it as an infinite medium.

The gamma radiation was detected with a CsI crystal and the resulting light pulses were converted into voltage pulses by a photomultiplier [scintillation counter] (type FEU-1C). The amplitude of the resulting pulses was determined by the anode resistor of the photomultiplier and was a function of the energy of the registered gamma radiation. The multiplier had a gain of about 2.5×10^6 . The multiplier and the cathode follower were supplied from a stabilized high-voltage supply (models BC-9 and BC-12). The voltage distribution on the dynodes of the multiplier was selected to assure good working stability of the multiplier for long periods of time (12-18 hours).

Fluctuations in the high voltage of ± 25 volts caused a change in the amplitude of the pulses of 1-2 percent. From the cathode follower the pulses passed to an amplifier in which they were ampli-

¹Translated from *Ispolzovaniye differentsialnoy gamma-spektometrii v neftiyanoy geologii: Prikladnaya Geofizika*, no. 23, p. 193-201, 1959.

fied to the point where their greatest amplitude would be about 90-100 volts. The gain was adjustable between the limits 0-1500. From the amplifier the pulses were fed into an amplitude analyzer essentially described in reference 3 [Fairstein].

The analyzer permits pulse-height analysis of the incoming pulses in the range of 0-100 volts in one-volt steps and with a gate width of 1, 2, 4, 8, or 10 volts. The pulses are counted with the conventional counting apparatus, type B-2.

The apparatus was tuned in the following way: Stability of operation of the circuits was tested without the crystal, and they were then calibrated and their linearity verified with a cobalt-60 source. First, the photomultiplier was placed in a light-proof box with a diaphragm in front of which was mounted a neon lamp of the type MH-3, acting as a source of light pulses. Curves were then plotted

of the relation of the number of pulses to the number of the channel (pulse-height). The measurements were repeated several times and gave good reproducibility. The whole apparatus was then calibrated with cobalt-60. The scale of energy, E , was calibrated by comparison with the peak at 1.33 Mev.

When working on the model, the voltage on the multiplier was set in such a way that the greatest amplitude of the recorded pulses was of the same order as the maximum obtained with cobalt-60. In that way linear operation of the circuits was assured. The scale was then calibrated again with cobalt-60 and with a polonium-beryllium source.

The results obtained with the model are shown in Figure 1. The calibration curve obtained with the Po-Be source is also shown there, con-

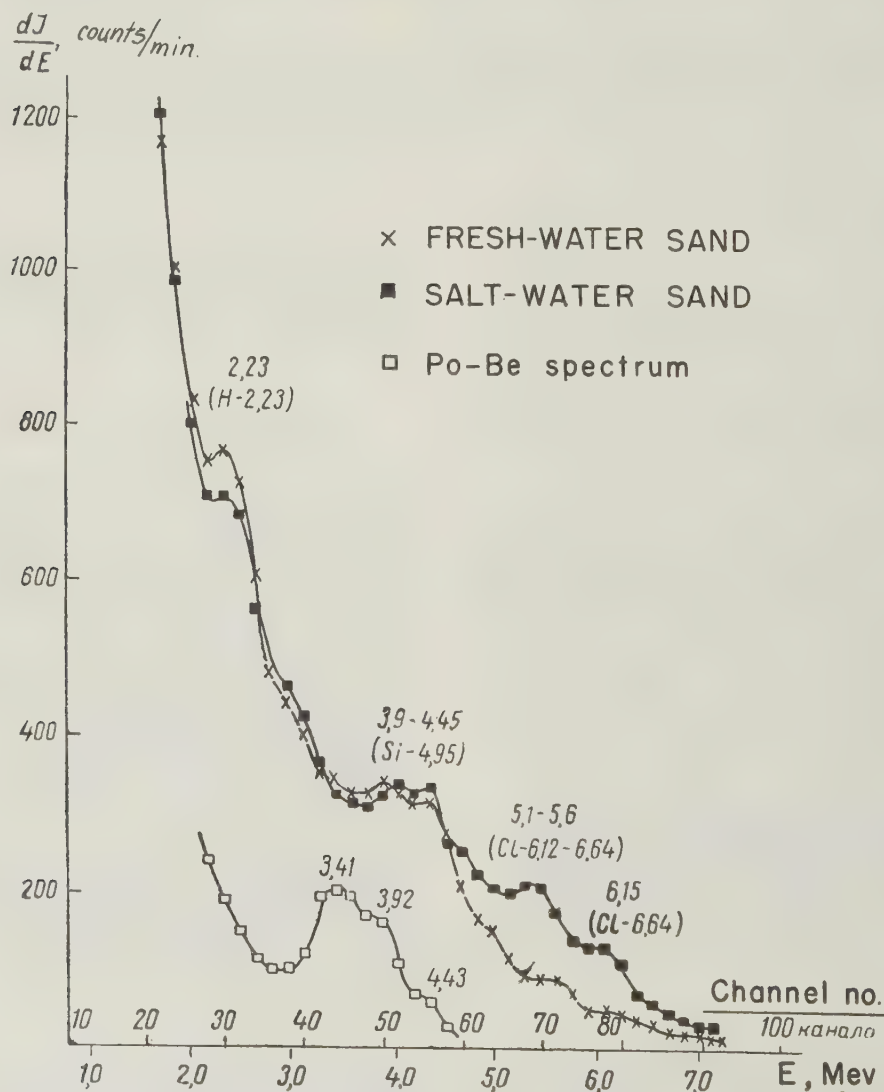


FIGURE 1. Spectra obtained with models in fresh-water sand, with salt-water sand, and with the polonium-beryllium source

taining the gamma-ray line at 4.43 Mev.

The model was made of sand saturated with fresh water (to simulate an oil-bearing sand) and of sand with mineralized water (to simulate a water-bearing sand).

As shown in Figure 1, the character and general shape of the two curves remains the same up to an energy of 4.5 Mev. Both curves show a maximum at 2.23 Mev. corresponding to the energy of the radiation emitted in the radiative capture of neutrons by hydrogen, and both indicate the line of silicon in the range 3.9-4.45 Mev which corresponds to the neutron-gamma radiation of silicon at 4.95 Mev. The upper part of the curves is different for the "fresh water" and "salt water" sands, which is caused by the presence in the "salt water" sand of chlorine, which has a higher neutron capture cross-section and thus gives a higher radiation intensity at the energy values of 6.12 and 6.64 Mev.

It can be seen from the curves that the spectrum of the "salt-water" sand shows maxima in the region 5.1-5.6 Mev and at 6.15 Mev, as a result of the Compton effect and pair production for these lines.

The model experiments confirmed the pre-supposition that differential spectrometry of neutron-capture gamma radiation is particularly useful for the solution of such problems as the determination of the liquid contained in the reservoir rock. The positive results of the laboratory studies provided the basis for the execution of experiments under the more complex conditions in the field.

APPARATUS FOR FIELD STUDIES

Conditions in the field differ from those in the laboratory primarily in the considerable distance (up to 5,000-10,000 feet) of the beds to be studied from the recording equipment at the surface. The deep-well detector, enclosed in a hermetically sealed metal shell, is lowered into the well and is connected with the surface equipment by a single-wire or, more frequently, a three-wire cable. The presence of a long cable in the detector-recorder circuit greatly complicates the recording of pulses which decay in shape and amplitude as they pass through the cable. This distortion is a function of the capacitance of the conductors of the cable to the earth, which varies for various types of cable from 0.2 to 0.5 microfarads, depending on the length.

Under field conditions one may study the spectra in two different ways: first, analysis of the spectra on the surface under optimum conditions of pulse transmission through the cable (without pulse attenuation), or second, measurement of the spectra in the deep-well probe by means of an automatically photo-recording apparatus.

The circuit diagram of a probe that passes

individual pulses up the cable is shown in Figure 2. In this equipment, a cesium iodide crystal is the detector with a type FEU-29 photomultiplier. The pulses from the anode resistor of the FEU-29 are amplified by tube L_2 .

Positive pulses from the plate of L_2 pass through the diode L_3 and charge the capacitor C_8 . The charge on C_8 is then proportional to the amplitude of the incoming pulses. The discharge of the capacitor passes through the diode L_4 as soon as the potential of the cathode of L_4 reaches zero. This discharge continues for a time t_p , determined by the circuit constants of the univibrator that consists of tubes L_7 and L_8 , and is triggered by the pulses to be measured. The rectangular pulses from the univibrator are differentiated by $R_{23}C_9$ and negative signals shut off tube L_5 by reducing the potential of its cathode to zero, whereupon the capacitor C_8 also discharges.

The choice of time constant t_p is based on the following considerations: the presence of the cable joining the probe to the surface recording equipment, which is equivalent to a loading of the probe output by a capacity of about 0.5 mfd. Such a capacity delays the rise and fall of the pulses and the time of this decay (the rise time to maximum amplitude) $t_d = R_{out} C_{cable}$ where R_{out} is the output resistance of the probe and C_{cable} is the equivalent capacity of the cable. It follows that R_{out} must not be large. A cathode follower is used in the circuit, consisting of L_9 . Its load consists of two resistances. The signal is taken from the smaller resistance $R_{out} = R_{37}$. The choice of R_{out} is based on the desire to receive pulses of maximum amplitude of the order of 1-2 volts, which for our circuit occurs at $R_{out} = 60$ ohms. Thus $t_d = 60 \text{ ohms} \times 0.5 \text{ mfd} = 30$ microseconds.

The essential requirement for transmission of pulses over the cable without loss of amplitude is that t_d be smaller than t_p , and with such delay time the pulses will retain their maximal amplitude. In our circuit t_p was chosen to equal 80 microseconds.

It follows that such a time delay will reduce the resolution of the probe circuit to about 10^4 equally-spaced pulses per second, or to about 10^3 pulses per second with a random input. The probe input intensity is essentially determined by the strength of the neutron source and by the spacing between the source and the detector (the length of the probe). Normally one uses polonium-beryllium sources of about 5-10 curies and a spacing of about 50-60 cm; the maximum input rate is then about 200 pulses per second and allows the apparatus sufficient resolution to assure its reliable operation.

The probe is attached to a three-wire cable, two wires of which are used to supply the power

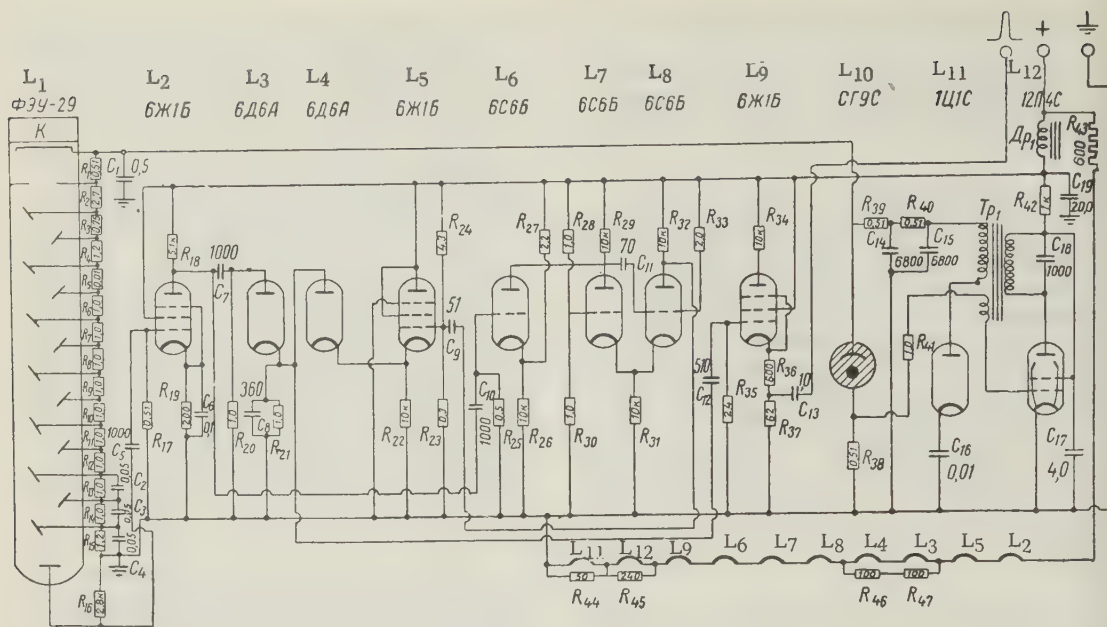


FIGURE 2. Schematic diagram of the probe circuit

(200 volts at 235 ma) and the third to transmit the signal to the surface.

The control of the operation of the probe is accomplished at the surface by monitoring the maximum amplitude of the received pulses. The amplitude of pulses from gamma quanta of maximum energy prior to the lowering of the probe into the well is regulated by the anode potential of the photomultiplier and may not exceed 1.2 volts so that the probe circuit operates linearly in this case, and the amplitude of the transmitted pulses is proportional to the amplitude of the pulses originating in the photomultiplier.

On the surface, the pulses are amplified and fed into an amplitude analyzer.

LOGGING FIELD STUDIES

The objective of the logging studies was the appraisal of the utility of gamma spectrometry and the evaluation of the suitability of the above mentioned apparatus for the study of the spectra of various rock layers. The secondary gamma-ray spectra of three materials were measured: water-bearing sand, oil-bearing sand and cement-filled cave (the essential components of the cement were CaO-65 percent, SiO₂-20 percent). The study took place in one of the wells of the Tuymazy field. The results of the measurements are shown in Figure 3.

The scale of energy values is calibrated with a polonium-beryllium source, emitting, as we have already mentioned, the characteristic gamma radiation with the energy E=4.43 Mev with peaks at 3.92 and 3.41 Mev, corresponding

to the Compton interaction of the gamma-ray with the CsI crystal and the production of electron-position pairs.

A single-channel differential pulse-height analyzer with a channel width of IV was used in the measurements. The range of measured amplitudes was 20-90 V. The resolution of the spectrometer for the greater part of the observations was 10-12 percent from the lines of the gamma-radiation of Co⁶⁰ (1.33 Mev).

The results of the logging studies essentially agree with the results obtained with the models. The differences in the curves of $dI/dE=f(E)$ can be explained by some difference in the mineralogical composition of the sands used in the laboratory and the producing sandstones of the Tuymazy field and also by the differences in porosity of the rocks and composition of the liquids saturating these sands and sandstones. It follows from the results of the logging studies that characteristic differences in the intensity of neutron gamma-radiation from the rocks studied fall into the hard part of the spectrum (3-7 Mev). In addition, barely resolved peaks were observed for all three media in the region of 2.2 Mev, corresponding to the radiative capture of neutrons by hydrogen (2.23 Mev).

As could be expected, the curve $dI/dE=f(E)$ for the water-bearing rock is higher than the curves for the oil-bearing rock and the cement, which is explained primarily by the different Cl content in these rocks. As is known, the principal lines of chlorine have the energies 6.12, 6.64, and 7.41 Mev. They also determine the character of the spectrum of the water-

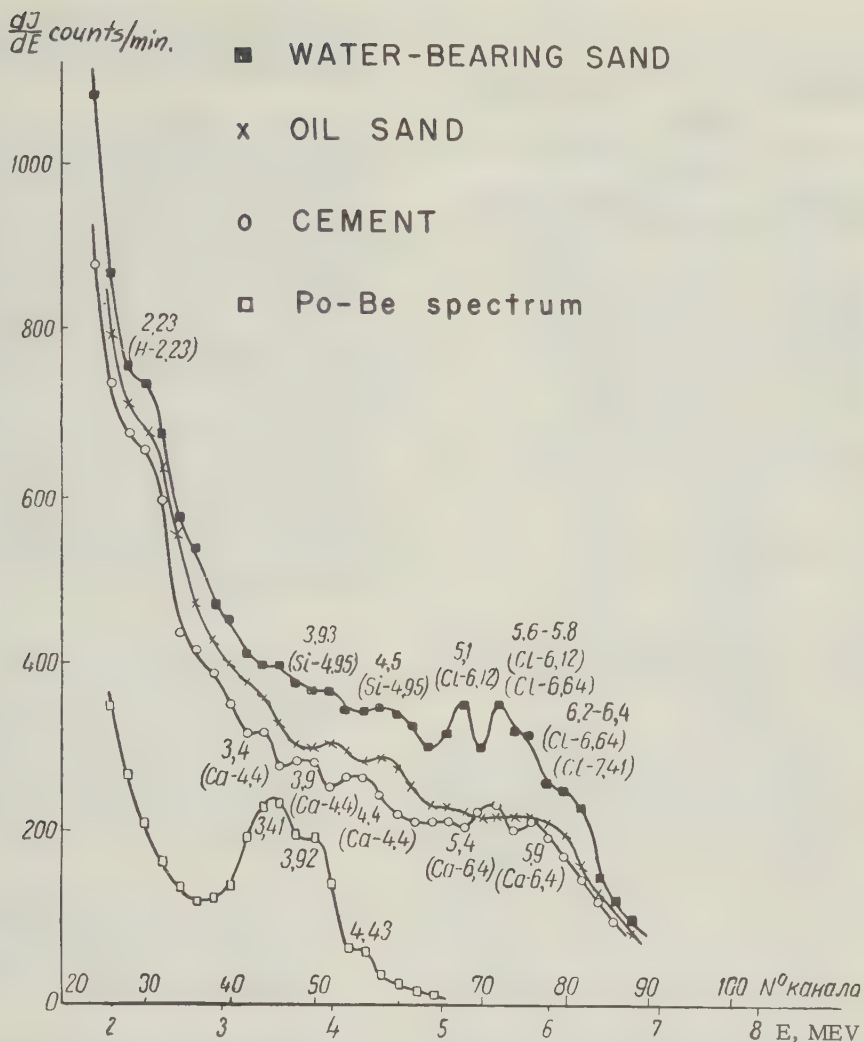


FIGURE 3. Spectra obtained in the well in water-bearing sandstone, oil-bearing sandstone cement-filled cave, and from the polonium-beryllium source

bearing rock. The clearly defined peaks in the regions of 5.1 and 5.6 Mev correspond to the energy 6.12 Mev (pair production) and to the energies 6.12 (Compton effect) and 6.64 (pair production) respectively. The less clearly resolved peak in the part of the curve between 6.1 and 6.4 Mev corresponds to the energies 6.64 Mev (Compton effect) and 7.41 Mev (pair production). On the same curve are clearly seen the peaks of silicon, 3.9 and 4.5 Mev corresponding to the Compton effect and pair production for the silicon gamma quanta of the energy 4.95 Mev.

The spectrum of the oil-bearing sandstone does not have characteristic peaks. Only the peaks of silicon stand out, analogous to those for the water-bearing rock.

In the spectrum of the cement, the calcium

line stands out. Two maxima correspond to the 6.4 Mev energy of the gamma-radiation of calcium: pair production - 5.4 Mev and Compton effect - 5.9 Mev. The calcium line at 4.4 Mev is recorded in three peaks at 3.4, 3.9 and 4.4 Mev.

The results of these studies show the unquestioned utility of inhole gamma-ray spectrometry. On the basis of the results obtained, one may already imagine ways of improving the effectiveness of solving such important problems of the petroleum industry as the determination of the fluid that saturates the reservoir rock. The spectral curves obtained offer the possibility of selecting optimum conditions for additional similar researches. The greatest differences between the spectral curves of oil-bearing and water-bearing strata are seen in the energy range 5-6 Mev. It is clear that the analysis of

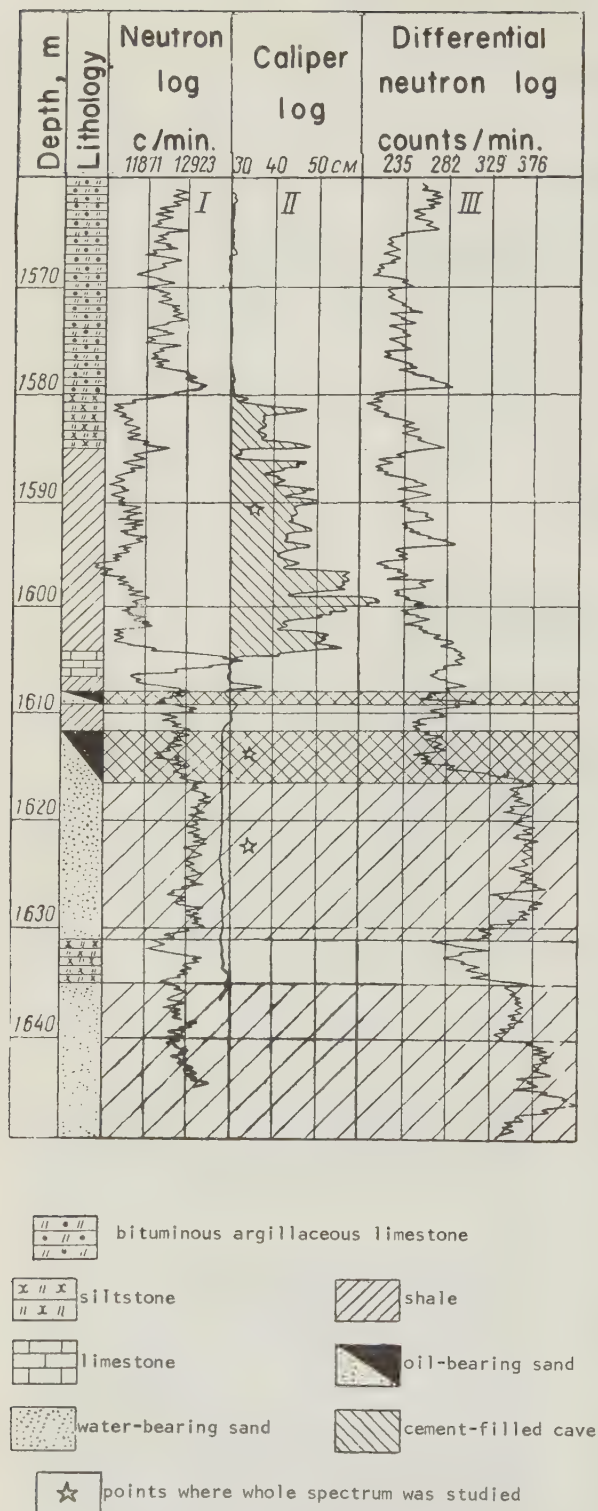


FIGURE 4. Neutron-gamma ray logs

the radiation only in this energy band would still give the essential criteria of difference between these two rocks.

A continuous neutron-gamma ray log of the energy interval 4.7 to 5.5 Mev was run in addition to these experiments and in the same hole in which took place the described series of measurements in the oil-bearing part of the section (see fig. 4, curve III). A standard neutron-gamma log, recording the intensity of all radiations was also run there (fig. 4, curve I). The stars (legend fig. 4, box 7) show the places where the stationary measurements shown in Fig. 3 were made.

One can see from the curves in Fig. 4 that the recording of gamma-radiation in the selected energy interval increases the measurable difference of gamma-ray intensity from oil-bearing and water-bearing strata from 6 to 38 percent, or by more than a factor of 6.

REFERENCES

1. Baranov, V. N., and Kuzmina, L. A., IONIVY METOD OPREDELENIYA VOZRASTA MORSKIKH ILOV [AN IONIUM METHOD OF AGE DETERMINATION FOR SEA BOTTOM SEDIMENT]: Doklady Akademii Nauk, SSSR, Nov. Ser., v. 97, no. 3, 1954.
2. Bressler, S. E., RADIOAKTIVNYE ELEMENTY [THE RADIOACTIVE ELEMENTS]: State Engineering Theory Publishing House, Moscow and Leningrad, 1952.
3. BYULLETEN KOMISSII PO OPREDELENIYU ABSOLYUTNOGO VOZRASTA GEOLOGICHESKIKH FORMATSII [BULLETIN OF THE COMMISSION OF THE ABSOLUTE AGE OF GEOLOGIC FORMATIONS]: Report no. 1, Akademii Nauk SSSR, Moscow, 1955.
4. Kurbatov, I. D., O SOOTNOSHENIYAKH AKTIVNYKH ELEMENTOV V DISPERSNYKH MASSAKH TYUYA-MUYUNA [RELATIONSHIPS AMONG ACTIVE ELEMENTS IN DISPERSE COMPLEXES OF THE TYUYA-MUYUN]: Doklady Akademii Nauk, SSSR., no. 17, 1930.
5. Kurbatov, I. D., Karzhauvina, N. A., and Samoilov, N. A., OPISANIYE METODA PRIGOTOV-LENIYA RASTVOROV DLYA OPREDELENIYA IONIYA V DISPERSNYKH MASSAKH TYUYA-MUYUNA [PREPARATIONS OF SOLUTIONS FOR IONIUM DE-

TERMINATIONS IN THE DISPERSED SYSTEMS OF THE TYUYA-MUYUN]: Doklady Akademii Nauk, SSSR, no. 4, 1930.

6. Melkov, V.G., MINERALOGO-GEOKHMICHESKIYE OSNOVY POISKOV, URANA MATERIALY PO POISKAM REDKIKH ELEMENTOV [MINERALOGICAL AND GEOLOGICAL PRINCIPLES OF URANIUM EXPLORATION CONTRIBUTIONS ON TRACE ELEMENT EXPLORATION]: Gosgeoltekhizdat, 1947.
7. Pylkov, A.N., POLYCHENIYE PREPARATA IONIYA IZ FERGANSKOY RUDY [CONCENTRATING IONIUM FROM FERGANA BASIN ORES]: Doklady Akademii Nauk, SSSR, (A), 1928.
8. Starik, I. Ye., and Melikov, O.S., K VOPROSU O MIGRATSII IONIYA V PRIRODNYKH USLOVIYAKH [THE PROBLEM OF IONIUM MIGRATION IN NATURE]: Doklady Akademii Nauk SSSR, Nov. Ser. v. 31, no. 9, 1941.
9. Starik, I. Ye., and Shchepotieva, Ye. S., METODY OPREDELENIYA RADIOKTIVNOSTI PRIRODNYKH OBRAZOVANII [MEASURING AND RADIOACTIVITY IN FORMATIONS]: Gosgeoltekhizdat, 1946.
10. Khlopin, V.G., K VOPROSU O MIGRATSII RADIOELEMENTOV V ZEMNOI KORE [THE MIGRATION OF RADIOACTIVE ELEMENTS IN THE CRUST]: Doklady Akademii Nauk SSSR, (A), September, 1926.
11. Khlopin, and Pasvik, M. A., MIGRATSIYA URANA I RADIYA V PREDELAKH GLAVNOI ZHILY TYUYA-MUYUNA [MIGRATION OF URANIUM AND RADIUM IN THE MAIN VEIN, TYUYA-MUYUN]: In: Izucheniu urana [Studies in uranium], v. 3, Akad. Nauk SSSR, Leningrad, 1928.
12. Hude, TRANSURANIUM ELEMENTS, v. 2, p. 1435, 1949.
13. Marckwald, W. and Russell, A., Radioakt. u. Elektronik, Bd. 8, no. 4, p. 548, 1911.
14. Picciotto, E. and Isaac, N., Nature, v. 171, no. 4356, p. 742, 1953.
15. Picciotto, E., and Wilgain, S., Nature, v. 173, no. 40405 [4405 ?], p. 632, 1954.

THE SPECTRUM OF SCATTERED GAMMA RADIATION IN ROCK STRATA OF VARIOUS MINERALOGICAL COMPOSITIONS¹

by

E.M. Fillippov

translated by Henry Faul

ABSTRACT

Curves of the dispersion of gamma-radiation in rocks are drawn on the basis of measurements on rocks of various compositions and density. The energy spectrum of scattered gamma-radiation shows an accumulation of softer rays. A decrease of the effective atomic number and of the density of the substance produces a shifting of the spectrum toward smaller energies of scattered radiation and vice versa. An increase in density of the substance and in its effective atomic number causes a decrease in intensity of gamma-radiation. In addition to soft rays the spectrum shows a considerable portion of rays with energies ranging from 1.25 to 0.212 Mev. Housings of gamma-gamma logging instruments should therefore be of materials which do not block the softer gamma-rays (for instance duraluminum walls less than 1 cm thick or steel less than 0.6 cm thick). In such cases all gamma-rays with energies down to 0.03 Mev will be registered. The use of the differential gamma-spectrometers permits the distinguishing of rocks and ores according to their mineralogical content. --S.T. Vesselowsky, courtesy Geophysical Abstracts, 178.

Understanding of the spectrum of scattered gamma radiation is important in the interpretation of all well logs based on the recording of gamma quanta. These include neutron-gamma logging, gamma-gamma logging and the logging of neutron-induced gamma activity.

The gamma-gamma logging method (GGL) has lately found application in the study of density and porosity of the geologic formations traversed by a borehole. The GGL method has been applied to such problems in mining [2, 4] and in the petroleum industry [3-6, 8, 13, 16-18].

The distribution of gamma radiation in a medium of density ρ can be described with the aid of the Boltzmann equation:

$$\vec{\omega} \text{grad } \varphi(\vec{\omega}, \vec{r}, k) + \tau_R \varphi(\vec{\omega}, \vec{r}, k) = \int_k^{k_0} dk' \int_{\Omega} M(k, k', \vec{\omega}, \vec{\omega}') h(k') \varphi(\vec{\omega}', \vec{r}, k') d\Omega' + s(k, \vec{r}), \quad (1)$$

where $\varphi(\omega, r, k)$ - is the distribution function of the number of gamma-ray quanta of energy k in units of electronic rest mass and of a direction characterized by the unit vector ω at a point at distance r from the source.

k_0 - is the energy of the primary gamma radiation of the source.

k - is the energy of the gamma radiation in the energy band of interest.

$h(k') = \frac{\lambda_\phi}{\lambda_R + \lambda_\phi} = \frac{\tau_R}{\tau_R + \tau_\phi}$ - is a function which takes into account photoelectric absorption of gamma-rays in the medium (with $\tau_R \gg \tau_\phi$ or $\lambda_\phi \gg \lambda_R$ the function $h(k')$ is equal to 1), λ_R and λ_ϕ are mean free paths of gamma quanta in the medium as regards the Compton scattering and photoelectric absorption, and $\tau_R = \frac{1}{\lambda_R}$ and $\tau_\phi = \frac{1}{\lambda_\phi}$ are the coefficients of Compton scattering and photoelectric absorption (Refs. 9, 10 and 12);

$d\Omega'$ - is the element of solid angle;

$s(k, \vec{r})$ - is the gamma-ray source function.

$$M(k, k', \vec{\omega}, \vec{\omega}') = a \frac{k^2}{(k')^2} \left[\frac{k'}{k} + \frac{k}{k'} - \sin^2 \theta_1 \right] \frac{1}{2\pi} \delta(\vec{\omega} \vec{\omega}' - \cos \theta_1)$$

¹Translated from *Issledovaniya spektra rasseyannogo gamma-izlucheniya v gornykh porodakh razlichnogo mineralogicheskogo sostava i razlichoy plotnosti*: Prikladnaya Geofizika, no. 19, p. 230-244, 1958. Reviewed by L. V. Spencer.

is the probability of transport of a gamma quantum from energy k' to energy k .

Here $\delta(\vec{\omega}\vec{\omega}' - \cos \theta_1)$ is Dirac's delta function;

$\vec{\omega}\vec{\omega}' = \cos \theta \cos \theta' + \sin \theta \sin \theta' \cos(\varphi - \varphi')$ is the direction of motion of the gamma quanta in spherical coordinates;

$\cos \theta_1$ is expressed in the following manner in terms of the energies of primary and scattered gamma quanta

$$\cos \theta_1 = 1 + \frac{1}{k'} - \frac{1}{k}, \quad a = 0,93 \varrho Z/A,$$

(where Z and A are the atomic number and atomic weight of the elements composing the rock). Instead of the real atomic number Z one takes the effective atomic number Z_{eff} , and the ratio Z/A will roughly equal 0.5 (within about 1 percent), so that $a = 0.495 \varrho$.

The solution of this equation is a difficult mathematical problem and is available only for simplified cases [9-11, 15, 19-21].

Solving this equation one could determine the spectral distribution of the scattered gamma-radiation in any medium. Some authors working in this direction, obtained only a rough qualitative evaluation of the spectral distribution [11, 15, 19]. In particular, these authors do not consider the photo effect [but they do!-Ed. note]. Compared to the Compton effect, the photo effect is less important there than it is in the gamma-ray logging of drill holes where both hard and soft radiation is recorded. The photo effect becomes appreciable at low energies (below 0.1 Mev) even in media of low density and low atomic number.

Experimental data on gamma-ray energy spectra in water [22, 23] and in sand [7] are available. However, the study of spectra in other media is complicated by the limited range of the spectrometers and the difficulties of modelling. A theoretical study of the spectrum of scattered gamma radiation in rock is, therefore, essential.

Expression (1) for the gamma-ray distribution function by energy only has the following form:

$$\tau_{\text{R}}\varphi(k) = \int_k^{k_0} \Gamma(k, k') h(k') \varphi(k') dk' + q(k), \quad (2)$$

where

$$\Gamma(k, k') = \int_{\Omega} M(k, k', \vec{\omega}, \vec{\omega}') d\Omega' = a \frac{k^2}{(k')^2} \left[\frac{k'}{k} + \frac{k}{k'} + \frac{1}{(k')^2} + \frac{1}{k^2} + 2 \left(\frac{1}{k'} - \frac{1}{k} - \frac{1}{kk'} \right) \right] -$$

is the differential effective Compton cross-section, expressed over the energy of the primary gamma radiation;

$\varphi(k) = \int_{\Omega} d\Omega' \int_V \varphi(\vec{\omega}', \vec{r}, k) d\vec{r}$ is the function that determines the number of quanta in the energy interval dk in the whole volume and $q(k) = 4\pi \int_V s(k, \vec{r}) d\vec{r}$ is the gamma-ray source function in all directions.

We may now solve equation (2) for the case of gamma distribution from a point source as applied in gamma-gamma logging. In that case $q(k)$ will have the following form:

$$q(k) = 4\pi \int_V \frac{Q\delta(\vec{r})}{4\pi} \delta(k_0 - k) d\vec{r} = Q\delta(k_0 - k),$$

where a is the quantity of gammas of energy k_0 (in units of electron rest mass) leaving the source per unit time.

Then equation (2) can be written:

$$\tau_{\text{R}}\varphi(k) = \int_k^{k_0} \Gamma(k, k') h(k') \varphi(k') dk' + Q\delta(k_0 - k).$$

Here we have an integral equation of the Volterra type of the second kind with the kernel $\Gamma(k, k')$, having a discontinuity of the first kind

$$\Gamma(k, k') = \begin{cases} \Gamma(k, k') & \text{with } k \geq \frac{k_0}{1+2k_0} \\ 0 & \text{with } k < \frac{k_0}{1+2k_0} \end{cases}$$

To solve this equation we shall replace function $\varphi(k)$ with a new function $\psi(k)$

$$\psi(k) = \tau_K \varphi(k) - Q \delta(k_0 - k), \quad (3)$$

with the result

$$\psi(k) = \int_k^{k_0} \Gamma(k, k') \frac{h(k')}{\tau_K(k)} \psi(k') dk' + Q \Gamma(k, k_0) h(k_0) \lambda(k_0), \quad (4)$$

In the given case, the second member on the right side represents as if a new source of gamma radiation and determines the spectral distribution of the once-scattered radiation.

Before we go on to calculate the desired function, we determine first the coefficients of Compton scattering and photoelectric absorption which enter into the subintegral function $h(k)$.

The energy dependence of the Compton coefficient is given by

$$\tau_K = \frac{\rho A_0 Z}{A} \sigma \approx \frac{A_0 \rho}{2} \sigma, \quad (5)$$

where ρ - is the density;
 A_0 - is Avogadro's number;
 Z and A - are the atomic number and weight of the elements of the medium (for rocks their ratio is 0.5);
 σ - is the overall Compton scattering cross-section.

Thus the Compton scattering coefficient in rocks is independent of their mineral composition and depends only on their density and the energy of the gamma radiation. The calculated energy dependence of the Compton coefficient in units of density of the medium is shown in Figure 1.

The energy dependence of the photoelectric absorption coefficient in media of various densities and mineral compositions is given by:

$$\tau_{cp} = \frac{\rho A_0 Z^5}{A} f(k) \approx \frac{\rho A_0 Z^4}{2} f(k), \quad (6)$$

where $f(k)$ is the function taking into account only the energy dependence of the photo coefficient.

Rocks have a complex chemical composition and instead of the atomic number Z we use an effective atomic number Z_{eff} . Table 1 gives our calculated values for various rock types [12].

From equation (6) and Table 1, one can see that the coefficient of photoelectric absorption as well as the Compton coefficient depend on the gamma energy, the density of the rock and on its mineral composition. For the rock types shown, the effective atomic number varies from 7 to 16 i.e. not far from the atomic number of aluminum ($Z = 13$).

Knowing the energy dependence of the photo coefficient for aluminum, we can calculate the energy relation for other media from the following equation [12].

$$\tau_{\Phi} = \tau_{\Phi, Al} \frac{\rho}{2.6} \frac{27}{A} \left(\frac{Z}{13} \right)^5, \quad (7)$$

where $\tau_{\Phi, Al}$ is the photoelectric absorption coefficient for aluminum; numbers 2, 6, 13 and 27 are

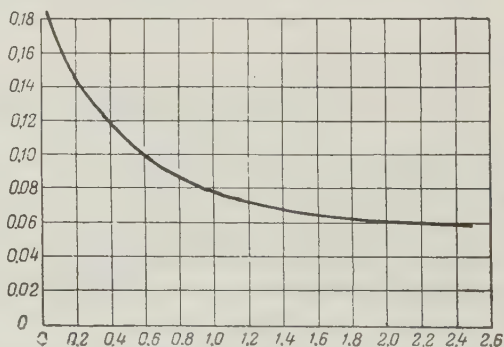


FIGURE 1. Dependence of the Compton scattering coefficient on the energy of the gamma radiation

TABLE 1.

Medium	$\rho, \text{g/cm}^3$	$\bar{\rho}, \text{g/cm}^3$	Z_{eff}	\bar{Z}_{eff}
Water	—	1.00	—	7.42
Coal	1.26—1.33	1.30	6.58—7.27	6.92
Sandstone	1.80—2.80	2.30	11.63—13.15	12.39
Shale	2.00—2.20	2.10	11.42—14.72	13.07
Marl	2.20—2.60	2.40	14.38—15.10	14.74
Limestone	2.30—3.00	2.65	14.84—15.53	15.18
Dolomite	2.44—2.90	2.67	13.67—13.92	13.80
Granite	2.46—3.10	2.78	13.28—14.00	13.64
Diabase	2.90—3.20	3.05	15.42—16.41	15.92
Aluminum	2.50—2.70	2.60	—	13.00

the density, atomic number and atomic weight of aluminum and ρ , Z and A are the same constants for the medium under study.

If we substitute the effective atomic number for a given rock, formula (7) becomes

$$\tau_{\Phi} \approx 0,4 \rho \tau_{\Phi, \text{Al}} \left(\frac{Z_{\text{eff}}}{13} \right)^4.$$

The values of the photo coefficient calculated with this formula for media of density 1, 2 and 3 g/cm³ and corresponding to the effective atomic numbers 7.42, 12.74 and 15.67 are shown in Figure 2. The photo coefficient drops sharply with increasing gamma-ray energy and it is highly for denser materials.

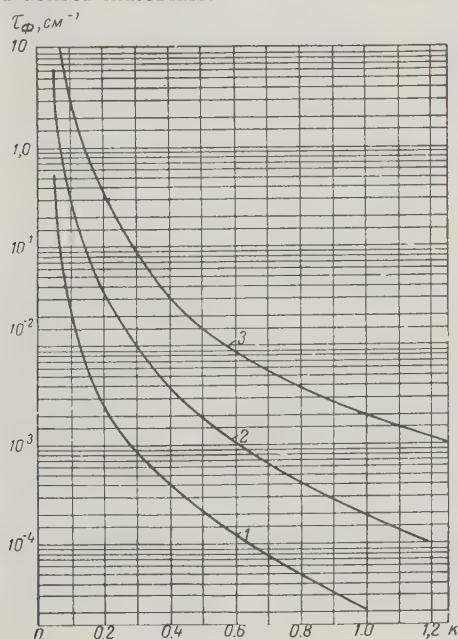


FIGURE 2. Dependence of the photoelectric absorption coefficient on the energy of the gamma radiation for media of densities 1, 2 and 3 g/cm³.

Neglecting photoelectric absorption in the study of scattered gamma-ray spectra can cause significant errors for the soft components. That is easily seen by examining the subintegral function $\rho \lambda_{\text{K}} h$ (coefficient ρ taken from the kernel $\Gamma(k, k')$), as shown in Figure 3.

Photo absorption can be ignored in considerations of scattered gamma-ray spectra only above 0.25 Mev ($k = 0.5$). In that case,

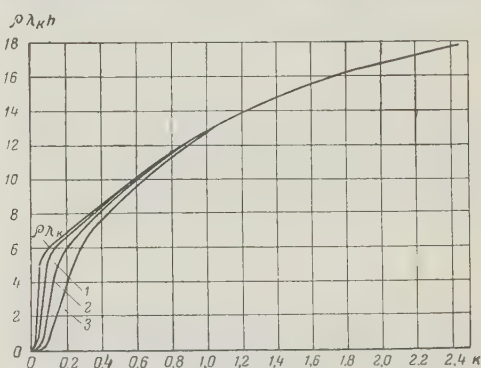


FIGURE 3. Dependence of the function $\rho \lambda_{\text{K}} h$ on energy of the scattered gamma radiation.

1, 2, and 3 - Compton and photoelectric absorption of scattered gamma radiation in media of density 1, 2 and 3 g/cm³, $\rho \lambda_{\text{K}}$ - Compton absorption only.

for media not denser than 3 g/cm³ with the corresponding effective atomic number not higher than 16, the error will not exceed 7 percent (table 2).

TABLE 2. Relationship of the function

$\rho, \text{g/cm}^3$	$k = 0.5$	0.2	0.1
1	1.04	1.03	1.15
2	1.03	1.15	1.93
3	1.07	1.75	6.67

The error in the determination of the energy spectrum rises sharply below 0.25 Mev. Thus, for example, in a medium of density 3 g/cm³, at $k = 0.2$ ($E = 0.1$ Mev) the error will

reach 75 percent and at $k = 0.1$ ($E = 0.05$ Mev) it will be 667 percent.

In the logging of boreholes the probe is usually in a steel shell no thicker than 1 cm, to protect it against hydrostatic pressure. Gamma-rays with an energy less than 0.08 Mev thus cannot reach the detector [12]. In the case of probes with walls thinner than 1 cm, more soft radiation will reach the detector.

To facilitate solving equation (4) we replace its kernel $\Gamma(k', k)$ with $\Gamma^*(k')$, in which $\cos \theta_1$ is replaced by the average value $\cos \theta_1$, which is a function of energy as follows [12]:

$$\overline{\cos \theta_1} = \frac{1}{\sigma(k)} \left[\frac{k^3 - k^2 - 6k - 3}{2k^4} \ln(1 + 2k) + \frac{-3k^4 + 8k^3 + 28k^2 + 15k + 31}{k^3(1 + 2k)^2} \right],$$

where

$$\sigma(k) = \frac{1+k}{k^3} \left[\frac{2k(1+k)}{1+2k} - \ln(1+2k) \right] + \frac{\ln(1+2k)}{2k} - \frac{1+3k}{(1+2k)^2}.$$

then if $k \ll 1$,

$$\overline{\cos \theta_1} = \frac{1}{\sigma(k)} \frac{k(16 - 58k + \dots)}{15},$$

where

$$\sigma(k) = \frac{4}{3} (1 - 2k + 5.2k^2 - \dots).$$

The substitution of $\overline{\cos \theta_1}$ for $\cos \theta_1$ in the subintegral function is possible because the scattering of gamma-rays is governed by the laws of statistics for strong sources and the sources used in logging do not have intensities below 10^8 gammas/sec. [sic].

The sharpest drop of $\overline{\cos \theta_1}$ occurs in the range of $k = 0.1$ to 1.0. For the energies of $k < 0.1$ the value of $\overline{\cos \theta_1}$ changes little. The angle of scattering is nearly 90° in that case.

The energy dependence of function $\Gamma^*(k')$ is shown in Figure 4 [as a dashed line]. The function $\Gamma(k_0, k')$ is plotted here as a function of energy [solid lines] and it may be seen that $\Gamma^*(k')$ comes closest to $\Gamma(k, k')$ at low energies when the angle of scattering is close to 90° . In that case, the scattering is essentially isotropic and use of the average cosine comes closest to the truth.

As a result of this substitution equation (4) becomes:

$$\psi(k) = \int_0^{h_0} \Gamma^*(k') \lambda_R(k') h(k') \psi(k') dk' + \lambda_R(k_0) h(k_0) Q \Gamma(k, k_0). \quad (8)$$

Differentiating, we obtain a heterogeneous first-order differential equation

$$\begin{aligned} \psi'(k) + \Gamma^*(k) \lambda_R(k) h(k) \psi(k) - \\ - Q \Gamma'(k, k_0) \lambda_R(k_0) h(k_0) = 0. \end{aligned} \quad (9)$$

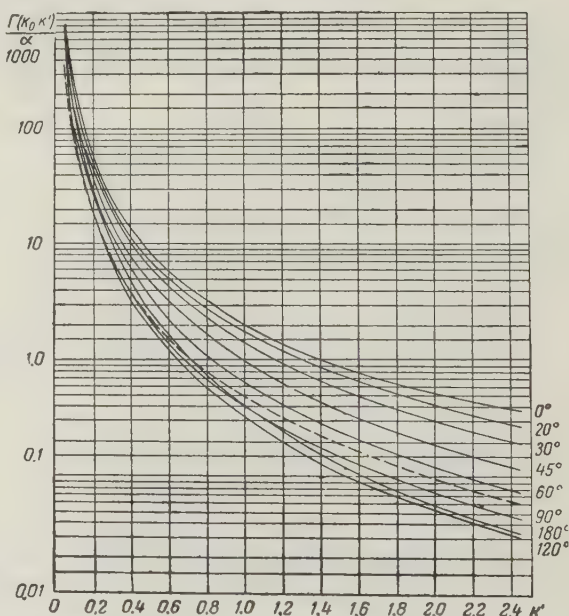


FIGURE 4. Relation of function $\Gamma^*(k')$ (dashed line) and gamma-ray energy k' (in units of rest mass energy) compared with actual values of function $\Gamma(k_0, k')$ evaluated for various angles of scattering.

Solving this equation we obtain

$$\psi_1(k) = Q\lambda_R(k_0)h(k_0)\left\{\Gamma(k_0, k_0) - \int_k^{k_0} \Gamma'(k', k_0) \exp\left[-\int_{k'}^{k_0} \Gamma''(k'')\lambda_R(k'')h(k'')dk''\right] dk'\right\} \times \exp\left[\int_k^{k_0} \Gamma''(k')h(k')\lambda_R(k')dk'\right]. \quad (10)$$

The energy dependence of the subintegral $\Gamma''(k')h(k')\lambda_R(k')$ for the rock densities 1, 2 and 3 g/cm³ is shown in Figure 5. It can

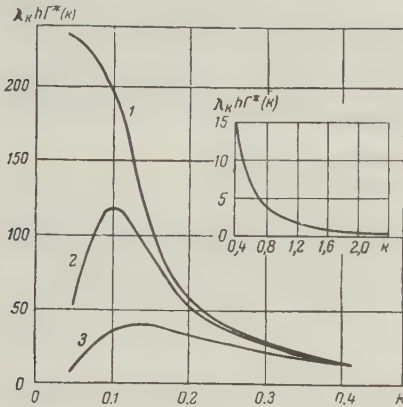


FIGURE 5. Dependence of the subintegral function $\lambda_R h \Gamma''$ on scattered gamma-ray energy (the numbers indicate densities of the media in g/cm³).

be seen that the function increases with decreasing energy and that the increase is greatest for the lightest medium.

Equation (9) holds only for energies k_0 to $k_0/(1+2k_0)$ because of the discontinuity of kernel $\Gamma(k, k')$, and we denote the desired function by $\psi_1(k)$. For energies below $k_0/(1+2k_0)$ equation (9) will have the form

$$\psi_2(k) = \int_k^{k_0} \Gamma''(k')\lambda_R(k')h(k')\psi_2(k')dk'. \quad (11)$$

Here

$$k_i = \frac{k}{(1-2k)}.$$

Differentiating with respect to k we obtain

$$\psi_2'(k) =$$

$$= F(k+\Delta k) - F(k), \quad (12)$$

where

$$F(k) = \Gamma''(k)\lambda_R(k)h(k)\psi(k),$$

$$\Delta k = 2k^2/(1-2k).$$

With the aid of well known rules of differen-

tiation equation (12) is easily reduced to

$$\psi_2'(k) = \frac{\partial F}{\partial k} \Delta k + \frac{\partial^2 F}{\partial k^2} \frac{\Delta k^2}{2} + \dots$$

Second order terms can be neglected and equation (12) becomes

$$\psi_2'(k) = \frac{\partial F}{\partial k} \Delta k. \quad (13)$$

Solving the derivative $\frac{\partial F}{\partial k}$, we obtain the homogeneous first-order equation

$$\psi_2'(k) - p(k)\psi_2(k) = 0. \quad (14)$$

Here

$$p(k) = \frac{2k^2 [\Gamma''(k)h(k)\lambda_R(k)]}{1-2k-2k^2\Gamma''(k)h(k)\lambda_R(k)}$$

Solving this equation, we obtain:

$$\psi_2(k) = C \exp\left[-\int_k^{k_0} p(k')dk'\right] \quad (15)$$

The energy dependence of function $[\Gamma''(k)h(k')\lambda_R(k)]$, which enters into the numerator of the function $p(k)$, is shown in Figure 6.

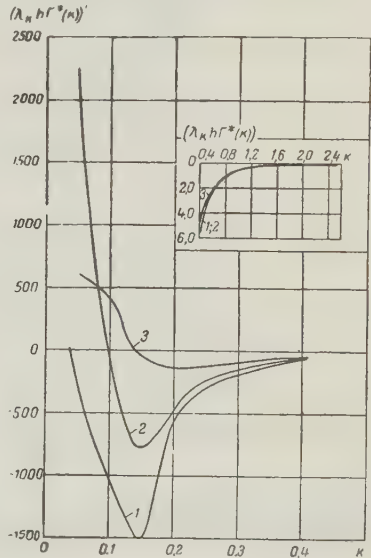


FIGURE 6. Dependence of the function $(\lambda_R h \Gamma'')$ on gamma-ray energy κ (the numbers indicate densities of the media in g/cm³).

The constant C is easily found from the equation

$$\psi_1\left(\frac{k_0}{1+2k_0}\right) = \psi_2\left(\frac{k_0}{1+2k_0}\right).$$

Using equations (10) and (15) we can calculate function $\psi(k)$ for all energy ranges. Multiplying the given function by the mean free path λ_R , according to (3) we obtain the desired function $\varphi(k)$. The energy dependence of the gamma-ray distribution (after removal of the gamma-ray source function) for media of densities 1, 2 and 3 g/cm³ and the corresponding effective

atomic numbers 7.42, 12.74 and 15.67 is shown in Figure 7.

Before we go on to describe the results shown in the graph, we shall calculate the integral spectra for these three media.

If the function of the integral spectrum of scattered gamma radiation is designated by $f(k)$, then it will be determined by the following integral

$$f(k) = \int_k^{\infty} \varphi(k) dk.$$

The results of this calculation are shown in Figure 8. Considering the data of Figures 7 and 8 we reach the following conclusions:

1. As one would expect, the energy spectrum of scattered gamma radiation is enriched in the soft components.

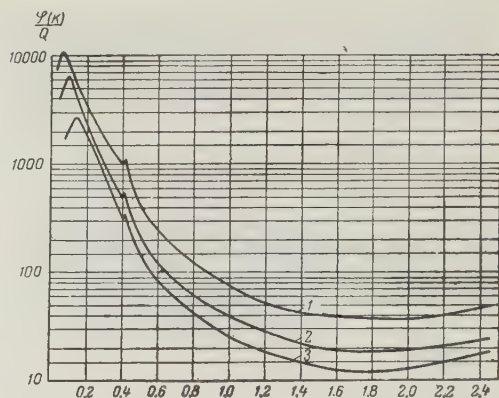


FIGURE 7. Energy dependence of the differential spectral distribution of scattered gamma-radiation for media of densities 1, 2 and 3 g/cm³.

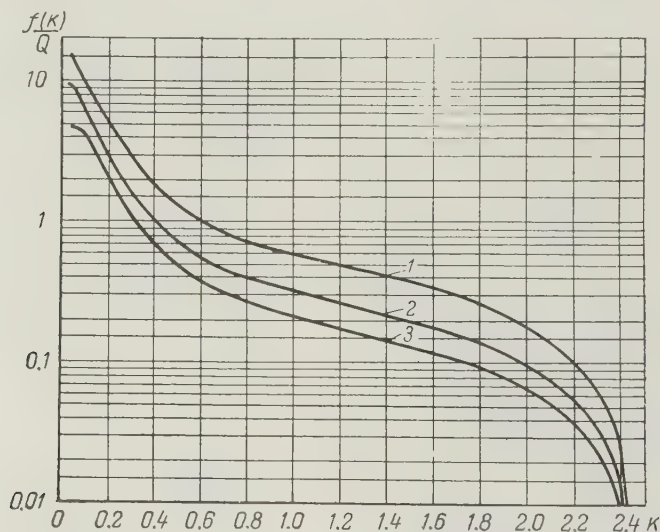


FIGURE 8. Energy dependence of the integral spectral distribution of scattered gamma radiation for three values of density: 1, 2 and 3 g/cm³.

2. The shift of the spectrum toward the soft end is greatest for the lightest medium and vice versa.

3. The intensity of scattered gamma radiation is lower in media of higher density.

4. A significant part of the soft component of scattered radiation consists of once-scattered radiation of 1.25 to 0.212 Mev (fig. 7 the maximum of this radiation shows up as a small peak).

On the basis of these results we may also consider the following practical applications: a) logging probes must be constructed so that the walls do not absorb the effective part of the soft radiation. For gamma-gamma logging of strata with densities above 2 g/cm³ the probe

walls should be of aluminum no thicker than 1 cm or steel no thicker than 0.6 cm. This makes it possible to record gamma-rays down to about 0.03 Mev ($k=0.05$); b) the use of differential gamma-ray spectrometers permits the determination of rocks and ores by [the effect of] their mineralogical composition on the intensity of the soft scattered gamma radiation. The heavy elements in ores will cause a shift of the spectrum toward higher energies because of the great photoelectric absorption of the soft radiation. This effect is also observed with gas-discharge [G-M] counters [14]. This increase of the hard component in the medium leads to a general decrease of all scattered gamma-ray intensity.

In conclusion I wish to thank S. A. Kantor for consultations.

REFERENCES

1. Akhiezer, A. and Pomeranchuk, I., I NEKOTORYE VOPROSY TEORY YADRA [SOME QUESTIONS OF NUCLEAR THEORY]: Tekhteoritizdat, 1950.
2. Voskoboinikov, G. M. and Deev, L. O., PLOTNOCTNOY KAROTAZH UGLER-AZVEDOCHNYKH SKVAZHIN [DENSITY LOGGING OF HOLES FOR COAL PROSPECTING]: Razvedka i okhrana nedr, no. 10, Gosgeoltekhizdat, 1956.
3. Dakhanov, V. N., INTERPRETATSIYA REZULTATOV GEOFIZICHESKIKH ISSLEDOVANIY RAZREZOV SKVAZHIN [INTERPRETATION OF THE RESULTS OF GEOPHYSICAL STUDIES OF BORE-HOLE SECTIONS]: Gostoptekhizdat, 1955.
4. ———, SOVREMENNOE SOS-TOYANIYE I PERSPEKTIVY DALNEYSHEGO RAZVITIYA RADIOMETRII SKVAZHIN [PRESENT STATUS AND PROSPECTS OF FURTHER DEVELOPMENT OF BOREHOLE RADIOMETRY]: Razvedka i okhrana nedr, no. 6, Gosgeoltekhizdat, 1956.
5. Itenberg, S. S., NEFTEPROMYSLOVAYA GEOFIZIKA DLYA GEOLOGOV [PETROLEUM GEOPHYSICS FOR GEOLOGISTS]: Gostoptekhizdat, 1957.
6. Komarov, S. G., TEKHNIKA PROMYSLOVOY GEOFIZIKI [TECHNIQUES OF INDUSTRIAL GEOPHYSICS]: Gostoptekhizdat, 1957.
7. Metveyev, A. D., and others, ENERGETICHESKOE RASPREDELENIE GAMMA-KVANTOV OT TOCHECHNOGO ISTOCHNIKA GAMMA-IZLUCHENIYA V BESKON ECHNOY PESCHANOV SREDE [ENERGY DISTRIBUTION OF GAMMA QUANTA FROM A POINT SOURCE OF GAMMA RADIATION IN AN INFINITE LAYER OF SAND]: Atomnaia Energia, Izd. Akad. Nauk, SSSR, no. 4, 1956.
8. NOVY GLUBINNY PRIBOR DLYA GAMMA-GAMMA-KAROTAZHA [NEW PROBE FOR GAMMA-GAMMA LOGGING]: Byulleten Nauchno-tekhnicheskoi Informatsii, no. 3, 21/I., 1956.
9. Ogievetskii, V. I., K TEORII RAS-PROSTRANENIYA GAMMA-LUCHEY CHEREZ VESHCHESTVO [THEORY OF GAMMA-RAY DISTRIBUTION IN MATTER]: Zhurn. Eksperim. i Teoret. Fiziki, v. 29, 1955.
10. Ogievetskii, V. I., VGLOVOE RAS-PREDELENIE GAMMA-IZLUCHENIYA NA BOLSHIKH GLUBINAKH PRO-NIKNOVENIYA V VESHCHESTVO [ANGULAR DISTRIBUTION OF GAMMA RADIATION AT LARGE PENETRATION DEPTHS IN MATTER]: Zhurn. Eksperim. i Teoret. Fiziki, v. 29, 1955.
11. Fano, V., YADERNYE REAKTORY [NUCLEAR REACTORS]: Sb. Statei, v. 1, 1956.
12. Filippov, E. M., K TEORII METODA GAMMA-GAMMA-KAROTAZHA (GGK) [THEORY OF GAMMA-GAMMA LOGGING]: Prikladnaia Geofizika, no. 17, Gostoptekhizdat, 1957.
13. ———, GAMMA-GAMMA - KAROTAZH [GAMMA-GAMMA LOGGING]: Primenenie Radiativnykh Izotopov v Neftianoi Promyshlennosti (sb. dokladov), Gostoptekhizdat, 1957.
14. Hayward, Evans, J. Appl. Phys., v. 25, no. 4, 1954.
15. Fano, V., Nucleonics, v. 11, nos. 8 and 9, 1953.
16. Measurement of soil density and moisture, Nucleonics, v. 8, no. 4, 78-80, 1951.
17. New logging technique measures density, porosity, World Oil, v. 139, no. 7, 142-156, 1954.
18. Rosoff, C., Bull. Assoc. Franc. Technique Petrol., no. 111, 275-310, 1955.
19. Spencer, L. V., Phys. Rev., 88, 793, 1952.
20. Spencer, L. V., and Jenkins, F. A. Phys. Rev. 76, 12, 1949.
21. Spencer, L. V., and Fano, V., Phys. Rev. 81, 464, 1951 and J. Res. Nat. Bur. Stds. 46, 446, 1951.
22. Thens, R. B., and others, J. Appl. Phys. 26, 294, 1955.
23. Weiss, M. M. and Bernstein, W., Phys. Rev. 92, 1264, 1954.

SOME PROBLEMS IN THE CONSTRUCTION¹ OF A BOREHOLE NEUTRON GENERATOR

by

E.A. Abb, V.M. Zaporozhets, R.I. Plotnikov and L.A. Khutsishvili

translated by Henry Faul

ABSTRACT

In designing neutron generators which will be put down bore holes, the usual vacuum techniques do not apply. Progress is reported in the development of an ion source that can operate effectively under conditions such that the pumping of gas is kept to a minimum, and in the design of special pumping systems specifically for bore-hole conditions. -- M. Russell.

INTRODUCTION

When neutrons are being produced by ions accelerated in a vacuum, gas is allowed to leak into the ion source of the apparatus. The effective pressure gradient produced by this leakage results from the fact that gas is best ionized at pressures of the order of 10^{-2} - 10^{-3} mm of mercury, but a vacuum of the order of 10^{-5} mm is needed to accelerate the ions.

In ordinary generators, this pressure drop is maintained by continuous pumping of the excess gas out of the accelerating sector.

For a small generator, particularly one that is to go down into bore holes, the usual vacuum techniques do not apply. This becomes clear when we consider the operating conditions for in-hole apparatus in general: Large hydrostatic pressure (up to hundreds of atmospheres), temperatures of the order of 120-300°F, restricted space (diameter only up to 4-5 inches), small power consumption, a limited number of connections for power supply and control, plus a great deal of vibration and mechanical shock. Under such conditions it is not possible to provide an exhaust for the fore-vacuum pump, and the action of the diffusion pump would be paralyzed by the high ambient temperature and the continuous agitation of the oil by the banging and spinning of the probe.

Two ways of attacking the problem present themselves: First, the development of an ion source that can operate effectively at a very low pressure, so that the pumping of gas can be kept to a minimum; second, the design of special pumping systems specifically for bore hole conditions.

Following we report some results obtained

during our research on basic problems of the in-hole neutron generator intended for the logging of bore holes.

ION SOURCE

The operation of a neutron generator with a zirconium-tritium target is considered satisfactory if 10^8 neutrons/sec. are produced with an accelerating voltage no greater than 150 kv [2]. The intensity of the ion beam necessary for this output depends on the proportion of atomic to molecular ions. Statements by various authors differ on the exact amounts, as a result of differences in the conditions of their experiments, but generally one can assume that an ion current of 50-100 microamperes with 20 percent atomic ions should be sufficient. However, the strength of the current does not exclusively determine the [choice of the] amount of gas that leaks from the ion source into the accelerating region. This leakage also depends on the pressure drop and conductivity (geometry) of the connecting tube.

From Table 1, compiled from published data,

TABLE 1

Power watts	Pressure microns of Hg	Leakage cm ³ /hour	Ion current microamps
Arc discharge sources			
2,000	3-5	up to 720	500,000
10,000	0.2-2	up to 600	300,000
20	0.8-3	2-8	300
High-frequency sources			
300	35	80	15,000
150	10	1	50
50	40	6	300

one can see that the magnitude of the ion current is not a simple function of the pressure. In existing generators, with an ion current recalculated to about 100 microamperes the gas flow

¹Translated from Nekotorye voprosy konstruirovaniya skvazhinnoy generatora neytronov: Prikladnaya Geofizika, no. 23, 1959.

would lie between about 0.3 and 8 cm³ [per hour]. This spread indicates that the problem of obtaining a given ion current with a minimal gas pressure in the source is not insurmountable and, as already mentioned, the small pressure does not limit performance.

We have built and studied several working models of ion sources and as a result of this work we designed a source that can work at a low gas pressure.

This source is shown schematically in Figure 1, where 1 is a cylindrical anode

solution of the problem of maintaining a high vacuum in the accelerating section, but also permits close approach to the problem of producing a tube with a permanent gas filling, in which the pressure in the accelerating section and in the ion source is the same.

APPARATUS FOR THE MAINTENANCE OF HIGH VACUUM IN THE ACCELERATING SECTOR

The ion source described here, working at a pressure of the order of 10^{-5} mm Hg can

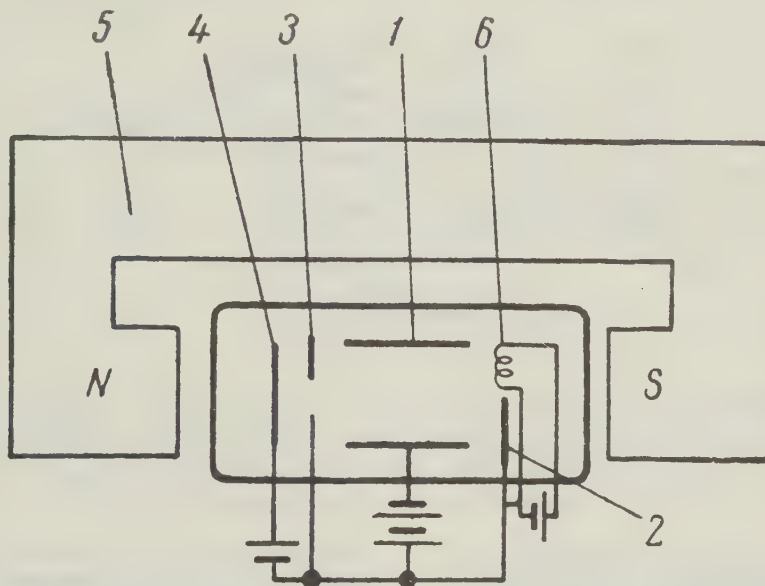


FIGURE 1. Schematic diagram of the ion source. 1-anode, 2-cathode, 3-second cathode, 4-target, 5-magnet, 6-filament.

about 20 mm in diameter and about 30 mm long, 2 is the first disc-shaped cathode and 3 is the second disc-shaped cathode with a hole in the center to allow the positive ions to pass to the target 4.

Due to the presence of the axial magnetic field of magnet 5, the electrons produced by the arc discharge are focused on the tungsten filament 6 and do not immediately fall on the anode, but oscillate for a time in the volume of the source. The oscillation substantially increases the probability of ionization at a comparatively low gas pressure. A source of stated dimensions has the following characteristics: Hydrogen pressure, 10^{-5} mm Hg; U_a , 1-2 kv; $I_{\text{discharge}}$, 500 microamperes; H , 600-800 gauss; U_{target} , -100 kv; I_{ion} , 70 microamperes.

It is easy to see that the choice of such an ion source not only substantially simplifies the

give an ion current no greater than 100 microamps. With the necessity of producing pulses of high-energy neutrons up to 10^9 n/sec and more, one must utilize very much higher ion currents and in that case one cannot avoid the need for a fairly high pressure in the source. The leakage in that case amounts to about 1 cm³/hour at 766 [sic] mm of Hg or 20 L/sec at 10^{-5} mm Hg [2].

Above we have cited the circumstances which make it impractical to use diffusion pumps or ion pumps. We have, therefore, undertaken a search for the most active getters that could independently or in combination with an electric discharge assure the necessary pumping capacity and speed. The materials normally used in vacuum technology (Ba-Ti, Ba-Ti-Al etc.) are altogether insufficient. A review of the literature showed that a number of authors [3, 4, 5] value highly the sorption properties of titanium and zirconium. Unfortunately, quantitative data are almost nonexistent, particularly for the

range of high vacuum, and information on the chemical composition of getters (impurities) and their technology is equally hard to find.

We obtained the pertinent information in a series of measurements of the sorption of hydrogen and air by different samples of titanium and zirconium under various conditions.

The apparatus used for the measurement of the speed of sorption and the capacity of absorbers is shown schematically in Figure 2.

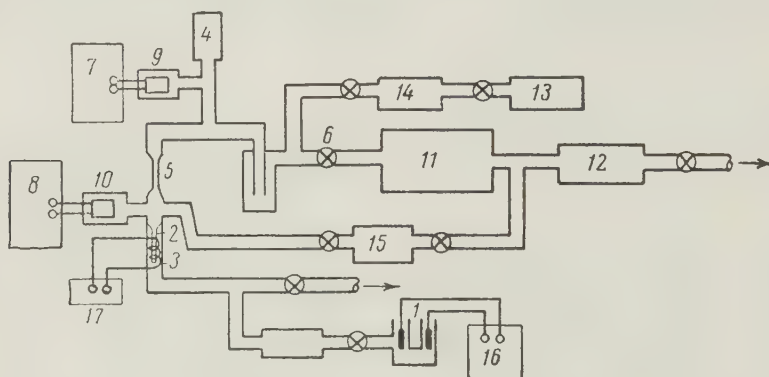


FIGURE 2. Schematic diagram of the apparatus for measuring the rate of sorption and the capacity of the absorbers. 1-electrolytic cell, 2-palladium tube, 3-tungsten filament, 4-getter being studied, 5-capillary tube, 6-high vacuum valve, 7,8-vacuum gauge VI-3, 9,10-LM-2/R, 11-high-vacuum pump, 12-fore-vacuum reservoir, 13-argon reservoir, 14-pipetting volume for argon, 15-pipetting volume for air, 16-power supply for electrolytic cell, 17-power supply for heating tungsten filament. Arrows indicate connections to fore-pump.

Hydrogen produced in the electrolytic cell 1 passes through palladium tube 2 heated by tungsten filament 3. At the same time, the hydrogen is cleaned of various possible admixtures and its quantity can be controlled by regulating the heat of the filament 3.

As a function of that, one or another quantity of gas per unit time is permitted to pass into the vessel 4 where the getter under study is placed. In the steady state, the rate of gas flow is determined as the product of conductivity of capillary tube 5, which joins the palladium tube to the vessel, and of the pressure drop measured.

Prior to the experiment, the system is evacuated by a regular pumping assembly 11 which can be closed off with valve 6 when the getters are being studied.

The apparatus permitted measurements under conditions corresponding to those in a neutron generator. The only difference was that instead of deuterium we used ordinary hydrogen, for which we corrected by using the appropriate factor, insofar as the ratio of sorption characteristics of hydrogen and deuterium is known [5].

The accuracy of results obtained is determined by the error of the vacuum gauges 8 and 9 [sic—probably should read 7 and 8; Tr.] which measure the pressure at each end of the capillary tube.

Vacuum gauges of type VI-3 were used. They have an error no greater than 10 percent, although the actual scatter of experimental data for numerous repeat measurements was much smaller.

We have made measurements on samples of massive, sublimated, and powdered titanium, the latter in various grain sizes and in various degrees of purity, on samples of massive and powdered zirconium, powdered "Ceto" alloy [Ce-Th-Al, a Telefunken trade mark; Tr.], powdered titanium hydride deposited and treated in various ways, and under various temperatures and pressures.

In addition to the sorption speed and capacity, the structure of the adsorbers was studied and the magnitude of the effective surface area of a number of samples was determined by electrochemical methods. The real area differs greatly from the geometric surface area which is simply determined.

Because a description of the physico-chemical results of this work falls outside the scope of this article, we present only a few of the many curves obtained (fig. 3-4).

The results of the whole series of measurements lead to the following fundamental conclusions of practical application:

1. Contrary to reports in the literature, titanium and zirconium, suitably prepared,

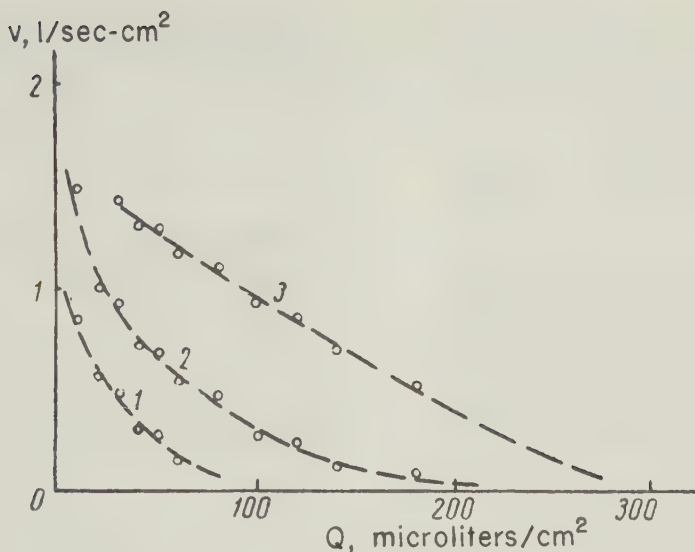


FIGURE 3. Sorption of hydrogen as a function of the quantity of gas already absorbed for powdered zirconium at room temperature. 1-first sorption, 2-second sorption, after heating, 3-third sorption, after heating

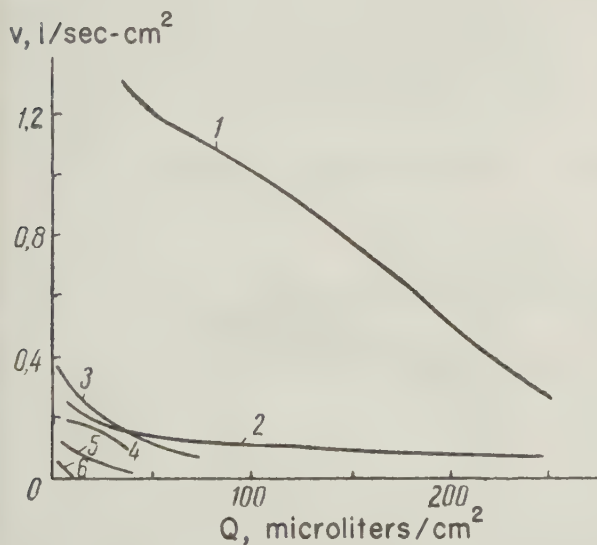


FIGURE 4. Rate of sorption of hydrogen as a function of the amount of gas absorbed at room temperature. 1-powdered zirconium, 2-powdered titanium covered by sublimated titanium, 3-powdered titanium, 4-titanium sublimated in an atmosphere of argon, 5-titanium sublimated in vacuo, 6-"Ceto" alloy at a temperature of 350°C.

absorb hydrogen with great speed in significant quantity at room temperature.

Raising the temperature to 100-200°C increases the speed of sorption and the capacity of the getter less than one order of magnitude.

2. The same getters analogously absorb air, but the capacity and speed are much lower in that

but the influence of increased temperature is pronounced.

3. The sorption of hydrogen by layers of powder is reversible. To reestablish the sorption characteristics, the getter first must be heated in a vacuum to a temperature of 800-850°C.

Sublimated layers, after analogous processing, are regenerated only to a negligible degree. For complete regeneration it is necessary to spray on [more getter] from the unused spare portion [left on the evaporator].

4. Per unit of geometrical surface area, the powdered getters are the most effective (about 250 microliters/cm², speed 1 L/sec).

Considering the weight of the getter, the sublimated layers are more effective. The best results are obtained with a layer sublimated in an argon atmosphere at pressures of the order of 10⁻² - 10⁻³ mm Hg (200 microliters/milligram, 2-5 L/sec).

5. Extremely effective is the sublimation of the getter onto a layer of powder of the same material to assure a bonding with a high degree of purity and a large surface area.

6. The use of binders for the application of the layers of powder clogs the surface area somewhat and reduces its effectiveness. Better results are obtained if the powder is baked

onto its base material by heating in a vacuum.

7. The "Ceto" alloy has little practical interest for it absorbs hydrogen with appreciable speed only at more than 300°C.

Our results on the evacuation of excess gas from the accelerating section of the borehole neutron generator permits the following conclusions:

A. A prepared coating of powdered getter of 200-300 cm² surface area (which corresponds roughly to the magnitude of surface area of the accelerating electrodes in the accelerating section) can absorb 30-50 cm³ of deuterium at 760 mm Hg without regeneration. The operation of the absorbing layer requires no external input of energy. Increase in temperature, such as may be encountered in the borehole, can only increase the effectiveness of the sorption. Use of the [getter] coating eliminates the necessity for pumping equipment. Once it is saturated (after working 40-70 hours) the tube must be replaced and taken to a vacuum laboratory for regeneration.

B. The sublimated layers we have studied cannot be applied directly to the electrodes, for the sublimation in the accelerating sector would cause short circuits between the electrodes.

The evaporator can be installed in a separate

volume connected with the accelerating sector. It will assure, with a sector about 15 cm long, the absorption of up to 20 cm³ of deuterium at 760 mm Hg without regeneration. For regeneration it is necessary to spray the additional part of the getter, which requires connecting the evaporator to a source of power of 100-200 watts at 5-6 volts for 2-5 minutes.

The supply of the getter can assure no more than 2 or 3 regenerations. The advantages of this or another design will be determined in practical application.

C. The significant capacity of the coatings we have studied permitted a solution of the problem of stabilizing the pressure in the ion source with escape of the gas into the accelerating sector. A filament of titanium wire 1 mm in diameter and 1-2 cm long and coated with titanium or zirconium powder saturated with deuterium at high pressure and then heated will evolve the necessary volume of gas. (The rate of desorption is controlled by the heating current.)

The availability of the ion source described in the first part of this paper and the enumerated characteristics of the getter coatings we have studied made it possible to go on immediately to the construction of working models of small accelerating tubes for the borehole neutron generator.

Two different models were designed, con-

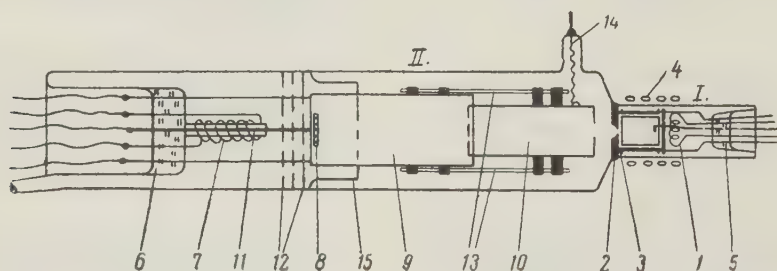


FIGURE 5. Schematic diagram of a working model of a small accelerator tube of a borehole neutron generator. 1-ion source sector: 1-desorber-reservoir gas supply, 2-glass diaphragm, 3-source electrodes: cylindrical anode and disc-shaped cathodes, 4-electromagnet, 5-press seal with connections, 11-accelerating sector: 6-press seal, 7-getter to be sublimated, 8-target, 9-second accelerating electrode, 10-first accelerating electrode, 11-quartz tube, 12-mica baffles, 13-quartz rods holding electrodes, 14-connection to first electrode, 15-guard sleeve.

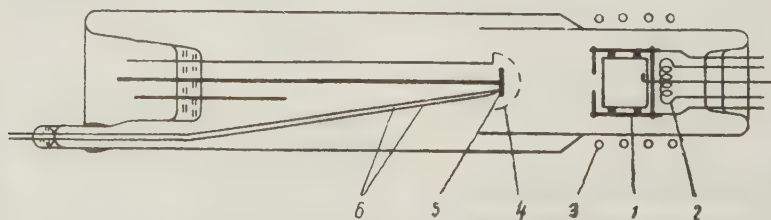


FIGURE 6. Schematic diagram of the working model of a small accelerator tube with "permanent filling." 1-ion source, 2-desorber-reservoir, 3-electromagnet, 4-anti-dynatron [secondary radiation] grid, 5-target, 6-thermocouple.

structed and studied: one with a "permanent filling" for the production of pulses of medium intensity and one with a "leak" for the production of stronger pulses.

The design of the two models is shown in Figures 5 and 6. The necessity of making models with a hydrogen filling and using molybdenum targets for the construction of the working parts was brought about by the fact that the study of working models, with the possibility of neutron beams being generated every time a switch is thrown could not go on in our laboratory which is not equipped for such measurements.

The characteristics obtained for tubes with a hydrogen filling correspond to those of similar tubes filled with deuterium.

The preliminary studies showed that the essential parameters of our models came up to expectations. The beam current of the tube with "permanent filling" was about 50-70 microamperes at a voltage of the order of 80 kv.

After the completion of the studies of service life times and some constructional changes concerned with improved cooling of the target under intensive operation, we plan to go on with the construction of working models of accelerating tubes for actual experiments in boreholes.

REFERENCES

1. Dushman, Saul, NAUCHNYE OSNOVY VA KUUMNOY TEKHNIKI [SCIENTIFIC FOUNDATIONS OF VACUUM TECHNIQUE]: GONTI [State Institute of Science and Technology] 1950, (originally published by John Wiley and Son, N. Y., 1949.
2. Zaporozhets, V. M., and Filippov, E. M., Prikladnaya Geofizika, vipusk 20, Gostoptechizdat, 1958 (Moscow).
3. Espe, Knolle and Wilder, Electronics, no. 23, p. 80, 1950.
4. Espe, Zirconium und seine Herstellung, 1954.
5. Stant and Gibbons, Jour. Appl. Phys., v. 26, p. 1448, 1955.

DETERMINATION OF COEFFICIENTS OF RADIOACTIVE EQUILIBRIUM AS A METHOD OF STUDY OF THE MIGRATION OF URANIUM, IONIUM, AND RADIUM¹

by

V.I. Malyshev

translated by Mark Burgunker

ABSTRACT

In the paper the problems of study of the migration of uranium, ionium and radium by means of definition of quantitative correlation between these elements are considered. Ratios of U:I, Ra:U and Ra:I given for rocks and minerals of the hypergene zone of three different deposits.

The author elucidates the conduct of uranium, ionium and radium in the zone of hypergenesis of the examined deposits by means of a graphic method which facilitates considerably the interpretation of data obtained. --Auth.

A certain constant proportion, a radioactive decay equilibrium, exists between radioactive elements in rocks with ages greater than one million years,² which have not been affected by secondary processes. The migration of a part of the radioactive parent or daughter element may upset the equilibrium; this migration may be consequent upon the chemical properties of the radioactive element in the hypergene zone. The time elapsed since the parent and daughter products were separated will also determine the extent to which the equilibrium is upset.

Until recently, most radioactive mineral deposits were classified on the basis of the radium-uranium ratio, even though this quantity cannot serve as a basis for inferences about the migration of either of these two elements. V. G. Khlopin [10, 11,] Ye. Starik [8, 9], and (even more definitely) V. G. Melkov [6] have asserted that the ionium-uranium ratio, in addition to the radium-uranium ratio, must be evaluated if any conclusions are to be drawn about the migration of the radioactive element. A number of methods of evaluating the ionium-uranium ratio has been developed [1, 3, 5, 7, 9, 12-15]. The best method of evaluating this ratio, in uranium ores and minerals, was developed by V. I. Baranova and L. A. Kuzmina. The great advantages which attach to this method derive

from the fact that other methods involve either excessively long intervals of time or extremely small ranges of variation, one percent of the uranium contents or less. The fact that the concentration of uranium X_1 is attained in only six months (inasmuch as the concentration of uranium X_1 can be substituted for the ionium concentration), constitutes the basis of the method developed by Baranova and Kuzmina. This procedure eliminates the necessity of precise measurements of the amounts of uranium and ionium present, inasmuch as the ratio between ionium and uranium X_1 does not vary under ordinary conditions. A number of thorium isotopes (thorium, radiothorium, radioactinium, ionium, uranium X_1 and uranium Y), then can be separated out by chemical analysis. Thorium, radiothorium, radioactinium and ionium give off alpha particles.

Ionium will be the chief source of alpha radiation if the quantity of radiothorium, and therefore the quantity of thorium, in the sample is small, inasmuch as the intensity of the alpha-radiation given off by radioactinium is only a few percent of the intensity for ionium, furthermore, this small intensity, decreases rapidly because of the short half life (8 or 9 days) of radioactinium; Uranium X_1 and Y give off beta radiation.

The radiation given off by uranium Y is very weak and attenuates rather rapidly, inasmuch as the half-life of this isotope is only about one day. Among the thorium isotopes, then, ionium X is the chief source of alpha radiation. Uranium X_1 is the chief source of beta radiation. Small amounts of the thorium isotopes are spread on metal surfaces in a thin, uniform layer with a mass of the order of 1 mg/cm²; the intensities of the alpha radiation from the ionium and the beta radiation from the uranium X_1 are then measured by specially positioned counters. The alpha and beta intensity values are converted to units of equilibrium uranium after calibration against appropriate standards.

¹ Translated from *Opredeleniye koeffitsiyentov radioaktivnogo ravnovesiya kak metod izucheniya migratsii urana, ioniya, radiya*: Sovetskaya Geologiya, 1958, no. 7, p. 138-147.

² The precision of time measurements computed from radioactive decay product equilibria, actually is based upon the fact that an ionium-radium equilibrium is established after fifteen thousand years, and ionium-uranium equilibrium after approximately 500 thousand years.

The ratio between the alpha and beta intensities, therefore, must have a value of unity (100 percent) if the uranium and ionium samples are in equilibrium. The amount of departure from this 100 percent value is a measure of the extent to which the equilibrium between parent and daughter elements is upset. This method is entirely feasible for the analysis of ores and minerals in which the uranium concentration is of the order of some multiple of 0.01 percent and a small amount of thorium is present (i. e., the thorium-uranium ratio is less than 0.1).

The precision of the ionium-uranium ratio determination by this method is entirely adequate for the purpose of ascertaining the existence of equilibrium between ionium and uranium; the errors, furthermore, are of the same order as those associated with radium-uranium ratio determinations. This permits a comparison of ionium-uranium and radium-uranium values. The standard deviation of the arithmetic mean ionium-uranium ratio is never greater than $\pm 10\%$. The fact that it is impossible to carry out ratio determinations for samples in which the uranium concentration is of the order of 0.001% by this method constitutes a disadvantage. We utilize the Baranova-Kuzmina method and other methods to determine the equilibria among uranium-ionium and radium in ores and minerals at a number of deposits for which the geology has been studied thoroughly.

Our problem was the study of the quantitative relationships among the radioactive elements (uranium, ionium, radium) in ores and minerals at various points in these deposits; we were concerned more specifically with the statement of conclusions and hypotheses about the migration of uranium, ionium and radium in the hypergene zones of these deposits.

A total of several mineral samples, 67 ancient stream channel and chimney samples were analyzed. The minimum number of analyses for each sample varied between 2 and 4; all errors were within the allowable experimental range.

The samples were taken at points which were selected in order to permit an evaluation of the ores along two vertical lines from the uppermost surface of the deposits to the lowest level exposed. The weights of all samples varied between 3 and 5 kg. As far as possible, monomineralic samples, selected on the basis of examination of specimens taken from chimneys under the binocular microscope, were tested.

It is a familiar fact that a rather large number of factors control the extent to which ore bodies, in the hypergene zone are altered; the most important of these are the time elapsed since secondary processes began to act, geo-

morphology of the district, climate, structural relationships, environment in which hypergene processes occur, and the shape of the portion ore body which lies in the hypergene zone. Each of these factors entails a different hypergene history even indifferent parts of the same ore deposit.

All of the factors affecting the behavior of radioactive elements with time can be taken into account only if each factor is studied in detail and the relationships among radioactive elements is determined. Each of the deposits we studied has its own characteristic patterns of radioactive decay and ratios between pairs of elements.

A graphic presentation of the data of radioactive equilibrium (figs. 1, 2, 3 and 4) is especially convenient; here the ionium-uranium ratio is measured along the abscissa, and the radium-uranium ratio is measured along the ordinate. This type of graph permits a grouping of all of the samples analyzed into definite equilibrium value classes.

All the points which represent samples taken in the oxidized zone (at all of the deposits studied) lie above the line $\frac{Ra}{U} = 100$ percent, and to the right of the line $\frac{Io}{U} = 100$ percent; i. e. these samples are deficient in "equilibrium" uranium. Most of the samples taken in the zone of cementation lie below the line $\frac{Ra}{U} = 100$ percent and to the right of the line $\frac{Io}{U} = 100$ percent; i. e. these samples are deficient with respect to uranium and ionium. Each deposit has its own characteristics, however, within the larger framework of these relationships.

The samples taken from the oxidized zone in the first deposit which we studied (fig. 1) may be divided into three groups with respect to the relationships among uranium, ionium and radium. It turned out that the samples were taken from various portions of the deposit. The samples which exhibited a considerable excess of radium and equilibrium between ionium and uranium (samples nos. 1-4, fig. 1) were taken from only slightly jointed igneous rocks which were enriched with respect to iron and manganese hydroxides. The radium excess apparently is consequent upon the absorption of the elements by these compounds. This adsorption had occurred within the last 15,000 years; otherwise the excess radium would have decayed until it had attained equilibrium with ionium.

The second group of samples taken from the oxidized zone of this deposit (sample nos. 5-7, fig. 1) exhibit equilibrium between radium and ionium, and a considerable uranium deficiency. These samples were taken from intensely fissured and folded igneous rocks with iron and manganese hydroxides. The weakly carbonate

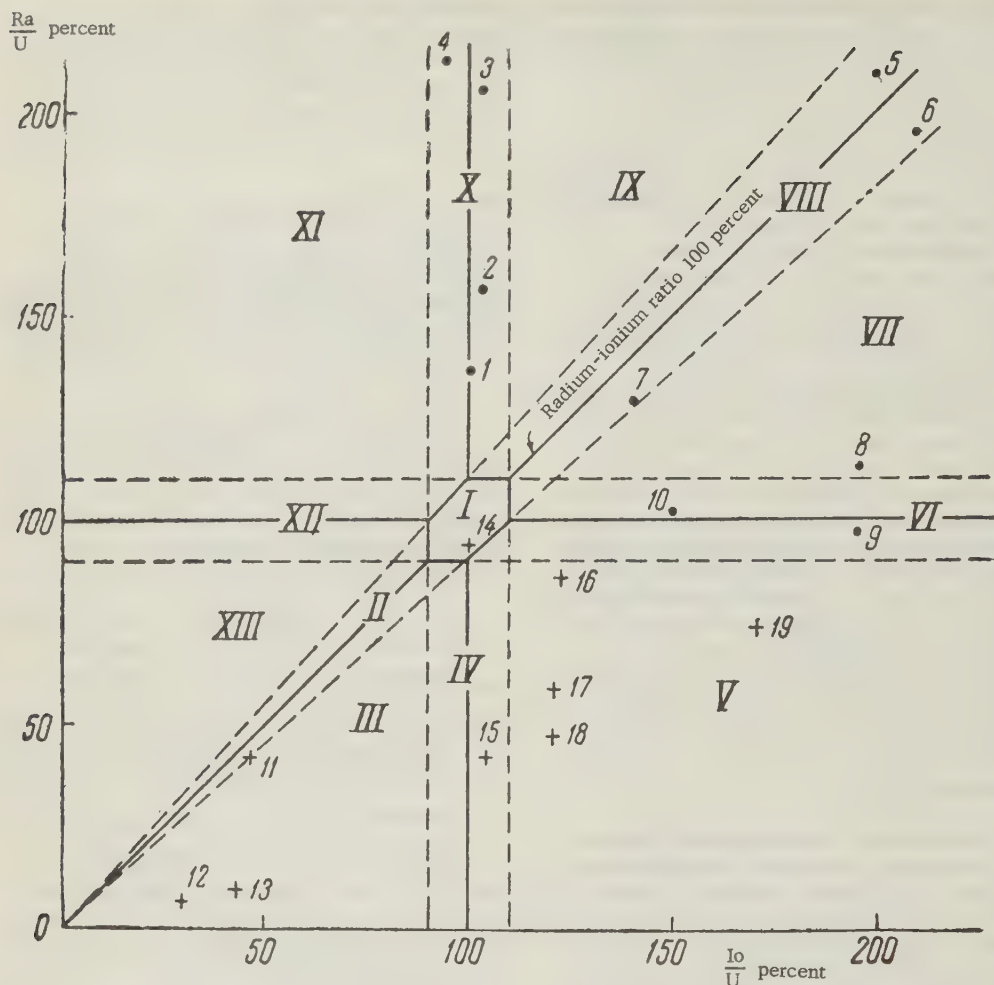


FIGURE 1. Proportions among uranium ionium and radium in samples taken from veins at first deposit. Fields on graph: I. Field of uranium-ionium-radium equilibrium; II. excess of uranium over ionium and radium; III. excess of ionium over radium, and uranium over ionium; IV. excess of ionium and uranium over radium; V. excess of ionium over radium and (to a smaller degree) over uranium; VI. excess of ionium over uranium and radium; VII. excess of ionium over uranium and (to a smaller degree) radium; VIII. excess of ionium and radium over uranium; IX. excess of uranium over radium and radium over ionium; X. excess of radium over uranium and ionium; XI. excess of radium and (to a smaller degree) uranium over ionium. XII. excess of uranium and radium over ionium; XIII. excess of uranium and (to a smaller degree) radium over ionium. Samples taken in oxidation zone represented by dots; samples taken in cementation zone represented by crosses

circulating waters here apparently removed only the uranium; the radium and ionium seemed to have remained in place. The removal of the uranium must have occurred over the last 500,000 years; otherwise the excess ionium and radium will have decayed to values at which equilibrium with uranium would have been established.

The third group of samples taken from the oxidized zone (sample nos. 8-10, fig. 1) exhibited a considerable excess of ionium and small amounts of uranium and radium; the latter two elements generally were in equi-

librium. These samples were taken from strongly fissured igneous rocks which, however, did not carry iron and manganese hydroxides. The same weakly alkaline carbonate waters apparently removed the uranium and radium here.

The samples taken in the cementation zone of the deposits (nos. 11-13, fig. 1) exhibited a large excess of uranium over ionium and radium; this may well have been consequent upon deposition of uranium, due to reduction of the latter element from the hexavalent to the tetravalent state, over the last 500,000

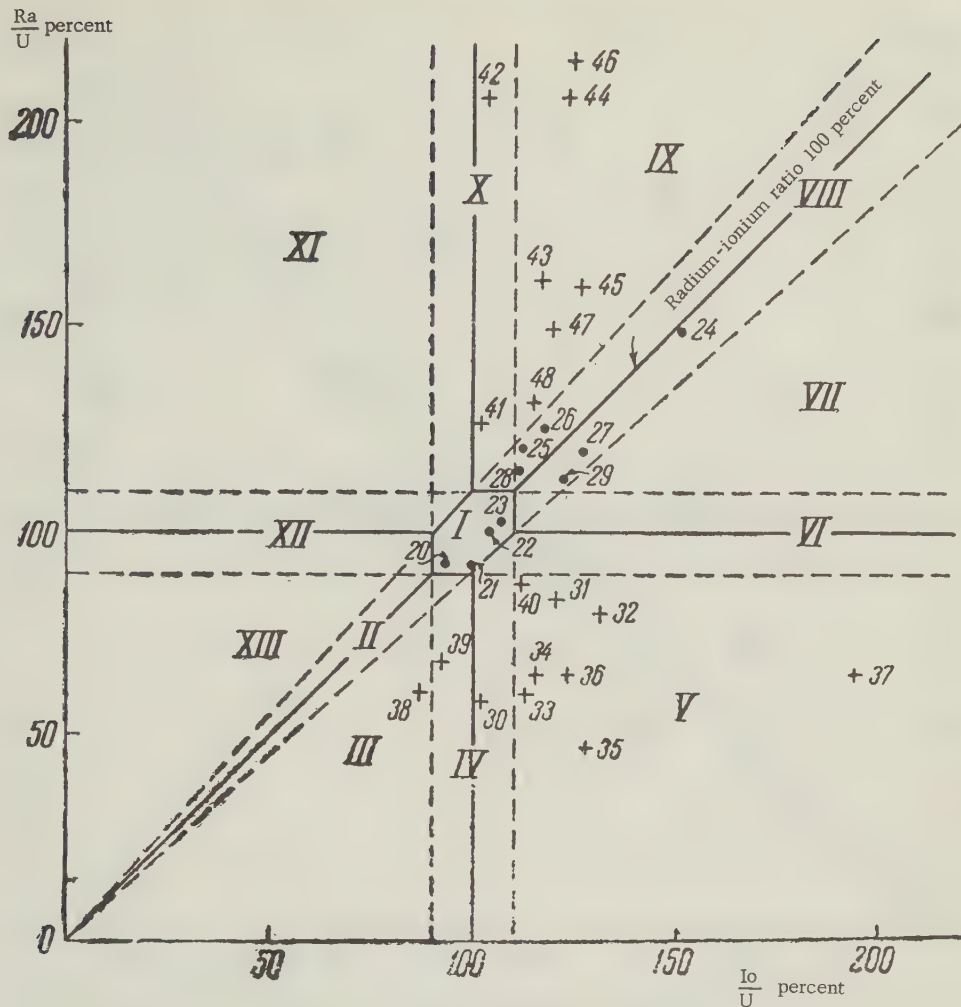


FIGURE 2. Proportions among uranium, ionium and radium in samples taken from veins at second deposit (Symbols the same as in figure 1)

years. The reduction of the valency of the uranium would have been consequent upon the presence of water with hydrogen sulfide in solution and minerals with bivalent iron. Ionium and uranium were in equilibrium, or nearly so, in the other samples (nos. 14 and 15, fig. 1) taken at this deposit. The samples in which equilibrium is approached closely but not attained (nos. 16-19) apparently were taken in the uppermost portions of the zone of cementation, where the beginning of removal of small amounts of uranium is to be observed in addition to a removal of radium. The amount of radium in almost all of the samples taken in the zone of cementation is not sufficient for equilibrium with uranium and ionium, i. e. this element has been undergoing removal by ascending hydrocarbonate-chloride-sodium waters during the last 15,000 years. An excess of radium over uranium in the circulating waters confirms this. The equilibrium among uranium,

ionium and radium in the samples taken from the second deposit which we studied (nos. 24-29, fig. 2) is either disturbed very slightly in the direction of a uranium deficiency or not at all (nos. 20-23, fig. 2). These samples were taken from veins; a comparison with uranium-ionium-radium relationships in secondary uranium mineral samples taken in the same zone there fore becomes a matter of considerable interest (see table 1 and fig. 4, nos. 1 and 4-8).

The equilibrium in the secondary minerals is shifted slightly in the direction of a uranium deficiency with respect to ionium and more strongly in the direction of a radium deficiency. The ionium-uranium ratio is such that an age of 27,000 years can be computed in only one mineral sample, a sample which consists of sharply defined tabular crystals of autunite which exhibit no marks of solution or corrosion.

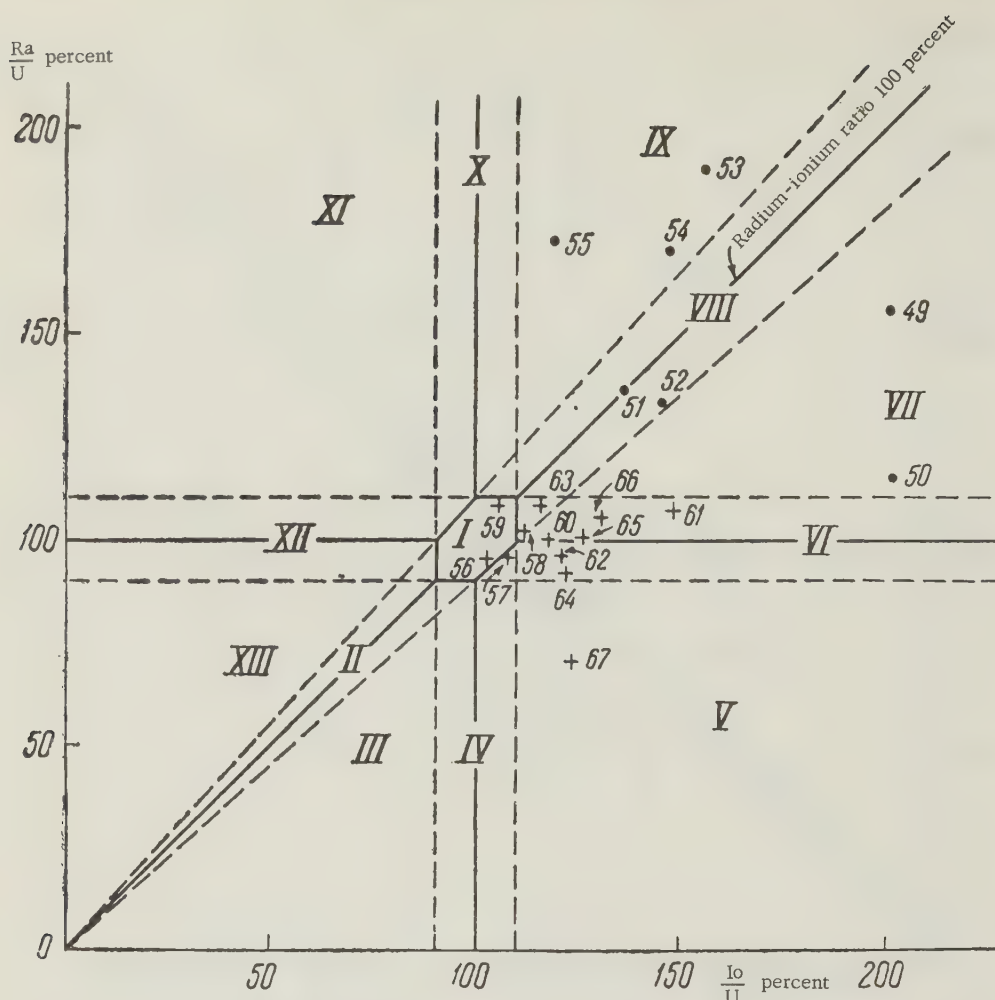


FIGURE 3. Proportions among uranium, ionium and radium in ore samples taken at third deposit
(Symbols the same as in figure 1)

TABLE 1. Experimental radioactive decay equilibrium values for uranium minerals

Sample no.	Mineral	$\frac{\text{Ra}}{\text{U}}$	$\frac{\text{Io}}{\text{U}}$	$\frac{\text{Ra}}{\text{Io}}$
1	Orlite	83	113	73
2	Torbernite	not determined	89	not determined
3	Uranophane + β - uranotyl	not determined	136	not determined
4	Kasolite	82	104	78
5	Uranophane I	75	117	64
6	Uranophane II	70	122	57
7	Uranospinite	66	112	59
8	decomposed uraninite - with uranium silicates	84	123	68
9	β - uranotyl I	101	100	101
10	β - uranotyl II	97	112	86
11	Autunite	1.7	20	8.5
12	Residual pitchblende	111	136	81
13	Regenerated-pitchblende	31	165	19
14	Uraninite I	96	100	96
15	Uraninite II	97	110	88
16	Uraninite III	92	100	92
17	Uraninite IV	4.4	10	44

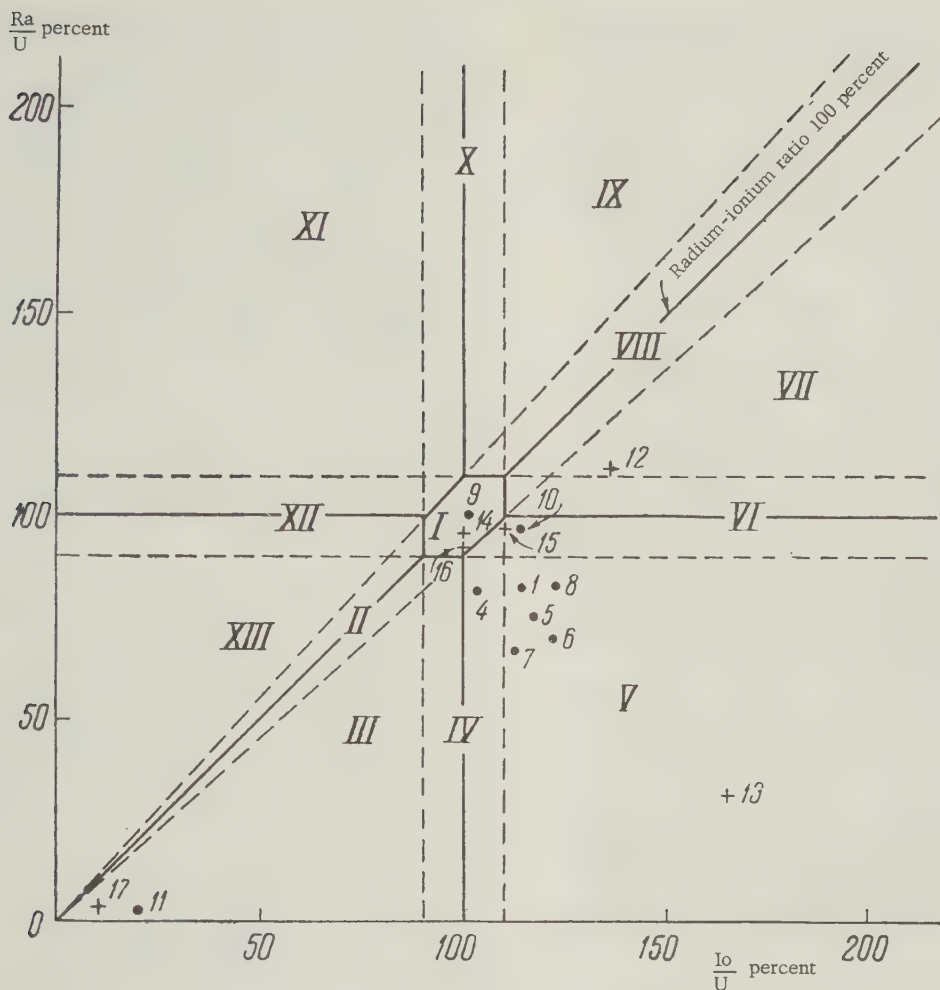


FIGURE 4. Proportions among uranium, ionium and radium in uranium minerals (Symbols the same as in figure 1)

These values are only rough approximations, inasmuch as the presence of relatively small amounts of radium indicates that the rock from which the samples were taken were attacked by secondary decomposition processes. These processes may have taken the form of leaching and possibly solution along minute and invisible hair cracks, capillaries; such alteration processes can entail profound changes in the ionium-uranium ratio.

Such relationships among radioactive elements, more specifically, can arise in secondary uranium minerals, in the main, if radium is leached out, and to a lesser degree because of the removal of uranium if the mineral undergoes partial solution. The leached radium minerals will be taken up by the surrounding rock if the circulation involves small amounts of water, and the water is alkaline. This is why we observe radium-uranium equilibrium in veins; minute amounts of uranium, however,

are carried somewhat further. A nearly negligible excess of ionium over uranium is observed in many samples taken from the cementation zone (see fig. 2.) This indicates that uranium was removed from some portions of the deposits over the last 500,000 years. This removal may have been consequent upon the circulation of weakly acid hydrocarbonate calcium waters. These samples, however, may be divided into two groups with respect to the behavior of the radium which they contain: the first group (sample nos. 30-40, fig. 2) is characterized by a considerable excess of ionium and uranium over radium.

It should be noted, however, that the amounts of uranium in these samples are generally less than those which would indicate equilibrium with ionium. These samples were taken from an ore body which actually consisted of soft, mylonitic igneous rock, virtually saturated with hydrous aluminum silicates and pitchblende. Here ap-

parently the radium and uranium were removed simultaneously by weakly acid hydrocarbonate-sulfate waters. The radium was sorbed by the intensely jointed country rock; this last inference was drawn on the basis of the uranium-ionium-radium ratios in the second group of samples; these samples were enriched strongly with radium and were taken from fine-grained country rock with especially low permeability (sample nos. 41-48, fig. 2).

The enrichment of such deposits with respect to radium is consequent upon the deposition of this element, and not only upon the removal of uranium; this can be inferred from the uranium-ionium-radium relationships.

It is not clear as yet which factor promotes the sorption of radium. It is possible that the chemistry of the waters which carry the radium and uranium undergo change. Apparently these waters undergo leaching and slow down when they pass from the open joints occupied by mineral grains into fine cracks, capillaries and pores. It is quite possible that the properties and composition of the host rock control the deposition of radium.

Many writers have noted similar relationships; a considerable excess of radium in rock samples poor in uranium and considerable radium deficiency in samples rich in uranium. This type of relationship may be due to the fact that the samples with small amounts of uranium are taken from ore bodies in which radium deposition has been intensive, and samples with large amounts are taken from bodies where circulating waters have removed radium.

The primary uranium minerals (e.g. uraninite) which we studied exhibited ratios between radioactive elements close to equilibrium values (sample nos. 14-16, fig. 4); this indicates good preservation of the minerals and the fact that the minerals came into being more than 500,000 years ago.

We encountered non-equilibrium relationships among uranium, ionium and radium in only one well-preserved sample (sample no. 17, fig. 4). It is entirely possible that this sample is of hypogene origin and has an age of the order of 10,000 years.

Interesting relationships among the radioactive elements were observed in pitchblende samples taken in the zone of cementation. The excess of ionium over uranium and radium in a sample of residual pitchblende indicates (most probably) a removal of uranium and radium at a substantially faster rate than ionium, i.e. the pitchblende can be regarded as having been subject to decomposition. A "regenerated" pitchblende sample exhibits an equilibrium shift in the direction of an ionium

excess. This points to the action of a large number of secondary processes which find expression as the decomposition of uranium in a reducing environment, which constitutes the zone of cementation during the early stages, when erosion lowered the zone of oxidation. An excess of ionium and radium over uranium is characteristic of the samples taken from the third deposit we studied [3]. The radium-ionium ratio is variable; it exhibits a deficiency of radium at some points, and excess at others. The ratios between radioactive elements indicate what is probably a removal of the uranium from the oxidized zone during the last 500,000 years (otherwise the excess ionium would have decayed until only the amounts necessary for equilibrium with uranium would have remained). The solution of uranium minerals (autunite) by the action of weakly alkaline hydrogen-carbonate-sodium waters and the formation of readily soluble higher compounds probably caused the removal of the uranium.

Radium is removed simultaneously with uranium, especially in intensely fissured rocks in which circulation is strong (sample nos. 49 and 50). Only uranium is removed at other points (sample nos. 51 and 52), and a deposition of radium occurs at still other points (sample nos. 53-55); this may be consequent of the fact that the radium is taken up into radiobarite, inasmuch as this mineral is present in the deposit. The radium was deposited during the last 15,000 years; otherwise the excess would have decayed until only the amount necessary for equilibrium with ionium would be left. The uranium, ionium and radium are in equilibrium in samples taken in slightly fissured, highly quartzose rocks in the cementation zone of the third deposit. This indicates that no transport of the uranium and ionium occurred during the last 500,000 years, and that no transport of radium occurred during the last 15,000 years.

A negligible uranium and radium deficiency is observed in samples (nos. 60-67, fig. 3) taken from more intensely fractured rock. The removal of the radium and uranium, apparently, has been consequent upon the action (circulating) weekly acid sulfate waters.

It is possible, then, to draw the following conclusions:

1. Hypogene uranium deposits may be identified by studies of equilibria among radioactive elements. This becomes especially important in deposits in which mineralogy cannot be taken as an indication of ore grade, and the extent of the radioactive equilibrium is the only reliable indicator of migration. The identification of hypogene zones is necessary for a prediction of the variation of ore grade with depth.

2. The uranium-ionium-radium proportions

permit the identification of sections with different characteristics and different intensities of removal and replacement; this is impossible on the basis of only the radium-uranium ratio. The identification of such sections is especially important in radioactivity mapping and reserve estimates. The identification of intensely fractured sections and beds, in addition, is important for metal reserves conservation, inasmuch as uranium is removed from such rocks most readily. The conservation aspect becomes particularly important when we remember that a change in the position of the water tables, consequent upon mining operations, may entail a rapid decomposition of uranium minerals.

3. The proportions among the radioactive elements is the basis upon which the migration of these elements is inferred. Uranium and radium are the most mobile elements in the hypergene zones of the deposits we examined, and ionium is the least mobile; uranium is the most mobile element in the zone of oxidation, and radium the most mobile element in the zone of cementation.

4. Rough estimates of the time intervals over which uranium, ionium and radium migrate are possible on the basis of the proportions among these elements. This is particularly important for the interpretation of either extremely large or extremely small concentrations.

5. Migration as well as radioactive decay controls the proportions among the elements in secondary uranium minerals. It is impossible, therefore, to determine the age of such minerals on the basis of uranium-ionium-radium proportions alone.

The study of the migration of radioactive elements with the aid of equilibrium proportion data will, without doubt, find broad application in geology and exploration. It will obviously be necessary, in the future, to increase the number of elements for which proportions are determined, and increase the sensitivity of the methods by which radioactive elements are located, in order to interpret correctly abnormal radioactivity in poorly consolidated Recent sediments, and facilitate the evolution of radioactive element proportion-determinations into a field method.

REFERENCES

1. Baranov, V. N., and Kuzmina, L. A., IONIVY METOD OPREDELENIYA VOZRASTA MORSKIKH ILOV [AN IONIUM METHOD OF AGE DETERMINATION FOR SEA BOTTOM SEDIMENT]: Doklady Akademii Nauk, SSSR, Nov. Ser., v. 97, no. 3, 1954.
2. Bressler, S. E., RADIOAKTIVNYE ELEMENTY [THE RADIOACTIVE ELEMENTS]: State Engineering Theory Publishing House, Moscow and Leningrad, 1952.
3. BYULLETEN KOMISSII PO OPREDELENIYU ABSOLYUTNOGO VOZRASTA GEOLOGICHESKIKH FORMATSII [BULLETIN OF THE COMMISSION OF THE ABSOLUTE AGE OF GEOLOGIC FORMATIONS]: Report no. 1, Akademii Nauk SSSR, Moscow, 1955.
4. Kurbatov, I. D., O SOOTNOSHENIYAKH AKTIVNYKH ELEMENTOV DISPERSNYKH MASSAKH TYUYA-MUYUNA [RELATIONSHIPS AMONG ACTIVE ELEMENTS IN DISPERSE COMPLEXES OF THE TYUYA-MUYUN]: Doklady Akademii Nauk, SSSR, no. 17, 1930.
5. Kurbatov, I. D., Karzhauvina, N. A., and Samoilov, N. A., OPISANIYE METODA PRIGOTOV LENIYA RASTVOROV DLYA OPREDELENIYA IONIYA V DISPERSNYKH MASSAKH TYUYU-MUYUNA [PREPARATIONS OF SOLUTIONS FOR IONIUM DETERMINATIONS IN THE DISPERSED SYSTEMS OF THE TYUYA-MUYUN]: Doklady Akademii Nauk, SSSR, no. 4, 1930.
6. Melkov, V. G., MINERALOGO-GEOKHIMI CHESKIYE OSNOVY POISKOV, URANA MATERIALY PO POISKAM REDKIKH ELEMENTOV [MINERALOGICAL AND GEOLOGICAL PRINCIPLES OF URANIUM EXPLORATION CONTRIBUTIONS ON TRACE ELEMENT EXPLORATION]: Gosgeoltekhizdat, 1947.
7. Pylkov, A. N., POLYCHENIYE PREPARATA IONIYA IZ FERGANSKOY RUDY [CONCENTRATING IONIUM FROM FERGANA BASIN ORES]: Doklady Akademii Nauk SSSR (A), 1928.
8. Starik, I. Ye., and Melikov, O. S., K VOPROSU O MIGRATSII IONIYA V PRIRODNYKH USLOVIYAKH [THE PROBLEM OF IONIUM MIGRATION IN NATURE]: Doklady Akademii Nauk SSSR, Nov. Ser. v. 31, no. 9, 1941.
9. Starik, I. Ye., and Shchepotieva, Ye., METODY OPREDELENIYA RADIOAKTIVNOSTI PRIRODNYKH OBRAZOVANII [MEASURING AND RADIOACTIVITY IN FORMATIONS]: Gosgeoltekhizdat, 1946.
10. Khlopin, V. G., K VOPROSU O MIGRATSII RADIOELEMENTOV V ZEMNOY KORE [THE MIGRATION OF RADIOACTIVE ELEMENTS IN THE CRUST]:

INTERNATIONAL GEOLOGY REVIEW

- Doklady Akademii Nauk SSSR (A)
September, 1926.
11. Khlopin, and Pasvik, M. A. MIGRATSIYA
URANA I RADIYA V PREDELAKH
GLAVNOI ZHILY TYUYA-MUYUNA
[MIGRATION OF URANIUM AND RADIUM
IN THE MAIN VEIN, TYUYA-MUYUN]:
in: IZUCHENIV URANA [STUDIES IN
URANIUM], v. 3, Akad. Nauk SSSR,
Leningrad, 1928.
12. Hude, TRANSURANIUM ELEMENTS, v. 2,
p. 1435, 1949.
13. Marckwald, W. and Russel, A., Radioakt
u. Elektronik, Bd. 8, no. 4, p. 548, 1911.
14. Picciotto, E. and Isaac, N., Nature, v. 171,
no. 4356, p. 742, 1953.
15. Picciotto, E. and Wilgain, S., Nature, v. 173,
no. 40405 [4405?], p. 632, 1954.

GEOLOGIC RECONNAISSANCE OF THE EASTERN PART OF THE MOUNTAINS IN QUEEN MAUD LAND, ANTARCTICA¹

by

M.G. Ravich, P.S. Voronov, L.V. Klimov and D.S. Solovyev

translated by Douglas Alverson

ABSTRACT

This reports on a four-man geologic reconnaissance of the eastern part of the mountains of Queen Maud Land, Antarctica. The German "Schwabenland" expedition of 1938-1939 had previously reported the so-called "oases" of ice-free lakes and dry land in the area. A description of the physiography and glaciology of the area includes a description of ice-character, fissures, heights of shelf and continental ice fields, and the nature of the coastlines. The "oases" include bedrock rolling lowlands, a nunatak zone, and block mountains. The geologic structure exhibits fault systems, block mountains, and some folding. Igneous and metamorphic rocks occur but no sedimentaries. Speculation on the development of known and probable mineral occurrences concludes that no great transportation difficulties would arise in mining and shipping ores. --D. C. Alverson

In February, 1959, a geologic party of the Fourth Soviet Antarctic Expedition, composed of M. G. Ravich (party chief), P. S. Voronov, L. V. Klimov, and D. S. Solov'yev, made a reconnaissance of the eastern part of the mountains in Queen Maud Land. The main area of investigation included the northern spurs of the mountains between 9° 25' E. and 18° 37' E., a distance of more than 300 km. A field camp was established in the center of the area, at 71° 19' S., 13° 13' E., at the base of the Wohlthat massif and 150 km south of Lazarev Station on the Princess Astrid Coast. Aerial flights totalling 1500 km were made in the mountains, and on the ground 10 localities were examined, at which 350 specimens were collected.

This region was first visited in 1938-1939 by the German expedition commanded by Captain A. Ritscher, which came to the Antarctic in the ship "Schwabenland." This expedition made geographic and meteorologic observations, and, examined the continent from the air, between 4° W. and 16° E., and up to 500 km inland, an area of about 350,000 sq km. Members of the expedition did not land on the continent. The main achievement of the expedition was the discovery of a high mountain belt about 150-200 km from the coast. By their intensive use of oblique aerial photographs, the German investigators were able to delimit this belt on the map of Antarctica, and very precise maps² at

scale 1:50,000 were compiled for two mountainous regions of the eastern part of Queen Maud Land. They were of considerable help in carrying out land and aerial geologic investigations in the south polar summer of 1959.

The German expedition took colored motion pictures from the air of an ice-free area of low, rocky hills and ice-free lakes (Schirmacher Lakes) entirely surrounded by ice. Thus a new type of landscape of Antarctica was discovered, which subsequently received the name "oasis" in the literature. By office study of the aerial survey data, the German scientists undertook the first attempt to give an orographic and geologic description of the regions which had been photographed. In a number of instances, however, this attempt led to erroneous results. For example, sequences of ancient schists were interpreted by them to be normal sedimentary rocks.

In the area under investigation, as elsewhere on the Antarctic continent, two principal types of relief should be differentiated: relief of the ice surface, and relief of the bedrock surface. The first type is underlain by snow and ice, and is quite characteristic of Antarctica, whereas the second type is underlain by rocks.

Among the macroforms of ice relief in this area are the coastal belt of shelf ice, and the border zone of the Great Ice Sheet. It is typical that the so-called "outlet glaciers", so common in the rest of Antarctica, are absent in this part of Queen Maud Land.

The average width of the ice shelf is 50 km. Almost everywhere its seaward edge floats on sea water, and is indented by a considerable number of angular bays and inlets, the waters

¹ Translated from *Rekognostsirovocnyye geologicheskiye issledovaniya vostochnoy chasti gor na Zemle Korolevy Mod v Antarktide: Informatsionnyy Byulleten Instituta Geologii Arktiki*, no. 16, 1959, p. 30-36.

² Another expedition to this part of Antarctica found these maps quite inaccurate. See Giaever, the White Desert (Official Account of the Norwegian-British-Swedish Antarctic Expedition), New York, 1955, pp. 59, 126, 145, 148. Tr.

of which are covered with old bay ice.³ Between 13° and 16° E., the shelf ice forms a peninsula | extending 80 km to the north. This peninsula was discovered by the German expedition in 1938-1939, but was shown incorrectly on their map as considerably to the west of its actual position. In 1959, Soviet investigators corrected this error and named the peninsula "Lazarev Ice Shelf". Lazarev Station (69° 58' S., 12° 55' E.) was built on its west coast, on the south shore of a long curved bay.

To the south of Schirmacher Oasis, the elevation of the ice surface begins to increase rapidly, and at the northern edge of the mountain belt, about 130-150 km from the Antarctic Ocean, it reaches 1,000-1,500 m. The mountain belt is a serious obstacle on the route of movement of the ice mass from the interior of the continent. At the southern edge of the belt, the surface elevation of the ice sheet is 2,500 to 3,000 m. The mountains thus create a 1,500 m north-south difference in elevation of the ice surface.

Inspection of the Lazarev Ice Shelf from the air confirmed the German scientists' hypothesis that a considerable part of it rests on islands or submarine banks. The presence of shallow water at some points along the coast, and hillocks and projections of crevassed light blue ice on the surface of the Lazarev Ice Shelf tend to confirm this. However, the ice surface is mainly flat, snow-covered, and rises evenly toward the interior of the continent. Near Schirmacher Oasis the shelf ice is gradually replaced by continental ice of the border zone of the Great Ice Sheet. Surface elevations of the ice mantle here average 150-200 m, while at the coast, elevations range from 30 m to 50 m.

Part of the ice does penetrate through to the north along narrow fault valleys, which cross the mountain belt in a number of places. In such instances, valley glaciers and hanging glaciers are common. There are also many avalanche and cirque glaciers in the mountains. However, the main outflowing of ice in this part of East Antarctica occurs at the eastern end of the mountain belt, along 15° - 16° E. Many crevasse zones and domes and ridges of light blue ice, features which indicate an uneven ice floor and more intense ice movement, are visible on the ice surface in this area.

The width of the ice crevasses is usually several meters, but in some instances reaches 15-20 m. Crevasses showing vertical displacement are quite frequently encountered. In addition, plicative distortion of the ice mantle is shown by bends in bands of morainal material. Most of the crevasses are covered by snow

bridges.

On the whole, the surface of the ice sheet may be characterized as a snow covered plain with numerous sastrugi⁴ trending east and south-east. The first system of sastrugi is formed by cyclonic winds, but the second is formed by the drainage type gravity winds of the Antarctic. On the surface of the ice sheet along the northern border of the mountain belt there is a wide zone of meltwater formation, the result of intense solar radiation. This zone is characterized by many small depressions in light blue ice, creating a very distinctive corrugated surface that is dangerous to the skis of landing aircraft.

On the ice surface near Schirmacher Oasis, there is a complex dendritic network of streams and creeks which collects meltwater into the lakes around the oasis.

Bedrock relief of this area may be subdivided into three categories: 1) low, rocky hills (Schirmacher Oasis); 2) the nunatak zone; and 3) the block mountain belt mentioned above.

Schirmacher Oasis occupies an area of about 30 square kilometers, and in plan has an elongate shape extending to the east-southeast, coincident with the strike of the bedrock which underlies it. The round hills of the oasis and the basins between them bear distinct traces of glacial scour. Elevations of the hilltops and dry basin bottoms range from 50 to 200 m. Many of the basins are occupied by lakes with fresh, probably relict, water. It is quite possible that the oasis is an area of the bedrock coast which has been freed from its ice mantle.

To the south and southeast of the Oasis there is a zone of nunataks, with elevations up to 2,200 m. One group of nunataks is situated between the oasis and the mountain belt, and another is the eastern continuation of the mountain belt beneath the ice (the nunataks Forposten, the Payer group, the Russkiye Mountains, etc.). The height of the nunataks above the surface of the ice sheet usually does not exceed 300 m.

A system of valley glaciers, of various widths, subdivides the mountain belt into a number of separate mountain massifs and ranges, such as the Wohlthat massif, the Humboldt massif, the Konrad Range, and others. All of them are situated in a belt up to 60 km wide, which has an undeviating northeast strike.

³ bay ice: sea ice remaining in its position of growth in bays and inlets along the coast. Tr.

⁴ sastrugi: long, low, linear, usually ridgelike dunes of snow or firn; where linear, generally aligned parallel to the direction of the prevailing wind; usually not over two feet high, but may reach several hundred yards in length. Tr.

From the Konrad Range the mountain belt may be traced further to the east towards Coats Land for a distance of several hundred kilometers. As a whole, this mountain belt is a complex system of sharply ribbed rocky heights, appearing as separate peaks and sharp, jagged ridges. Their elevations reach 3,000-3,500 m.

Most of the mountain peaks of this area, including the nunataks, have a definitely alpine appearance, which is caused mainly by the unusual force of the physical rock-weathering processes. At the same time, the mountains themselves are young, of fault-block origin, and their uplift doubtless continues at the present time. Only in this way can the great elevations of the mountains be explained, in view of the rapidity of their destruction by the action of frequent sharp changes of temperature and winds of hurricane force.

Enormous masses of fragmental material, from fine-grained sediments to angular rock fragments of various sizes, are the products of this physical weathering, and they form broad, thick diluvial debris trains around the mountains, gradually grading into wide moraine fields. A study of the material in moraines showed that in this area there are two types of moraine. The first consists of fragments of local rocks, and the second, of well-rounded "foreign" rocks, which came from somewhere in the interior of Antarctica in an epoch of more intense glaciation. In spite of very careful search, nowhere were fragments of sedimentary rock found. The morainal material consists entirely of Precambrian igneous metamorphic rocks.

Several varieties of schist and gneiss of the deep granulite facies of regional metamorphism are present in the eastern part of the mountains in Queen Maud Land. On the whole they are rather poorly migmatized, but in places contain many concordant or discordant veins of pegmatites, and, more rarely, of leucocratic granites and aplites. The vast majority of the schists and gneisses are noticeably cataclastic, and in places brecciated, forming typical porphyroclastic rocks. All these rocks probably date from the early Precambrian, by analogy with other regions of East Antarctica, where schists and gneisses comprise the crystalline basement of the East Antarctic Platform.

In the Konrad Range (Lodochnikov Mountains) there is a large massif of porphyritic granite with veins of various fine-grained granitic rocks, including some syenite and lamprophyre, that is younger than the gneisses. Such massifs and accompanying vein facies are probably rather abundant within this area, as the rocks comprising them were found continually as boulders in many moraines. In several parts of the area there are individual dolerite dikes.

At least five main groups can be distinguished among the schists and gneisses: 1) garnet-biotite, in places garnet-sillimanite-biotite gneiss, predominantly mesocratic and leucocratic; 2) biotitized pyroxene gneiss and schist, predominantly melanocratic; 3) granulite with pyroxene or garnet, predominantly leucocratic; 4) amphibolite and amphibole-biotite schist; and 5) marble, calciphyre and diopside rocks with scapolite or amphibole.

In addition, there are gneissic and cataclastic basic intrusive rocks, including anorthosite and anorthosite dikes.

Boulders and fragments of granitic rocks, gneiss, and schist predominate in the composition of the morainal deposits; rarely dolerite boulders, and exceptionally fragments of metamorphic greenschists are noted. Although our investigations were brief, the above tends to confirm the supposition that in this area Paleozoic formations are of small extent, or are completely lacking. The andesites and trachyandesites found as boulders appear to be Cenozoic, but may be Mesozoic.

Without describing the rocks listed above in detail, some general features in the geologic structure of this area, which differentiate it from other areas of the crystalline basement of the East Antarctic Platform, will be stressed.

Together with the predominance of the usual types of gneiss and schist of the granulite facies, the calciphyres and diopside rocks have wide development. The latter more or less equally saturate all sequences of gneisses, independently of their composition. This indicates the wide development of sedimentary formations in the Precambrian rocks, which served as initial material for the formation of the regionally metamorphosed rocks.

Migmatization of the gneisses and schists occurred weakly, which indicates that this area is in the peripheral part of the regional zone of migmatization. Veins of pegmatite, and sometimes aplite, which are related to the latest stages of migmatization, predominate here. The absence of migmatite fields, of whatever thickness, is characteristic of these rocks. The formation of migmatites has a particularly local character, and is related mainly to the intrusion of residual melts of quartz-feldspar composition.

The processes of deep cataclasis and related partial recrystallization of metamorphic rocks in the solid state are developed only exceptionally. The rather constant trend of the gneiss and schist is marked; a latitudinal or sub-latitudinal strike and south-southeast or northwest dip seem to be characteristic. All of the small but widespread deviations from the indicated attitudes are connected with folding, which took place everywhere in the period of regional metamorphism. The extreme variations in dip angles, from 20°-30° to

60°-70° and even vertical angles, is explained by the variable character of the folds at various points in this area; some are wide and flat, others are narrow and steep, or even isoclinal.

Regional faulting is widely developed in two systems. The southwest trending faults subdivide the mountains into a number of uplifted blocks and depressions, which are filled by glaciers and without bedrock outcrops; such depressions are located in areas bounded by 16° and 17° E., 13° and 14° E., and 10° and 11° E. The north-northwest trending faults in turn break up the uplifted blocks into separate mountain chains, with the same trend. The time of faulting is as yet unknown. However, as the faults are rather old, movement on them probably has been renewed periodically, especially from the earliest Tertiary to the beginning of glaciation.

The large massifs of porphyritic hornblende granites with vein facies of fine-grained granites, porphyritic granodiorites and aprites, are younger than the gneisses and schists. The dikes of normal dolerite were formed still later. The youngest rocks are possibly the granosyenite porphyry dikes.

The discovery of mineral deposits was not to be expected during such short and hurried investigations of such an extensive area as the eastern part of the mountains of Queen Maud Land. However, the rich disseminations of graphite in the calciphyres of the Zhelannaya Mountains, and the pegmatite veins in the northern spur of the Konrad Mountains may be counted as discoveries.

It may be presumed that industrial deposits of pegmatitic muscovite are present in a number of extensively muscovitized pegmatite veins formed in alumina-enriched gneisses.

The discovery of industrial phlogopite is quite probable in veinlike diopside-scapolite bodies, where veinlets of fine, flaky phlogopite have been found (Forpost Mountains, Zhelannaya Mountains, etc.). Discoveries of rich iron ores, together with boron minerals, are quite possible in metamorphic bodies related to regionally metamorphosed sequences of former carbonate beds. The weak degree of migmatization of this area is favorable for

concentrations of ore minerals.

These are not the only discoveries determining the prospects of the area with regard to mineral deposit exploration. Also favorable are large massifs of granitic rocks and other intrusive bodies, with typical discordant contacts, massive shape and numerous veins of different types developed in and around them. Many such massifs were observed during aerial reconnaissance flights. A complex of hydrothermal ore deposits may be related to each such intrusion.

In view of the short duration of the investigations, it is not possible to clarify further the geologic structure and the prospects for mineral deposits exploration of these block mountains in Queen Maud Land, which extend almost 900 km latitudinally from 18° E. to 6° W., most parts of which are still unexplored. Our investigations confirmed the presence of an extensive mountain area, for the most part well exposed, and of area not less than 60,000 sq km, in the interval 18° to 4° E. The first information on the geology of this region, presented above, indicates the possibility of discovery of a number of valuable mineral deposits within it.

This mountainous area is not far south, only 150-200 km of the Antarctic coast. At the center of this part of the coast the new Soviet Lazarev Station has been built. The shelf and continental ice on the route to the mountains is suitable for movement of mechanized land transport. The absence of crevasses along almost the whole north ice border of the mountains, and also the presence of excellent sites for ice airfields, suitable for practically any type of aircraft, at the foot of the mountains, make work in them possible, with the help of all types of modern air and land transport.

All this permits us to recommend further study of the mountain belt with the aims of making a geologic map of scale about 1:1,500,000, understanding the geologic structure and prospects for mineral deposit exploration, and solving a whole series of theoretical problems related to the genesis of regionally-metamorphosed and ultra-metamorphic rocks, and to the processes of neotectonics and contemporary glaciation.

ON THE AGE OF METAMORPHISM IN THE JAPANESE ISLANDS¹

by

Masao Minato²

translated by Reiko Fusejima

ABSTRACT

The distribution, lithology, and previously held theories on age of metamorphic activity in Japan are outlined. Precise age determination of each metamorphic complex is still uncertain. The latest was probably Miocene, the earliest either Precambrian or as late as Devonian. Miocene metamorphism affected the so-called green tuff region of the Inner zone of Japan. The Hida gneiss is the result of the oldest age of metamorphism. Absolute age determination of 230×10^6 years has been made of minerals in the Ryoke gneiss although recurring metamorphism has been shown for its area. Considerable granite emplacement occurred during the Cretaceous and early Tertiary. The age of metamorphism resulting in the Sambagawa-Mikabu complexes is much in dispute but is probably older than late Triassic. --M. Russell.

INTRODUCTION

A considerable number of metamorphic zones have been defined in the Japanese Islands. It is questionable, however, whether the division of these zones was reasonably based on geologic structures. Some zones may manifest only the geographic distribution of metamorphic rocks.

Before we criticize the hitherto accepted division of the metamorphic zones, we shall review how the Japanese metamorphic rocks were treated in the discussion of geologic ages. By the "age of metamorphic rocks" is generally meant the following three different periods, i. e. 1) the time when the original rocks formed, 2) the time when metamorphism took place, and 3) the time when the metamorphosed rocks, after having been exposed, came to constitute a structural unit such as folded mountains. The present paper deals chiefly with the period of the formation of the original rocks, referring to the past hypotheses and related discussions.

The study of the age of metamorphic rocks in Japan has undergone three chronologic stages. The first stage is the middle term of the Meiji Era [T. N.; 1868-1912] when all the gneisses and crystalline schists reported by Naumann were considered Archean in age. The second stage is between the latter part of the Meiji Era and World War II, during which the original rocks of all metamorphics were thought to be Paleozoic or younger. The third stage, to the present, is characterized by the hypo-

thesis that some of the Hida gneisses and other gneisses may be assignable to pre-Paleozoic. [fig. 1 shows the distribution of the metamorphic zone of Japan].

PRE-PALEOZOIC THEORY OF THE MEIJI ERA

Edmund Naumann, Toyokichi Harada and Bunjiro Koto presumed that the Japanese metamorphic rocks, especially gneisses, are all Archean in age, as their papers reveal.

With regard to crystalline schists, however, Harada and Koto seemed to have had less confidence in the pre-Paleozoic origin than Naumann (1885) did. Harada (1890) stated that some crystalline schists in foreign countries were apparently derived from Paleozoic rocks, hence examples of such may be found in Japan, although he admitted that the greater part of the Japanese crystalline schists are older than Paleozoic.

Koto (1888) determined that the Sambagawa series is the oldest geologic system in the Kanto Mountains, but he was extremely prudent about age determination of the System. According to Koto the rocks of the Sambagawa series are on the whole similar to the rocks of Saxony, Granulit Mittel Gebirge, Arden and Tanus. It had been clarified by J. Lehman that the Saxony metamorphic rocks are a product of metamorphism of a Cambrian graywacke. Koto maintained that sericite schist of the Sambagawa series was metamorphosed from coarse-grained graywacke, epidote-sericite gneiss from fine-grained sandstone, chlorite-amphibole schist from basic tuff, and graphite-sericite schist from coaly shale. He emphasized the fact that these rocks bear a close resemblance, in their initial characteristics, to the crystalline schists southeast of Granulit Mittel Gebirge and to the Paleozoic, especially pre-Carboniferous, rocks

¹ Translated from the Japanese; in Jubilee Publication in the commemoration of Professor Jun Suzuki, M.J.A. Sixtieth birthday (1956), p. 1-16, 1958.

² Institute of Geology and Mineralogy, Faculty of Science, Hokkaido University.



FIGURE 1. Metamorphic zones in Japan

of the Chichibu district. What Koto called "pre-Carboniferous rocks" may correspond to the present Sakahara formation and the Kashiwagi formation reported by Haruyoshi Fujimoto.

Koto also noticed that the highly metamorphosed crystalline schists of the Alps are not as old as pre-Paleozoic but represent a metamorphosed facies of Paleozoic or Mesozoic rocks.

Koto did not correlate the Sambagawa system with the Precambrian bedrocks but predicted that the system represents a metamorphosed facies of Mesozoic or younger folded mountains. This revealed his excellent foresight when geologic research in Japan was still in a pioneer stage.

As mentioned already, Naumann and Harada believed that all Japanese gneisses were Archean. It must be kept in mind, however, that in those days dividing the Precambrian rocks into Archeozoic and Proterozoic was not practised as yet, so that "Archean" by Naumann and Harada meant no more than "as old as pre-Paleozoic" and not necessarily the Archeozoic of our present knowledge. As far as the antiquity of the gneisses was concerned, Koto agreed with the above two geologists. Koto divided the metamorphic rocks of the Abukuma Mountains into two parts, and assigned the lower part to Laurentian. He subdivided the upper part into the Takanuki series and the Gozaisho series in ascending order, and correlated the latter with Huronian.

Why did Koto, who showed utmost caution in dating the Sambagawa series, accept without hesitation the Archean origin for the gneisses? It is true that he was attempting a hypothesis on the stratigraphic position of the gneiss complexes, on the basis not only of the lithologic similarity but also of the distribution of metamorphic rocks hitherto reported in Japan. His attention was attracted to the zonal arrangement of gneisses which are distributed chiefly in the inner part of the Japanese Islands and are surrounded respectively by the Sambagawa series, the Mikabu series that was known as the Lower Chichibu system, and the Chichibu Paleozoic formation, in outward order. This zonal arrangement is obvious at least in central to southwestern Japan. Koto, judging from the geologic structures, inferred a great time gap between the Naumann's gneiss system and the crystalline schist system.

Thus, Koto was convinced that the gneiss system is a remnant of a shield and is Archean in age, from both the lithologic character and the structural position.

According to Koto, part of the gneiss system, for instance the Gozaisho series, consist chiefly of green massive schists originated for the

most part in pyroclastics, and part of the system consists of an alternation of green schist and quartzite or alternation of green schist and mica schist, so that the gneiss system as a whole resembles the clastopyroxinite of the Mikabu formation or the green schist of the Sambagawa series. In those days the Mikabu formation was considered a member of the lower part of the Chichibu Paleozoic formation. It is probable, therefore, that Koto expected to find part of the gneiss system separable from the bedrocks, although he apparently attributed the greater part of the gneiss system to pre-Paleozoic.

Summarizing the above, we realize that already in the beginning period of geologic research in Japan the age determination of metamorphic rocks was more or less confused. With an exception of Koto who was more or less skeptic about the Archean origin of the Sambagawa series, the majority of geologists supported the pre-Paleozoic theory for the greater part of metamorphic rocks, especially for the gneiss system. This was really a unique period in the history of the study of age determination of the Japanese metamorphic rocks.

PALEOZOIC-MESOZOIC THEORY

The second period in the history of research on the Japanese metamorphic rocks is represented by the view that no Precambrian rocks were anywhere exposed in the country.

Such a view must have been established as a result of research works of many people and gradually came to be accepted as an authentic theory. It is not easy to trace the history of theoretical vicissitudes simply through by past references. The above-mentioned theory is not so modern as some people insist, because it was advocated as early as the end of the Meiji era.

The geologic map of the Japanese Empire at scale of 1:1,000,000 published by the Geological Survey of Japan in 1898 described the metamorphic rocks as gneisses and crystalline schists, following the nomination by Naumann and Harada, whereas on the 1:2,000,000 geologic map, published in 1910 by the Geological Survey of Japan, gneisses were called schistose granites, and the Sambagawa and Mikabu formations were treated as pre-Carboniferous rocks. Thus, it is evident that the schistose granites and the pre-Carboniferous rocks were distinguished from the Precambrian metamorphics of Korea.

The first chapter of the *Geology and Mineral Resources of the Japanese Empire* (in English) published by the Geological Survey of Japan in 1929 began with a sentence "Japan seems to lack in the Archean system."

By then, the pre-Paleozoic theory must have vanished altogether. The section on the Ryoke metamorphics in the book was written by Kiyohiko Ishii who studied not only the gneisses of the Ryoke system but also other gneisses reported by Harada.

Harada's gneiss system comprises the following rocks in which he noticed a resemblance to the gneisses of the Liaotung Peninsula and Shantung Province [T. N. ; of China].

1) Kashio gneiss: Porphyroidal rock exposed at Kashio, Ina-gun, Nagano Prefecture, characterized by platy exfoliation.

2) Biotite granite: Local facies of granite gneiss (5), distributed in the Kitakami Mountains, the Abukuma Mountains, the Akaishi Mountains, in Awaji Island, in northern Shikoku, in southwestern Kyushu, at Yanai of Setouchi, and in the Sonogi Peninsula of Nagasaki Prefecture.

3) Ryoke schist: Rock resembling corubianit [T. N. ; sic] is probably a derivative of graywacke or clay slate contact-metamorphosed by granite.

4) Amphibole gneiss and amphibole schist: Distributed in Toyama and Ishikawa Prefectures, well exposed along the Miya and Takahara Rivers, consisting chiefly of granite gneiss, gneiss, amphibole gneiss and amphibolite, intercalated with crystalline limestone, tremolitic rock, graphite gneiss, granulite and quartzite.

5) Granite gneiss: Distributed in southern Kitakami Mountains and in such mountains as Abukuma, Akaishi, Suzuka, Kasagi, Katsuragi, as well as in southern Kyushu and Mino-Hida plateaus. It was considered the oldest granite in Japan.

With regard to the crystalline schist system, Harada held that the Mikabu formation in the Kanto Mountains should be separated from the Sambagawa formation and the latter be included in the crystalline schist system. In other regions, however, Harada assigned all metamorphic rocks other than the gneiss system to the crystalline schist system. For example, he regarded the rocks, which were to be grouped later into the Mikabu system of the Inner Zone, as constituents of the crystalline schist system. Therefore, not only the schists distributed in Wakayama, Shikoku, Nagasaki and Sonogi Peninsula but also the schists exposed in Abukuma, Hida, in the vicinity of the Eukiya mine of Chugoku region and near Mitsuishi of Hokkaido were all included in the crystalline schist system.

In short, according to Naumann and Harada, the gneiss system and the crystalline schist

system comprised the metamorphic rocks of all zones of metamorphism presently known as the Hidaka, Kamuikotan, Kitakami, Abukuma, Ryoke, Sangun, Motoyama, Higo, Sambagawa, Mikabu and Hida metamorphic zones. Only the Misaka and a few other zones escaped their attention.

Then, what was the reason that the age of those metamorphic rocks, which had once been believed Archean for the great part, was later determined to be Paleozoic or even younger? It can be summarized as follows:

In the first place, as more observations were made, it was realized that part of the initial rocks of sedimentary origin graded into the unmetamorphosed Chichibu Paleozoic rocks or Mesozoic rocks.

In the second place, fossils indicating Paleozoic or younger ages were found in some of the weakly metamorphosed rocks and even in the strongly metamorphosed ones.

In the third place, the age of igneous activity, as far as the resultant igneous rocks are closely related to the origin of schistose and gneissic rocks, was assumed to be Mesozoic.

Lastly, in some rocks, like Kashio gneiss, the formation of mylonite was shown to be Paleozoic or younger.

Kashio Gneiss

Besides Harada, the rock was studied by Chu Hiki (1893), Shintaro Nakamura (1906), Masao Oba (1920), Shutaro Ushimaru (1927), Kyojo Shinoda (1930), Ken'ichi Sugi (1933) and Ryuji Sugiyama (1939). Oba pointed out that the Kashio gneiss comprises various rocks which could hardly be called gneiss. He concluded that the "Kashio gneiss" is piezo-crystallized igneous rock intruded along the structural line and suffered crustal movement in the course of ascent and solidification until it finally presented a special lithologic facies.

Oba's view prevailed for a long period. It was later shown, however, that his structural line was the Median Dislocation Line and so the Kashio gneiss could not be as old as Archean, and this opened the way for a new view that at least part of Naumann's gneiss system is much younger. According to Ryuji Sugiyama, the Kashio gneiss locally intrudes rocks of the Outer Zone, hence mylonitization which is a characteristic of the Kashio gneiss must have occurred after the Median Dislocation Line. Furthermore, Sugiyama confirmed that the so-called Kashio gneiss contains not only rocks of igneous origin but also rocks derived from Paleozoic sedimentary rocks. Thus, the age of the Kashio gneiss became much younger.

Ryoke Metamorphics

According to Harada, the Ryoke metamorphics originated in graywacke and clay slate which were contact-metamorphosed by granite intrusion. Kiyohiko Ishii (1929) confirmed that the schistose rocks in the Tenryukyo district grade into unmetamorphosed Paleozoic rocks. In the vicinity of Mikawa he recognized the same transitional relation and made it clear that rocks similar to the Ryoke schists grade into spotted biotite slate, a member of the Chichibu Paleozoic formation. Ishii also maintained that the contact-metamorphic rocks resulted from granite intrusion, such as those distributed in the Kasagi, Yanai, Mt. Tsukuba, Abukuma, Hida and Oki regions, could not be as old as Archean because their original rocks have a transitional relation with Paleozoic rocks. Later, Hiroshi Koide (1949), Shuichi Iwao (1937) and George Kojima studied the Ryoke schists and corresponding metamorphic rocks in the Dando Mountains of Aichi Prefecture, in the Tenryukyo district of Nagano Prefecture and in the Yanai district, Yamaguchi Prefecture. Their study has revealed that the formation of the Ryoke metamorphics is attributable to at least two plutonic activities and associated two metamorphisms. That is to say, rocks derived from Paleozoic formations were contact-metamorphosed, or granitized, by intrusion of older granites before or after the regional metamorphism, and later were intruded by younger granites, thus forming doubly metamorphosed rocks.

The above-mentioned works revealed that metamorphism occurred twice during or after the Paleozoic era, but none of them could indicate the exact age of the metamorphism. Koide studied the pebbles collected by Nobuo Kurata from the Torinosu formation, and concluded that some of the pebbles are similar to the Ryoke schists and associated granites. Hence, had correlation of the pebble-bearing formation been correct and the source of the pebbles is as maintained by Koide, the Ryoke schists must have been formed during the latter part of the pre-Jurassic period.

Metamorphic Rocks of the
Abukuma Mountains

Koto established the stratigraphy of the metamorphic rocks of the Abukuma Mountains on the basis of the exposures on the highway along the Same River between Yumoto and Ishikawa-machi.

Archean	{	Upper Division
		α: Gozaisho series (Huronian)
		β: Takanuki series
	{	Lower Division
		Laurentian

Nearly contemporaneous with the work of Koto (1892), the Geological Survey of Japan was proceeding with geologic mapping which disclosed many new facts. Sen'ichi Otsuka (1892) correlated Koto's Gozaisho series with the Mikabu formation and part of the Takanuki series with the Ryoke schists. Such correlation had been anticipated already by Koto who had noticed a similarity not only between the Gozaisho series and the Mikabu formation but also between the lower half of the Takanuki series and Harada's Ryoke schists. Much later, Manjiro Watanabe (1920) and Haruyoshi Fujimoto (1924) discovered Carboniferous (Visean) corals from a bed correlated with Koto's Gozaisho series. According to them, in southern Abukuma Mountains the bed containing Carboniferous fossils is underlain by continuous complexes of Gozaisho and Mikabu types and by the Ryoke schists. By that time, the Paleozoic origin of the Ryoke schists began to be generally accepted, and so the metamorphic rocks of the Abukuma Mountains were thought to contain no rocks as old as Archean, whether fossiliferous or not. The geologic maps of Sukegawa compiled by Kameki Kinoshita (1932) and Nakoso compiled by Kyukichi Watanabe and Motoo Sato (1934) treated both the Gozaisho series and the Takanuki series as Paleozoic.

The metamorphic rocks of the Abukuma Mountains were studied further by Jun Suzuki (1927), Seitaro Tsuboi (1930) and his students, by Ken'ichi Sugi (1935) and Masao Gorai (1941). Suzuki studied chiefly the rocks which Manjiro Watanabe called the Ayukawa formation. As the age of this formation was already known, Suzuki did not go into details of correlation, but expounded that the region had suffered two kinds of metamorphism--as already maintained by Watanabe--dynamic-metamorphism and contact-metamorphism.

With regard to the age of metamorphism in the Abukuma Mountains, Sugi thought that the lower limit must be late Paleozoic or post-Paleozoic for the reason that part of the original rocks are Carboniferous, and the upper limit is older than Late Jurassic on the basis that the Torinosu series of the Soma district is not metamorphosed. His view has been supported by Gorai and others to recent times.

When the type locality reported by Harada is taken into consideration, correlation of the Hida gneisses with Harada's amphibole gneiss and amphibolite would meet little opposition. Lithologically these gneissic rocks of Hida are considerably different from the so-called Ryoke schists and gneisses. This difference, however, was attributed to the kind of original rocks, as the Ryoke metamorphics are a product of contact-metamorphism between granites and Paleozoic beds scarcely containing limestone, whereas the Hida gneiss was derived from limestone-rich Paleozoic beds which were con-

tact-metamorphosed by granites. Thus, the two metamorphic complexes were considered contemporaneous. This view, advocated by Ishii (1926), was succeeded by Nobuoki Kondo (1942) and Teiichi Kobayashi (1941).³

Other Gneisses

Included in Harada's gneiss system, in addition to the above, were biotite gneiss and granite gneiss that are widely distributed throughout the country. After later studies some of these rocks were included in the Ryoke metamorphics. As it became gradually known that the original rocks of sedimentary origin were Paleozoic in age and the Precambrian theory for the Kashio gneiss, Ryoke gneiss and Hida gneiss had to be denied, controversy over age of the metamorphic rocks waned. The above-mentioned biotite gneiss and granite gneiss were considered much younger than the Ryoke and Hida gneisses, because of newly recognized facts which made a correlation possible between the intrusion of granitic rocks and the Cretaceous phase. Some of the granitic rocks were assigned to Paleogene. Study of the hybrid and plutonic rocks of the Hidaka zone commenced much later. Yasushi Ohira (1928), Mitsuo Funahashi and Seiji Hashimoto (1951) and their students concluded that the age of the metamorphism of the Hidaka zone ranges from Cretaceous to early Paleogene.

Hence, all constituents of the gneiss system which had been assigned to Archean by earlier geologists of the Meiji era became much younger.

Sambagawa Formation⁴ (including Mikabu Formation)

That Koto was dubious about the Archean origin of the crystalline schist system has been mentioned already. He believed, however, that the crystalline schists were the oldest rocks in the Kanto Mountains and was convinced about the stratigraphic sequence Sambagawa--Mikabu--Chichibu Paleozoic beds. Yabe agreed with this view. Afterwards, views on the age of the Sambagawa formation were split into two groups; I) one group insisted that the Sambagawa formation (and part of the Mikabu formation) is a metamorphic facies of the Chichibu system, and II) the other supported the stratigraphy proposed by Koto and Yabe.

View I was advocated by Takuji Ogawa (1929). It was deduced from various theories abroad

concerning metamorphic zones of shields and folded mountains, rather than was based on positive evidence. Ogawa's view later split into two theories, namely I₁ and I₂. Theory I₁ led by Reiichi Kobayashi persisted that the metamorphic rocks represent a metamorphosed facies of the Chichibu Paleozoic formation, and theory I₂, advocated by Haruyoshi Fujimoto (1938), maintained the Paleozoic-Mesozoic origin on the basis that not only are Paleozoic rocks contained but also Mesozoic rocks, and specifically rocks of Jurassic age as substantiated by Jurassic-type radiolarian fossils.

View II, originated in the theory of Koto and Yabe, also separated into several theories. Theory II₁ was advocated by Takeo Kato (1923, 1926), who maintained that the Sambagawa formation shows no vertical relation with the Paleozoic formation but constitutes a structural unit, and that the nature of the formation's metamorphism suggests a Precambrian age, of the Algonkian era to be exact. Theory II₂, advocated by Shintaro Nakamura (1931) and Jun Suzuki (1932), is roughly similar to II₁ in assigning the Sambagawa formation to Precambrian; only greater importance was attached to petrologic features in age determination. It is worthwhile to notice that Fujimoto in those days asserted the Sambagawa formation and Mikabu formation are in an unconformable relation. His view undoubtedly paved the way for the acceptance of later theories, such as II, II₁ and II₂, even after Precambrian origin of the gneiss system was denied. Afterwards, support view II waned as the resemblance between the original rocks of the Sambagawa-Mikabu formation and the Chichibu Paleozoic rocks proved undeniable and fossils were discovered in those metamorphic rocks. One of the most important discoveries was of crinoid stems by H. Fujimoto and Yun Yamada (1947, 1949) and others at the type locality of the Sambagawa formation in the vicinity of Yorii. These fossils disproved the Precambrian theory for the Sambagawa formation. The presence of fossils in the Mikabu formation, has been known for many years. Denkichiro Yamashita (1896) discovered fossil crinoids south of Yatsushiro. Hisao Otani (1926) found corals and fusulines in the Tatsumine zone. Verbeekina was collected by Tatsuro Matsumoto and Tetsuo Totsugi (1949). At that time, however, the fossiliferous part was excluded from the Mikabu formation, that is, the beds for the very reason that they contain fossils were distinguished from the typical Mikabu formation. Today, these beds are accepted as a member of the Mikabu formation on the basis of distribution and lithology.

As already stated, it was held by many people that the Carboniferous formation at Hitachi reported by Watanabe and Fujimoto was correlated with the Gozaisho series and the latter was thought to correspond to the Mikabu formation.

Fossil crinoid stems and radiolarians from a few localities do not permit exact age de-

³ Kobayashi previously held that the Ryoke metamorphics were formed later than the Hida metamorphics.

⁴ Harada's crystalline schist system was re-defined by Jun Suzuki in 1926, and the so-called regional metamorphics of the Inner Zone were excluded from the Sambagawa-Mikabu system in a narrow sense. The metamorphic rocks of the Nagasaki triangle area were also treated separately.

termination of the Sambagawa formation. Nevertheless, it is certain that the fossils indicate an age between Lower Carboniferous (Visean) and Middle Permian. Hence, if the above-mentioned view II is correct, the Sambagawa formation should be older than Carboniferous (Visean), whereas according to view I an exact age cannot be determined but is generally assigned to Paleozoic. Thus, probability of occurrence of Jurassic rocks in the Sambagawa formation became very small, as was pointed out by Teiichi Kobayashi (1941) and many others. According to Tatsuro Matsumoto (1949) the oldest bed containing pebbles of the constituent rocks of the Sambagawa formation is the Ryoseki series of Wakayama Prefecture, and the oldest bed in which piedmontite occurs as a constituent mineral of sedimentary rocks is, according to Koji Fujii (1956), the Upper Jurassic Sakamoto formation of the Yatsushiro district.

Crystalline Schists Other Than the Sambagawa Formation

Included in Harada's crystalline schist system are the Mikabu formation of the Inner Zone, the weakly metamorphosed rocks of the present Sangun-Motoyama zone and the crystalline schists of the Kamuikotan zone. Miyoji Sambonsugi (1938), Hisakatsu Yabe and Toshiro Sugiyama (1939) and Ken'ichi Otatsume (1942) disclosed that part of the original rocks of the Kamuikotan zone are Jurassic. This does not imply that all the constituent rocks of the Kamuikotan (or Hidaka) zone were derived from Mesozoic beds, but it at least offers strong evidence that the age of metamorphism was the latter half of the Mesozoic. Hasakatsu Yabe (1901) and Jun Suzuki correlated these rocks with the Franciscan formation of North America. Similar rocks seem to be widely developed in Sakhalin and the Maritime Province of Siberia. According to Obruchev (1926), metamorphic rocks initially thought to consist of rocks at least as old as Paleozoic, ultimately yield Jurassic fossils.

CENOZOIC THEORY

There is no room for doubt that the Fossa Magna and the Inner Zone or the Chishima arc, Honshu arc and Ryukyu arc experienced similar structural history since the Neogene period (Minato, Yagi and Funahashi, 1956). In the above regions are developed younger plutonic and metamorphic rocks, although their distribution is limited. The Tanzawa block of the Fossa Magna is characterized by various metamorphic rocks ranging between green schist facies and amphibolite facies. As the result of studies by Banzo Murakami (1909), Tetsunosuke Kato (1910), Fujio Homma (1924) and Ken'ichi Sugi (1931), these rocks were believed to correspond to the fossiliferous Misaka formation. However, some geologist hold view that the highly metamorphosed rocks should be correlated with the Sambagawa formation and so are dif-

ferent from the Misaka formation.⁶ However, the quartz diorite that occurs in the center of the metamorphic zone [T. N.; of the Tanzawa block?] is known to have intruded during the Miocene epoch and contact-metamorphosed the surrounding rocks. On the other hand, the greater portion of the metamorphism of this area must have been completed before the intrusion of diorite. At any rate, a conclusive age determination of the Tanzawa metamorphic rocks is a problem for future study. The writer only wishes to attract attention to the latest tendency to date as Neogene the granites of the so-called Outer Zone of western Japan and the Ryukyu arc and the younger granites of the so-called green tuff regions, although they are not necessarily contemporaneous. It has lately been shown that marked mylonitization took place in the Hidaka zone during of after the Neogene.

PRE-PALEOZOIC THEORY OF THE PRESENT DAY

By the 1940's it became established theory that no bedrock of pre-Paleozoic age is exposed in Japan. Yet, some geologist still held that Harada's amphibole gneiss and amphibolite, i. e., Hida gneisses, must be older than pre-Paleozoic. As far as the writer knows, the view was advocated by Hiroshi Koide, Hisashi Kuno and Masao Gorai. After World War II, the age of the metamorphic rocks again became the subject of active discussion. Kokichi Ishioka (1949) discovered staurolite in the lower reaches of the Kurobe River. Setsuo Kamei (1941) began his study of the Gotlandian system in the vicinity of Fukuchi, and the petrological study of the Sakagami district was commenced by Hideo Kobayashi (1949). Tamotsu Nozawa (1949) started the geological survey of Kamioka and vicinity.⁶ Later, research work on the Hida Mountains was begun under Haruyoshi

⁵ According to Takeo Watanabe.

⁶ The writer himself surveyed the region in 1949, 1952 and 1954. The result of the survey were not published, but the stratigraphy established by the writer in 1949 will be outlined below. Here the Murakami conglomerate T.N.; not shown in the stratigraphy is referred to those enormous boulders in the vicinity of Kami-saka. The Murakami conglomerate in the village of Murakami contains fusuline fossils. The conglomerate resembles the Tobigamori formation's conglomerate which contains schist pebbles.

Kamisaka (Conglomerate of metamorphic pebbles)
Gotlandian formation

Lower reaches of Kurobe River { Clay slate
Quartzite, limestone

So-called Hida metamorphics

Fujimoto. In consequence, a number of new facts were disclosed, although no positive evidence was acquired for the assumed unconformable relation between the Hida gneisses and the overlying Gotlandian system. Hideo Kobayashi and his students disclosed the following: a) The amphibole gneiss of Hida closely resembles the Archean amphibole gneiss of the Liao-tung Peninsula, previously reported by Michitaka Sawatari (1935). This was just as predicted by Richthofen and Koide. b) As is known in the gneiss regions of Ryoke, Hidaka, Abukuma and Kitakami, Paleozoic and Mesozoic rocks affected by thermal-metamorphism exhibit various stages of metamorphism ranging from hornfels to intrusion gneiss and to infiltration gneiss. In the Hida Mountains, on the other hand, all gneisses are amphibole gneiss revealing uniform metamorphism and no transitional relation between metamorphosed and unmetamorphosed rocks. This is characteristic of shield gneisses. c) The Hida gneiss region is encircled by the Gotlandian formation which is further surrounded zonally by Carboniferous and Permian formations, as if it reveals the process of accumulation of the Paleozoic formations on the remnant of a shield. The above information may not be a decisive clue to the age of the Hida gneiss but at least it does not counteract the theory of Precambrian origin.

In the Hida Mountains, various granites of different ages were discovered one after another. For example, there are the Shirakawa granite penetrating the Tetori formation, the Funatsu granite which contact-metamorphosed the Hida gneisses and the Paleozoic rocks and is unconformably overlain by the Tetori formation, and the gray granite which is thought to intrude only the Hida gneisses. If pegmatite should be found in association with the gray granite it would help determine the age of the Hida gneisses.

An Archean age for the Hida gneisses has been argued for an entirely different reason. Toru Tomita (1954) noticed that the color of zircon in granites varies with the age of intrusion. According to him, the Hida gneiss exposed in Oki Island is contemporaneous with the Archean granite of Shansi Province [T. N. ; of China], and gneiss of other regions [T. N. ; than Oki?] corresponds to the Tai-shan granite of Shantung Province.

Tomita held that not only the Hida gneisses but also the Higo gneisses belong to the Archean era, and stated that granites similar to the above are distributed in the Abukuma Mountains.

Outlined so far is the seventy-year-long his-

tory of research for the dating of the following Japanese metamorphic rocks:

a) Hida and Higo gneisses (part of them include the metamorphic rocks of the Abukuma Mountains), b) metamorphic rocks of the Sambagawa-Mikabu formations and of the Sangun-Motoyama metamorphic zones, which originate in the Paleozoic rocks of Gotlandian or younger age and for the most part are a product of regional metamorphism, c) the Ryoke metamorphic rocks which were derived from Paleozoic rocks due to thermal metamorphism, d) rocks that were derived mostly from Paleozoic rocks, partly from Mesozoic rocks, affected by thermal metamorphism of younger ages than the Ryoke rocks, e) thermally metamorphosed rocks originating in Mesozoic rocks, such as those of the Hidaka zone, and the dynamically metamorphosed rocks as exemplified by those of the Kamuikotan zone, f) rocks of the regions intruded by younger plutonic rocks, like those in the Fossa Magna, the green tuff regions, and the Outer Zone of southwestern Japan.

SUPPLEMENT TO PAST KNOWLEDGE

The writer concludes by expressing his personal views as a supplement to past results.

a) The stratigraphy, interrelations, lithology and thickness of the Paleozoic formations in southern Kitakami Mountains are being clarified. This will furnish important information for the study of the stratigraphic position of the original rocks of the Japanese metamorphic rocks as well as for the history of metamorphism in Japan.

1) Formations younger than the Onimaru series abound in pyroclastics. Of them, the Ohno series and the Nakazato series are characterized by predominance of keratophyre tuff and scarcity of diabasic rocks. According to Jun Suzuki, this keratophyre tuff could be the original rock of the Oboke gneiss.

2) The metamorphic rocks that were correlated with the Mikabu formation [T. N. ; Sambagawa formation?] are known to range from the Onimaru series to the Kanokura series on the basis of fossil evidence. Hence, it may not be erroneous to assume that the Sambagawa formation includes beds corresponding not only to the Onimaru series but also to the underlying formations. Despite all the research of George Koyama and his students, the stratigraphic sequence of the Sambagawa formation is still not clearly defined, an indication of the difficulty in establishing the stratigraphy of metamorphic complexes. Therefore, in dating metamorphic rocks we must not be prejudiced by an initial apparent stratigraphic sequence but must carry out intensive studies of lithology, thickness

⁷ Ken'ichi Sugi (1935) once stated that to consider the original rocks of the metamorphic rocks of the Abukuma Mountains all Paleozoic would be premature, because part of them may be Precambrian.

and sequence between the metamorphic rocks and the unmetamorphosed Paleozoic formations of which original rocks are known. The same may be said about the Sangun and Motoyama metamorphic rocks.

b) Some structural geologists of Japan held a view that the Japanese Islands during the Paleozoic remained an area of sedimentation, and that tectogenesis, metamorphism and igneous activity was restricted to the Mesozoic, especially in the latter half. However, this view must be criticized because Paleozoic tectonic movement has been disclosed in the Kitakami Mountains. A marked unconformity seems to exist beneath the Tobigamori series of the Kitakami Mountains, and the unconformity beneath the Hikoroichi series, Onimaru series, Nagaiwa series, Sakamotosawa series, Kanokura series and Inai series has been already verified.

1) Folding of the Setamai stage below the Sakamotosawa series has been proved in other regions such as Abukuma, Hida (Anama area), Taishaku, Nagato and Kyushu.

2) The latest information available (Jitsutaro Takubo, and others, 1953), Indicates the age of the pegmatite accompanying the granite related to the Ryoke gneisses to be 216×10^6 years. This can be correlated with Late Pennsylvanian or the Setamai stage.

3) In the Upper Permian system of Japan the Usuginu-type conglomerate is widely distributed from the Kitakami Mountains in the north to the Ryukyu Islands in the south. Granite pebbles occur also in several horizons of the Triassic system.

4) The source of those granite pebbles is unknown, but their derivation can be surmised as follows: During the Setamai stage, the geosynclinal basin, before it was upraised to form the Japanese Islands, experienced deep-seated plutonic activity which was the beginning of later uplift movement. The resultant plutonic rocks, especially their superficial part, began to be denuded during late Permian, and the Usuginu conglomerate and other granite pebbles resulted.

5) By the end of the Mesozoic era the greater part of the plutonic rocks must have been eroded away, leaving only the deepest part as the so-called Ryoke zone.

c) As far as the observations in the Kitakami Mountains indicate the Shimizu stage prior to the Onimaru transgression represents a tectogenesis much more important than the Setamai stage.

1) With regard to tectogenesis in the Soma district of the Abukuma Mountains, the

research by Jun'ichi Iwai, Hiroshi Okano and others, although their results are still unpublished, has contributed a great deal. The writer himself studied the Soma district and reported an unconformity beneath the Onimaru series and an occurrence of metamorphic rocks beneath the unmetamorphosed Onimaru series. As previously mentioned, the above metamorphic rocks are similar to those of the Takanuki series.

2) According to the latest study by Toshihiko Sato, the stratigraphic position of these metamorphics is probably lower than the Tobigamori series.

3) The writer, in collaboration with Jun Suzuki, previously disclosed the existence of pebbles of crystalline schists and plutonic rocks in the conglomerate of the Tobigamori series. The source of these pebbles may be attributable to the above-mentioned "Takanuki-type metamorphic rocks." That a great unconformity occurs beneath the Tobigamori series and that such beds [T. N. ; conglomerates?] are distributed not only in the Kitakami and Abukuma Mountains but also in the Hida Mountains (especially at Kamisaka) have been stated already.

4) Hence, it [T. N. ; the source of the pebbles?] is assumed to lie in the Ryoke-type metamorphic rocks (the Takanuki metamorphic rocks were included up to the recent times) or in the rocks older than the Setamai stage.

5) In the Abukuma Mountains, however, even the beds corresponding to the Onimaru series are thermally metamorphosed, as seen at Hitachi. This indicates that the region underwent igneous activity during the Mesozoic era, by which the "younger granites" were intruded. Judging from the mineral age which was calculated as 131×10^6 years, the last igneous activity must have taken place during Late Jurassic or Early Cretaceous.

d) Although it is generally believed that the Hida metamorphics, for the most part, belong to the pre-Paleozoic, further research is required for precise age determination. The writer is inclined to regard the rocks as contemporaneous with the Takanuki metamorphics.

Taking the nature of the Paleozoic tectogenesis into account, the possibility that the Hida metamorphics constitute the basement of Paleozoic beds seems to be small.

e) With the progress of the study of the Sakashu unconformity and the Kurosegawa tectonic zone by Noboru Yamashita and Koichiro Ichikawa and the research works on the Mesozoic rocks in various parts of the country, it has become known that the age of metamorphism of the Sambagawa and Mikabu

formations is not as young as the Sakawa stage. Nevertheless, there still remains the question whether the period of these regional metamorphisms can be definitely restricted to Late Paleozoic and Early Mesozoic. As the thermal metamorphisms varied in age, namely, Precambrian?, pre-Onimaru stage, pre-Sakamotosawa stage, Cretaceous and Tertiary, the age of regional metamorphisms may be rea-

sonably assigned to various periods. The results of the Cefüge analyses of metamorphic rocks by George Kojima, Teiji Kamiyama and Giichi Horikoshi support the above assumption.

f) The age of the formation of the metamorphic zones in the Japanese Islands, taken from the latest and most reliable information, is summarized in Figure 2.

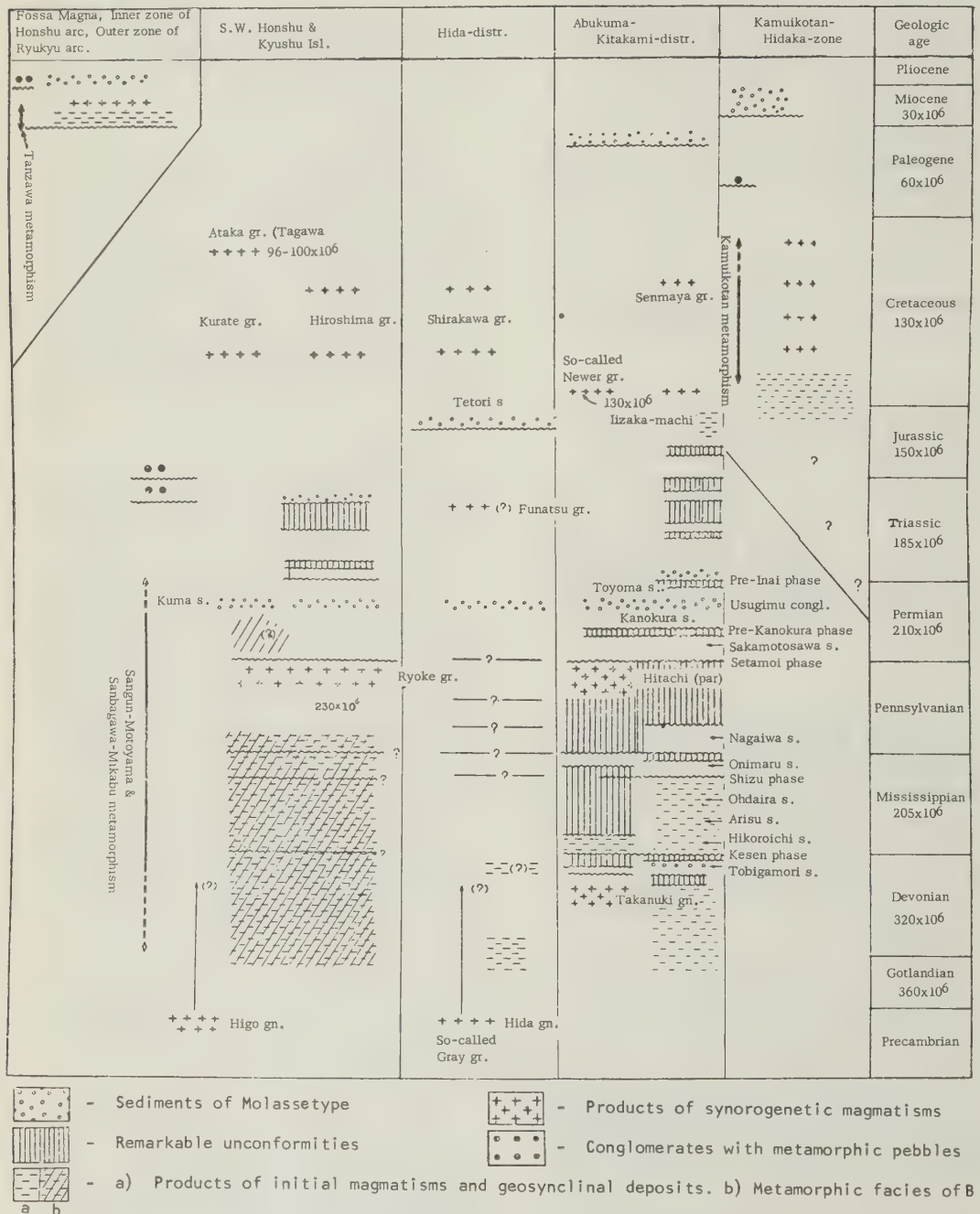


FIGURE 2. Age of the Metamorphisms in Japan

In conclusion, the writer's sincere gratitude is expressed to my respected teacher Dr. Jun Suzuki for his continuous guidance and encouragement. It is a great pleasure for the writer to dedicate this paper in commemoration of Dr. Suzuki's sixtieth birthday.

REFERENCES

- Fujimoto, H., and Yamada, J., 1940, DISCOVERY OF A CRINOID-LIMESTONE IN A CRYSTALLINE SCHIST OF THE NAGATORO SYSTEM OF THE KWANTO MOUNTAINLAND: Proc. Japan Acad., v. 25, no. 5, p. 175.
- Funahashi, M., and Hashimoto, S., 1951, GEOLOGY OF THE HIDAKA ZONE, HOKKAIDO: Monograph of the Assoc. for Geol. Collaboration, no. 6.
- Gorai, M., 1944, PETROLOGICAL STUDY ON THE PLUTONIC ROCKS OF GOSAISHO-TAKANUKI DISTRICT, SOUTHERN ABUKUMA PLATEAU: Mem. Fac. Sci. Kyushu Imp. Univ., ser. D, v. 2, p. 239-321.
- Harada, T., 1890, DIE JAPANISCHEN INSELN: Kaisrl. jap. [sic] Geol. Bundesanst.
- Kato, T., 1923, THE PERIODS OF IGNEOUS ACTIVITY IN JAPAN, WITH SPECIAL REFERENCE TO METALLOGENY: Proc. Pan-Pacific Sci. Congr., p. 806.
- Kobayashi, Hideo, and Kobayashi, Naoki, 1951, A STUDY OF THE HIDA METAMORPHIC ZONE: Jour. Geol. Soc. Japan, v. 57, no. 667, p. 121-134. [In Japanese].
- Kobayashi, T., 1941, THE SAKAWA OROGENIC CYCLE AND ITS BEARING ON THE ORIGIN OF THE JAPANESE ISLANDS: Jour. Fac. Sci. Imp. Univ. Tokyo, sect. 2, v. 5, pt. 7.
- Koide, Hiroshi, 1949, DANDO GRANO-DIORITES AND DANDO METAMORPHIC ROCKS: Mem. Assoc. Geol. Collaboration in Japan, no. 1. [In Japanese].
- _____, 1958, DANDO GRANO-DIORITIC INTRUSIVES AND THEIR ASSOCIATED METAMORPHIC COMPLEX: Japan Soc. Promotion Sci.
- Kojima, G., 1953, CONTRIBUTIONS TO THE KNOWLEDGE OF MUTUAL RELATIONS BETWEEN THREE METAMORPHIC ZONES OF CHUGOKU AND SHIKOKU, SOUTHWESTERN JAPAN, WITH SPECIAL REFERENCE TO THE METAMORPHIC AND STRUCTURAL FEATURES OF EACH METAMORPHIC ZONE: Jour. Sci., Hiroshima Univ., ser. C, v. [?], no. 3, p. 17-44.
- Koto, B., 1888, ON THE SO-CALLED CRYSTALLINE SCHISTS OF CHICHIBU: Jour. Col. Sci., Imp. Univ., v. 2, pt. 2.
- _____, 1892, THE ARCHEAN FORMATION OF THE ABUKUMA PLATEAU: Ibid., v. 5, pt. 3.
- Minato, M., 1950, ZUR OROGENESE UND ZUM VULKANISMUS IN JÜNGEREN PALEOZOIKUM DES KITAKAMI-GEORGES, HONSHU, JAPAN: Jour. Fac. Sci., Hokkaido Univ., 7.
- _____, 1955, ZUR STRATIGRAPHISCHEN LÜCKE DER PRA-ONIMARU-SERIE (OBER VISE): Jour. Fac. Sci., Hokkaido Univ., 9.
- Minato, M., Yagi, K., and Funahashi, M., 1956, GEOTECTONIC SYNTHESIS OF THE GREEN TUFF REGIONS IN JAPAN: Bull. Earthquake Res. Inst., v. 34, pt. 3.
- Nakazawa, Keiji, Shiki, Tsunemasa, and Shimizu, Daikichiro, 1954, THE MESOZOIC AND PALEOZOIC FORMATIONS IN THE VICINITY OF AIDA-GUN, OKAYAMA PREFECTURE: Jour. Geol. Soc. Japan, v. 60, no. 702, p. 97-105. [In Japanese].
- Naumann, E., 1885, UBER DEN BAU UND ENTSTEHUNG DER JAPANISCHEN INSELN.
- Sugi, K., 1931, ON THE METAMORPHIC FACIES OF THE MISAKA: Japanese Jour. Geology and Geography, v. 9, no. 1-2.
- Suzuki, J., 1930, PETROLOGICAL STUDY OF THE CRYSTALLINE SCHIST SYSTEM OF SHIKOKU, JAPAN: Jour. Fac. Sci., Hokkaido Imp. Univ., 1.
- _____, 1934, ON THE ROCKS OF THE SO-CALLED KAMUIKOTAN SYSTEM: Jour. Geol. Soc. Tokyo, v. 41.
- Tomita, T., 1954, GEOLOGIC SIGNIFICANCE OF THE COLOR OF GRANITE ZIRCON AND THE DISCOVERY OF THE PRE-CAMBRIAN IN JAP: Mem. Fac. Sci., Kyushu Univ., ser. D, v. , no. 2.
- Yabe, H., 1917, PROBLEMS CONCERNING THE GEOTECTONICS OF THE JAPANESE ISLANDS; CRITICAL REVIEWS OF VARIOUS OPINIONS EXPRESSED BY PREVIOUS AUTHORS ON THE GEOTECTONICS: Sci. Rept. Tohoku Imp. Univ., Sendai, 2nd ser. (Geology), v. 4, no. 2.
- Yamashita, Noboru, 1957, MESOZOIC: Chigaku Sosho [Geoscience Series], p. 43-48. [In Japanese].

ALKALIC ROCKS OF THE NEMURO PENINSULA WITH SPECIAL REFERENCE TO THEIR PILLOW LAVAS¹

by

Kenzō Yagi²

translated by Kinkiti Musya

ABSTRACT

Mafic alkalic rocks occur as lava flows, sheets or laccoliths in the Upper Cretaceous rocks in the Nemuro Peninsula, Hokkaido, Japan. Crystallization differentiation owing to gravitational separation of olivine and pyroxene is observed in some sheets or laccoliths, while remarkable pillow structure is observed in some sheets or lava flows. Pillows are mostly 50 cm - 2 m in diameter and usually ellipsoidal in shape. Difference in crystallinity and mineral composition is observed in a pillow; i. e., its central portion is holocrystalline dolerite and its margin is tachylite with very high water concentration. Origin of the pillow lavas in this district is interpreted as follows. Very fluid doleritic lava was erupted on deep ocean bottom, sometimes intruded into thick wet sediments. Quenching by water or sediments and convection current resulted in the formation of ellipsoidal cracks in the lava flows or sheets. Under such conditions there was not much difference between lava flows and sheets. Because of its high partial pressure the water diffused into the lava along the cracks, developing high marginal water concentration, and formed individual pillows. As the increase of water content in the melt decreased its temperature of crystallization, the wetter marginal portion might have a crystallization temperature somewhat lower than that of the dryer central portion, and consequently crystallization in a pillow proceeded from the core to the margin, forming tachylite at the last stage. Abundance of analcite or natrolite is the result of enrichment of soda in some portions by the diffusing water vapor, though spilitization which is fairly common in pillow lavas is absent in the present case. --author.

INTRODUCTION

In the Cretaceous rocks of the Nemuro Peninsula, Hokkaido, occur lava flows, sheets, and laccoliths of mafic alkalic rocks, mainly dolerite. Some of the rocks exhibit a well-developed pillow structure which is particularly remarkable in Nemuro-machi and the Cape of Hanasaki. The pillow lavas are popularly called "Kurumaishi" (wheel rocks) and have attracted the attention of many people. Also, there are sheets and laccoliths which present remarkable crystallization differentiation due to sinking of early formed crystals. These rocks are rich in potassium, form a peculiar petrologic province in Japan, and suggest many interesting problems. In this paper, particular consideration will be given the pillow lavas.

During the present study kind guidance was given by Dr. Jun'ichi Takahashi, Professor emeritus of Tohoku University, Dr. Manjiro Watanabe, President of Akita University, and Dr. Jun Suzuki, Professor of Hokkaido University. In the field work, instruction and assistance were given by Messrs. Masao Minato, Hatsutarō Ito, and Yutaka Yoshimoto; in the

laboratory work valuable instruction was given by the late Dr. N. L. Bowen and Dr. H. S. Yoder, Jr. Moreover, as to the measurement of index of refraction, assistance was afforded by Mr. Ken'ichiro Aoki. The writer takes this opportunity of thanking them.

It is a pleasure for the writer to publish this paper, which is closely related to Prof. Jun Suzuki's studies, in this Jubilee Publication to one who has rendered a brilliant contribution to the petrology of Hokkaido.

BRIEF SUMMARY OF THE GEOLOGY

The Nemuro Peninsula exhibits flat terrace topography formed by abrasion, and the highest point is a triangulation mark 55.3 m above sea level north of Nishiwada Station. The surface of the terrace has been slightly eroded by shallow rivers, and swamps and lakes are distributed in places. Inconsequence rocks are poorly exposed, but along the coast outcrops are generally good (fig. 1).

The basement of this district is a marine Cretaceous formation mainly consisting of shale and sandstone. Its geologic age has been considered upper Senonian on the basis of *Inoceramus schmidtii* which occurs at Nikkamap. Throughout the peninsula a monoclinic structure is developed, striking N 50° - 80° E and dipping 50° - 30° toward SSE. The lower part of this formation exposed at Nokkamap consists of conglomerate, basalt of calc-alkalic rock series, lava flow of andesite, and tuff. Toward the top

¹Translated from the Japanese: in Jubilee Publication in the Commemoration of Professor Jun Suzuki, M. J. A. Sixtieth Birthday (1956), p. 287-298, 1958.

²Institute of Petrology, Faculty of Science, Tohoku University.

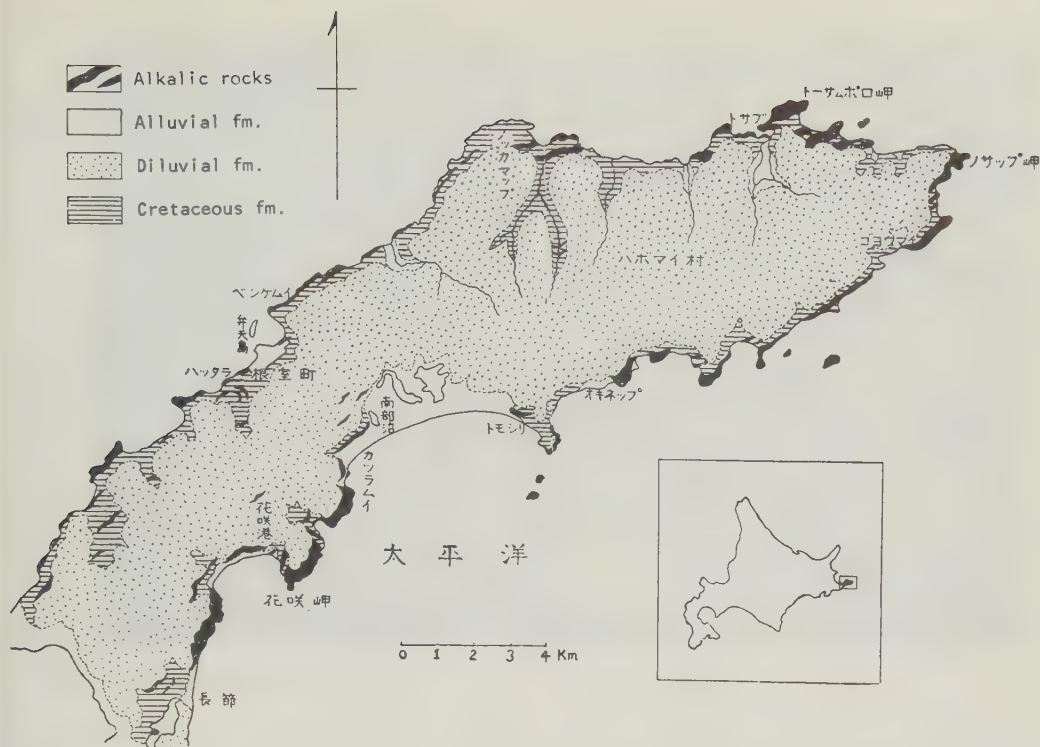


FIGURE 1. Geologic map of Nemuro Peninsula

pyroclastic rocks decrease and shale and sandstone become predominant.

The Diluvial formation overlying the Cretaceous formation is extensive and consists mainly of sand and gravel. In the upper part pumice and volcanic ash, considered to be eruptives of the Akan volcano group, are intercalated with soil. In swamps peat is developed. On the coast and around lakes the Alluvial formation consisting of sand and mud is distributed.

Alkalic rocks occur in the Cretaceous formation as lava flows, sheets, laccoliths, and occasionally as dikes. The alkalic rocks occur throughout the peninsula, particularly along the coast, but are not very extensive. According to Yasuo Sasa (1934), similar alkalic rocks are distributed widely in the Cretaceous of Shikotan Island. Chuji Tsuboi (1954) who made a gravity survey of Japan revealed that the Bouguer anomaly in the Nemuro Peninsula is +225 milligals, the highest in Japan. This anomaly suggests that dolerite or a rock which contains more olivine and is of high specific gravity is distributed extensively at depth from the Nemuro Peninsula to Shikotan Island.

MODE OF OCCURRENCE OF PILLOW LAVAS

The so-called "Kuruma-ishi" is a spherulitic or elliptical rock body found in the dolerite

and has a well-formed radial structure. Fujio Homma (1930) who studied the rock for the first time considered it to be different from pillow lavas. However, the characteristics of this rock body are quite identical with those of pillow lavas. The best-developed structure of this rock is found below a lighthouse on the Cape of Hanasaki. In this locality this rock occurs in a sheetlike form conformably on the Cretaceous formation, and has metamorphosed the underlying sandstone and shale. The upper surface assumed to be in contact with the overlying bed cannot be seen but a hardened shale with a grayish white color occurs in places. In the upper and lower parts are developed platy joints parallel to the bedding plane of the Cretaceous rocks and columnar joints in the inner side. Moreover, in the central part of the rock body, is the structure of well-formed pillow lavas. In some cases the boundary between the columnar joints and the pillow structure is obviously discontinuous, but in many cases the former gradually grades into radial joints which change again into perfect pillow lavas. Consequently this is not a complex rock body but a single one (fig. 2). The distribution of the pillow lavas is fairly irregular. The individual rock body (to be called merely a pillow from now on) is mostly elliptical like a pillow or straw rice-bag elongated rather horizontally. The pillow is mostly one or two meters in size, but some are over 4 meters and elongated like a tube. In the center of a pillow is a cavity, in



FIGURE 2. Pillow lava in the Cape of Hanasaki. Pillow structure is developed between the upper and lower columnar joints.

which an aggregate of analcite or natrolite is commonly found. Radiating from the center, joints extend like spokes. Toward the margin appear concentric joints perpendicular to the radial joints,

and the outermost part is coated with a thick tachyitic substance (basaltic glass), 3 to 5 cm, the surface of which is cracked in hexagonal pattern. The large spaces between pillows are



FIGURE 3. Pillow lava in the Cape of Hansaki (the so-called "Kuruma-ishi" or wheel rock). Pillow in the left side is more than 4 m in diameter.

sometimes filled with shaly rock³ (fig. 3).

Pillow lavas with a similar mode of occurrence are also observable in the vicinity of Lake Nambu-numa. In this locality pillow lavas are found in the middle of a part where columnar joints are developed, and on the pillow surfaces is wavy undulation, like ripple marks, 5 to 8 cm wide and 2 to 3 cm high. This suggests that when pillows were half solidified they rolled along producing the undulatory surface.

On the coast of Nokkamap dolerite occurs between the alternating beds of Cretaceous sandstone and conglomerate. Pillow lavas are developed in the lower half of the dolerite and perpendicular columnar joints in the upper half. The lower pillow lavas gradually pass into tuff breccia or a compact lava flow horizontally and the upper dolerite is in contact with the underside of sandstone tachylite. The boundary between the upper and lower halves is clearly observable and the both halves differ petrologically, though slightly. Consequently it is supposed that either the pillow lavas followed by the basalts flowed in quick succession, or the basaltic sheet intruded above the pillow lava after deposition of the overlying bed.

The above-mentioned rock body shows characteristics of both sheet and lava, so is hardly

determinable to which of the two the rock belongs. As will be described later, this rock body may have a mode of occurrence which is intermediate between the two. In either case, it is noteworthy that the part of pillow lavas seems to have moved fairly freely.

In contrast, an undoubted lava flow is found on the coast of Tosabu. In this locality somewhat rounded dolerite blocks 10 to 50 cm in diameter form a stratum about 2 m thick, and the stratum grades upward into shale through an agglomeratic part. The dolerite has not metamorphosed the underside of the shale, so it is a lava flow beyond doubt. The surface of each block is thinly coated with glass, but there are no radial joints as seen in "Kuruma-ishi." Most probably this stratum of dolerite blocks is pillow lava produced under somewhat different conditions (fig. 4). Shale containing similar pillow lavas occurs in a few other localities.

Excellent "Kuruma-ishi" is in places developed in a stratum which is undoubtedly a sheet. On the coast of Hattera in Nemuro there is a stratum of dolerite 10 to 20 m thick parallel to shale beds. The shale above and below the dolerite was metamorphosed and became dark gray and compact. Tachylite occurs in the dolerite near the contact, suggesting that the



FIGURE 4. Pillow lava flow in Tosabu.

dolerite is a sheet which intruded into the shale. In the upper and lower parts of the sheet are platy joints parallel to the shale, and in the central part radial joints like "Kuruma-ishi" are developed grading into pillow lavas. How-

³This may be palagonite, but it has not been confirmed.

ever, in this case there is no pillow of irregular form like those in the Cape of Hanasaki and Nambu-numa. The tachylite mantle is also thin, and the spaces between pillows are not very large.

Beneath the dolerite mass in the Cape of Hanasaki mentioned before, two sheets are found parallel to the mass, and in the upper part where the sheets are in contact with the dolerite a pillow lava structure is found, though imperfect. In the sheet near Katsuramui a small number of large "Kuruma-ishi" are found between the joints.

Summarizing the foregoing, the mode of occurrence of pillow lavas in this district is classified as follows:

1) Pillow lavas which occur as distinct lava flows, 2 to 4 m thick. Example: Tosabu and Nokkamap.

2) Pillow lavas which occur in distinct sheets 10 to 20 m thick. Radial joints are developed between columnar joints, and the radial joints pass into pillow lavas. Example: Hattara and Katsuramui.

3) Pillow lavas exhibiting a complex mode of occurrence intermediate between lava flow and sheet. The most representative structure of "Kuruma-ishi" or wheel rock is exhibited in this type. Example: Cape of Hanasaki, Nambu-numa, and coast of Nemuro.

Besides these, sheets and laccoliths more than 50 m thick are developed in the Cape of Nosap, Benkemui, Cape of Tosamporo, and near Goyomai. Among these is known a type manifesting a remarkable in place crystallization-differentiation where the gravitational sedimentation of olivine and augite of earlier crystallization had resulted in the formation of pikritic dolerite in the lower part and monzonite in the upper part, and then in the final stage of crystallization syenite aplite dikes were formed and porphyritic basalt came into existence in the zone of contact with the Cretaceous rocks (Yagi, 1948, 1953b). This phenomenon will be discussed in another paper.

PETROLOGY OF THE PILLOW LAVAS

Pillows of pillow lavas assume various shapes such as pillow, ricebag, bulb, bun, flat convex, and long tube. Of these, elliptical ones like a pillow or rice-bag are predominant. The diameter (longer diameter) and curvature of 1017 samples of pillows collected in the pillow lavas in this district are shown in Tables 1 and 2. As shown in the tables, most of the pillows are 50 cm to 2 m in diameter and more than half have a curvature between 1.0 and 1.5 (curvature = longer diameter/shorter diameter).

TABLE 1. Longer diameter of pillow

Longer diameter (cm)	Number	Percent
0-50	44	4.3
50-100	237	23.3
100-150	290	28.6
150-200	241	23.7
200-250	77	7.5
250-300	48	4.7
300-350	36	3.5
350-400	22	2.2
400-1100	22	2.2
Total	1,017	100.0

TABLE 2. Curvature of pillow

Curvature	Number	Percent
1.0	72	7.2
1.0-1.5	632	62.8
1.5-2.0	226	22.5
2.0-2.5	46	4.6
2.5-3.0	17	1.7
3.0-3.5	8	0.8
3.5-6.0	4	0.4
Total	1,005	100.0

Lava flows and sheets forming pillow lavas consist of dolerite and are fairly homogeneous throughout this district. However, as distinctly seen at a glance, the structure and texture are fairly different in different parts of a pillow. In order to clarify this difference one of the pillows of the pillow lavas from Lake Nambu-numa was chosen and the petrological character of various parts was examined. Sampled parts are as follows (fig. 5).

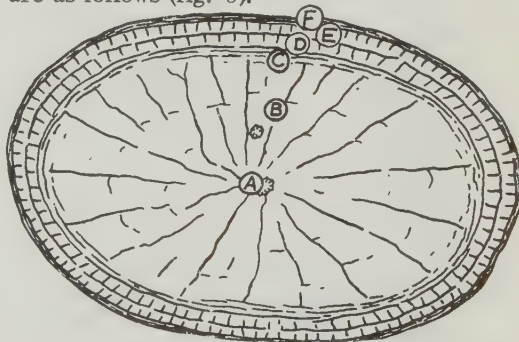


FIGURE 5. Pillow (Sample No. 48090204) from Nambu-numa. The longer diameter is 4.5 m.

Sample number	Position	Distance from the center
48090204 A	Center	0 cm
48090204 B	Middle part of inner core	75 cm
48090204 C	Outer part of inner core	135 cm
48090204 D	Inner part of intermediate layer	150 cm
48090204 E	Outer part of intermediate layer	160 cm
48090204 F	Margin	165 cm

A and B in the above list are coarse-grained holocrystalline dolerite almost identical. This type of dolerite constitutes the greater part of thin sheets and lava flows. This rock contains phenocrysts mainly of plagioclase (An_{46-50}), augite ($\alpha_{\min} 1.690$, $\gamma_{\max} 1.717$, $2V \gamma 460-570$, $Ca_{43}Mg_{38}Fe_{19}$), olivine (decomposed into chlorite and calcite), and magnetite, and the groundmass consists mainly of plagioclase (An_{40-55}), anorthoclase ($\alpha 1.526$, $\gamma 1.533$), augite ($\alpha_{\min} 1.690$, $\beta 1.696-1.703$), and magnetite together with small quantities of alkali-hornblende, apatite, and titanite. In addition, large quantities of analcite and natrolite are also contained. The alkali-hornblende is very small crystals, has deep bluish green to brownish green pleochroism, and its double refraction is low. Of the augite, there is slightly greenish soda-augite. However, no aegirine augite is contained, nor is there aegirine-augitization of augite due to natrolite described by Jun Suzuki (1938).

C and D are almost the same as A and B in mineral composition, but the crystals are much smaller and the groundmass is finer-grained. The rocks contain phenocrysts of plagioclase (An_{46-50}), augite ($\alpha_{\min} 1.690$, $\gamma_{\max} 1.717$, $2V \gamma 46-57$, $Ca_{43}Mg_{38}Fe_{19}$), olivine (decomposed into chlorite and calcite), and magnetite, and the groundmass consists of plagioclase (An_{45}), augite, anorthoclase, titanite, magnetite, and apatite. Besides, large quantities of analcite and natrolite are contained. There is a small quantity of soda augite but no alkali-hornblende.

E is less crystalline and lacks olivine. Phenocrysts of plagioclase (An_{60}), augite ($\alpha_{\min} 1.690$, $\gamma_{\max} 1.717$, $2V \gamma 530-550$, $Ca_{45}Mg_{37}Fe_{18}$), and magnetite are scattered in the groundmass which consists of augite and large quantities of brown glass with abundant crystallites. The greater part of F consists of brown glass. The phenocrysts consist of plagioclase (An_{53-61}) and augite ($\alpha_{\min} 1.692$, $\beta 1.697-698$) and the groundmass mostly brown glass with a small quantity of acicular plagioclase (An_{37-40}). The index of refraction of the glass is 1.533-1.541, relatively low for a basaltic glass. This may be due to a large amount of water in the glass as will be discussed later. Crystallites occur radiating from the matrix plagioclase. Perlitic cracks are developed.

The chemical compositions of these samples are shown in Table 3. A, B, and C are almost identical. E is relatively close to A, B, and C, but is lower in alkali and particularly soda. F is strikingly different from A, B, C, and E, and is characterized by much smaller content of silicic acid and alkali and very large content of H_2O^+ and H_2O^- . Column 6 of Table 3 shows the chemical composition of the central part of a pillow of the pillow lavas from Tosabu. When compared with the chemical compositions of the pillow lavas from Lake Nambu-numa, this

sample contains somewhat smaller quantities of alkali and magnesia, and larger quantities of lime and H_2O^+ . This rock is a basalt of remarkable porphyritic structure. The phenocrysts, excepting plagioclase (An_{66}), have been completely chloritized. The groundmass is holocrystalline and consists of plagioclase (An_{43-48}), anorthoclase, magnetite, chlorite, and apatite. In order to compare with them, the chemical compositions of each type of the laccoliths in the Cape of Nosabu are shown in Table 4. The chemical composition of the pillow lava (A, B, C) most nearly resembles that of porphyritic monzonite. The magnesia and lime content is lower and alumina and alkali content higher than the porphyritic basalt which is considered to be allied to the parental magma of the laccoliths.

Tables 3 and 4 show that the alkalic rocks in this district are relatively rich in potassium as shown by the presence of anorthoclase and soda-orthoclase. This is a remarkable characteristic, for example, as compared with the alkalic petrographic province of the Morotsu district, Sakhalin (Yagi, 1953 a) which is rich in soda. These rocks constitute a unique potassium-rich alkalic petrographic province.

ORIGIN OF THE PILLOW LAVAS

Pillow lavas occur in various places in the world and in various geologic ages. Their peculiar shape has attracted attention since ancient times and numerous theories on their origin have been proposed. Of these, a generally accepted view is that basaltic lava which was effused in a form of fissure eruption in the sea bottom and entered into the bottom deposits of volcanic ash, ooze, and fine sand was cooled and solidified rapidly (Lewis, 1914; Shrock, 1948; Jun Suzuki, 1954).

It is beyond doubt that the pillow lavas in Tosabu and the lower half of the composite lava flow in Nokkamap were produced as a result of submarine eruption. But, the occurrence of pillow lavas in sheets as seen at Hattara and Katsuramui suggests that such structure produced from peculiar jointing when a sheet is cooled, even if there is no rapid cooling due to water. The presence of pillow lavas as sheets has been noticed by several geologists, and Homma considers that, unlike the pillow lavas described in foreign countries, the "Kuruma-ishi" of this district are an aggregate of spherical blocks having radial cracks produced in sheets by cooling.

However, the pillow lavas exhibiting the mode of occurrence of described above in the Cape of Hanasaki and Lake Nambu-numa (mode 3) cannot be regarded as a mere aggregate of spherical blocks within a sheet. As Table 3 shows, the tachylite mantle of a pillow

TABLE 3. Chemical compositions of various parts of a pillow of the pillow lava from Lake Nambu-numa.

	1	2	3	4	5	6
SiO ₂	52.40	52.30	50.74	52.58	42.93	49.76
TiO ₂	0.80	0.76	0.98	1.00	0.82	0.54
Al ₂ O ₃	17.92	16.90	16.16	16.39	17.25	19.38
Fe ₂ O ₃	3.87	4.38	4.26	3.76	5.21	2.66
FeO	4.74	4.14	4.52	4.23	4.17	2.31
MnO	0.12	0.36	0.12	0.15	0.13	0.17
MgO	3.82	3.91	3.59	3.63	3.99	1.77
CaO	7.40	6.84	8.40	8.98	8.63	11.27
Na ₂ O	3.35	3.33	3.81	2.26	1.96	2.90
K ₂ O	4.16	4.42	3.48	3.92	1.13	3.66
H ₂ O+	1.75	2.18	1.74	1.90	7.78	5.06
H ₂ O-	0.20	0.78	2.00	2.00	6.10	0.94
P ₂ O ₅	0.22	0.22	0.22	0.06	0.65	0.08
Total	100.75	100.52	100.02	100.86	100.75	100.50
Specific gravity	2.68	2.66	2.66	2.59	2.44	-

1. Central part (48090204 A)

2. Middle part of inner nucleus (48090204 B)

3. Outer part of inner nucleus (48090204 C)

4. Outer part of intermediate layer (48090204 E)

5. Marginal part (48090204 F)

6. Central part of pillow of pillow lava from Tosabu

[Analyzed by Yagi].

TABLE 4. Chemical compositions of each rock type of the laccoliths from the Cape of Nosabu.

	1	2	3	4	5	6
SiO ₂	45.58	50.16	51.35	51.98	55.65	51.05
TiO ₂	0.80	0.70	0.62	0.85	0.13	0.59
Al ₂ O ₃	10.57	15.82	16.86	18.39	17.79	16.43
Fe ₂ O ₃	5.66	4.20	5.36	4.45	2.05	2.81
FeO	5.56	4.81	3.27	2.27	0.98	5.18
MnO	0.16	0.28	0.12	0.12	0.14	0.17
MgO	10.86	6.14	3.27	2.77	4.11	6.18
CaO	11.93	9.88	9.11	6.69	3.61	7.67
Na ₂ O	1.60	2.49	3.80	2.99	2.82	3.45
K ₂ O	1.91	2.92	4.02	4.52	7.84	3.38
H ₂ O+	2.96	3.05	2.88	3.80	3.38	2.19
H ₂ O-	2.05	0.25	0.10	0.89	2.05	0.79
P ₂ O ₅	0.18	0.19	0.18	0.88	0.31	0.42
Total	99.82	100.89	100.94	100.60	100.86	100.31*
Specific gravity	2.97	2.75	2.66	2.57	2.46	-

1. Picritic dolerite (lower part)

2. Porphyritic basalt (lowermost contact part)

3. Porphyritic monzonite (upper part)

4. Red monzonite (middle part)

* In the original paper total 100.26.

5. Syenitic aplite (middle and lower parts).

(The above rocks were analyzed by Yagi.)

6. Monzonite from Benten Island in the Nemuro Harvor (Analyzed by Umekickhi Ushijima (Homma, 1930).

contains more than 13 percent H₂O. So high a water content is rarely found even in pitchstone (Yoshinori Kawano, 1950). The water content of basaltic magma has been considered generally to be less than 3 percent, so it is impossible that so large a quantity of water is juvenile. Hence, it is supposed that, as a result of contact of red-hot lava with sea water or watery ooze, water was absorbed into the lava.

According to Goranson's experiments (1931, 1937), high pressures are necessary to make large quantities of water dissolve into silicate

solution. Therefore, even if lava comes in contact with sea water, it is impossible for such large quantities of water to be absorbed.⁴ But when deposits having fairly high partial pressure of water are heated by the intrusion of lava, should sufficient pressure prevent the

⁴ It is noteworthy that no pillow lava was produced when lava flowed into the sea in the recent volcanic activities such as those of Sakura-jima and Miyake-jima.

escape of water, the partial pressure of water increases rapidly with the result that the water which cannot escape anywhere diffuses into the lava (Kennedy, 1955). Thus, it is expected that the marginal part of the lava becomes rich in water.

Then, in what way were elliptical pillows produced? Osborn (1949) observed that when optical glass is cooled rapidly in water, elliptical cracks are produced in the inner part of thick plate glass because of convection from rapid cooling and he connected this phenomenon with the origin of pillow lavas⁵. Green (1887) reported that during the 1859 eruption of Mauna Loa elliptical joints were produced in red-hot lava and blocks which fell separately in the sea.

Based on the above descriptions, the writer considers the origin of the pillow lavas in this district to be as follows: Highly fluid doleritic lava was effused in the deep sea floor and flowed on the sea floor or intruded into the watery deposits of ooze or fine sand. Within this lava elliptical cracks were produced by cooling and convection. Then, water having a high partial pressure percolated through these cracks and a highly watery layer was formed in the marginal part. Thus, individual pillows were formed to constitute the whole pillow lava. As pointed out by Suzuki (1954), it is difficult to distinguish lavas flows from sheets in a deep sea floor thickly covered by ooze.

Increased water content causes a remarkable fall of crystallization temperature. For example, the experiment made by Yoder and Tilley (1956), confirmed that when a large quantity of water is added to basalt the crystallization temperature falls as much as 300°C. Hence, when the marginal parts of pillows become watery, even if cooled rapidly, the temperature of these parts is still above crystallization temperature, and consequently it is possible that crystallization progresses from the inner part to the marginal part. The facts that olivine phenocrysts are found abundantly in the inner part and lacking in the marginal part, and the An percent of groundmass plagioclase decreases from the inner part to the outer part may be explained easily by assuming that crystallization progressed from the inner part to the outer part and finally tachylite was consolidated. Homma also considers that crystallization began in the inner part and ended at the glassy marginal part. In the pillow lavas found

in Ogi, Sado Island, olivine is present in the inner part but lacking in the outer part, and here also it is considered that crystallization progressed from the inner part to the outer part (Eisuke Tokushige, 1934).

It has been experimentally confirmed that in super-heated vapor under high pressure alkali-silicate, especially soda-silicate, is highly soluble (Morey and Hesselgesser, 1952). In this case also it is considered that soda taken away from basaltic lava especially from tachylite in the marginal part progressed to the inner part of pillows, resulting in crystallization of analcite and natrolite, so that in the final stage beautiful crystals were formed in the central cavities. However, spilitization as seen in pillow lavas did not take place, possibly because the parental magma was rich in potassium.

SUMMARY

1) Ferromagnesian alkalic rocks occur as lava flows, sheets, and laccoliths in the Upper Cretaceous rocks of the Nemuro Peninsula and make up a peculiar alkalic petrographic province which is rich in potassium.

2) Crystallization differentiation is remarkable in thick sheets and laccoliths, but sometimes pillow lava is developed in lava flows and sheets. The mode of occurrence is roughly divided into 3 types.

3) The pillows range generally from 50 cm to 2 m across. The inner part consists of coarse-grained holocrystalline dolerite. In the margin is developed a tachylite mantle containing more than 13 percent water.

4) The genesis of pillow lavas is considered as follows: Part of the highly fluid doleritic lava effused in the deep sea floor was intruded into the deposits of ooze; elliptical joints were produced by rapid cooling and convection; through the joints water was diffused; and individual pillows were formed.

5) Due to the fall of crystallization temperature that accompanied the addition of water, crystallization progressed from the inner part to the marginal part, and finally tachylite was produced. Moreover, due to the migration and concentration of soda by the water content analcite and natrolite were produced, but spilitization did not occur at all.

REFERENCES

- Goranson, Roy W., 1931, THE SOLUBILITY OF WATER IN GRANITE MAGMAS: Amer. J. Sci., v. 22, p. 481-502.

Silicate-water systems, 1937, "OSMOTIC

⁵ It is interesting that the late Dr. E.E. Wright who saw the photographs shown in Fig. 2 and 3 of this paper at the meeting of the Geological Society of America in 1950 told the writer that the pillow lavas in Nemuro are a natural example most closely resembling the elliptical cracks produced in optical glass by rapid cooling, which he had studied.

- PRESSURE" OF SILICATE MELTS: Amer. Miner., v. 22, p. 485-490.
- Green, W. L., 1887, VESTIGES OF THE MOLTEN GLOBE, PT. 2. THE EARTH'S SURFACE FEATURES AND VOLCANIC PHENOMENA: Honolulu.
- Homma, Fujio, 1930, PROBLEMS ON THE IGNEOUS ROCK GEOLOGY IN JAPAN: Papers on Geoscience in Commemoration of Dr. J. Ogawa's 60th Birthday, p. 383-434.
- Kawano, Yoshinori, 1950, A STUDY ON THE GLASSY ROCKS FROM JAPAN: Rept. Geol. Surv. Japan, no. 134, 1-29.
- Kennedy, George E., 1955, SOME ASPECTS OF THE ROLE OF WATER IN ROCK MELTS: SYMPOSIUM ON CRUST OF THE EARTH: Geol. Soc. Amer. Sp. Paper, no. 62, p. 489-504.
- Lewis, J. V., 1914, ORIGIN OF PILLOW LAVAS: Geol. Soc. Amer. Bull., v. 25, p. 591-654.
- Morey, G. W., and Hesselgesser, J. M., 1952, THE SYSTEM $H_2O-Na_2O-SiO_2$ at 400°C: Amer. J. Sci., Bowen Volume, p. 343-371.
- Osborn, E. F., 1949, CELLULAR STRUCTURES IN GLASS AS RELATED TO STRUCTURES IN LAVAS: J. Geol., v. 57, p. 73-78.
- Sasa, Yasuo, 1934, A PRELIMINARY NOTE ON THE GEOLOGY OF THE ISLAND OF SHIKOTAN, SOUTHERN TISIMA (SOUTH KURIL ISLANDS): Fifth Pacific Sci. Congress, Proc., p. 2479-2482.
- Shrock, R. R., 1948, SEQUENCE IN LAYERED ROCKS; A STUDY OF FEATURES AND STRUCTURES USEFUL FOR DETERMINING TOP AND BOTTOM OR ORDER OF SUCCESSION IN BEDDED AND TABULAR ROCK BODIES: McGraw-Hill, New York, p. 359-366.
- Suzuki, Jun, 1938, ON THE OCCURRENCE OF AEGIRINE-AUGITE IN NATROLITE VEINS IN THE DOLERITE FROM NEMURO, HOKKAIDO: J. Fac. Sci. Hokkaido Univ., Ser IV, no. 4, p. 183-191.
- _____, 1954, ON THE PILLOW LAVAS FROM HOKKAIDO: Geol. Comm. Hokkaido, Bull., no. 26, 11-20.
- Tokushige, Eisuke, 1934, PILLOW LAVA IN OGI, SADO IS.: Rep. Historic Sites, Scenic Places, and Natural Monuments, in Niigata Prefecture, no. 4, p. 31-47.
- Tsuboi, Chuji, [no date], GRAVITY SURVEY ALONG THE LINES OF PRECISE LEVELS THROUGHOUT JAPAN BY MEANS OF A WORDEN GRAVIMETER, PT. 4. MAP OF BOUGUER ANOMALY DISTRIBUTION IN JAPAN BASED ON APPROXIMATELY 4,500 MEASUREMENTS: Earthq. Res. Inst. Bull., Sup. v. 4, p. 125-127.
- Yagi, Kenzo, 1948, BASALTS IN THE CAPE OF NOSAP, HOKKAIDO: Kagaku (Science), v. 18, p. 323-326.
- _____, 1953a, PETROCHEMICAL STUDIES ON THE ALKALIC ROCKS OF THE MOROTU DISTRICT, SAKHALIN: Geol. Soc. Amer., Bull., v. 64, p. 769-810.
- _____, 1953b, ON THE DIFFERENTIATION OF BASALTIC MAGMA: Chikyu-Kagaku (Science of the Earth), no. 14, p. 17-22.
- Yoder, H. S. and Tilley, C. E., 1956, NATURAL THOLEIITE BASALT-WATER SYSTEM: Geol. Soc. Amer., Bull., v. 67, p. 1746-1747.

Reference Section

RUSSIAN AND EAST EUROPEAN GEOLOGIC ACCESSIONS OF THE LIBRARY OF CONGRESS

This section is devoted to a listing of selected geologic items appearing in the two publications of the Library of Congress: Monthly Index of Russian Accessions, and East European Accessions Index. These lists are intended as a means of indicating to researchers in the earth sciences some of the material most recently available for screening, further review, and translation. For this reason the lists do not include material now, or soon to be, published in English. Emphasis is placed on Russian material; the extent to which items from East European sources are listed depends on the country and language involved.

A major function of the AGI translations program is the screening of foreign literature for material that should be made available to the English-speaking scientist. Researchers who need such material are urged to review these lists and send us their recommendations for consideration by the editors; the translation needs of all geologists will be served better thereby.

-- Managing Editor

MONTHLY INDEX OF RUSSIAN ACCESSIONS

Volume 13, No. 5

August 1960

PART A—MONOGRAPHIC WORKS

12. GEOGRAPHY & GEOLOGY

AKADEMIIA NAUK URSR, Kiev. Institut geologichnykh nauk. [Problems in studying underground waters of the Ukrainian S. S. R. ; Pytannia vyvchennia pidzemnykh vod Ukrain's'koi RSR. Kyiv, 1959. 162 p.

AKADEMIIA NAUK URSR, Kiev. Institut geologichnykh nauk. [Tectonic pattern of the Ukrainian S. S. R. and Moldavian S. S. R. ; explanatory text to the tectonic map of the Ukrainian S. S. R. and Moldavian S. S. R. made on a 1:750 000 scale] Tektonika terytorii Ukrain's'koi RSR ta Moldav's'koi RSR; poiasniuvai'na zapyska do tektonichnoi karty Ukrain's'koi RSR i Moldav's'koi RSR. Masshtab 1:750 000. Kyiv, Vyd-vo Akad. nauk URSR, 1959. 217 p.

ALIEKSTIEVA, O. M. [Comparative investigation of physical properties of stone meteorites and some rocks] Dosvid porivnial'nykh doslidzhen' fizychnykh vlastyvoستي kam'ianykh meteorytiv ta deialykh hirs'kykh porid. Kyiv, Vyd-vo Akad. nauk URSR, 1958. 47 p.

BÄRBOT DE MARNI, A. V. [Deposits of basic building materials in northern Kazakhstan (in region of virgin and waste lands); explanatory notes, cadastral survey, and a map; Mestorozhdeniia osnovnykh stroitel'nykh materialov v severnoi chasti Kazakhstana (v raionakh tselinnykh i zaleznykh zemel'); ob'iasnitel'naia zapiska i kadastr s kartoi. Alma-Ata, Izd-vo Akad. nauk Kazakhskoi SSR, 1960. 375 p.

PONDARCHUK, V. H. [Geology of the Ukraine] Geologia Ukrainy. Kyiv, Vyd-vo Akad. nauk URSR, 1959. 831 p.

BUBNOV, S. N. [Basic problems in geology] Osnovnye problemy geologii. Pod red. E. E. Milanovskogo. [Moskva] Izd-vo Mosk. univ., 1960. 232 p.

GALAKHOV, A. V. [Rischorrites in the Khibiny alkali massif] Rischorrity Khibinskogo shchelochnogo massiva. Moskva, Izd-vo Akad. nauk SSSR, 1959. 169 p.

GORSKII, N. N. [Secrets of the ocean] Tainy okeana. Izd-vo Akad. nauk SSSR, 1960. 218 p.

GVOZDETSKII, N. A., and others. [Physical geography of the U. S. S. R. ; selected lectures for students attending geography faculties of correspondence schools] Fizicheskaja geografiia SSSR; izbrannye lektsii dlia studentov-zaochnikov geograficheskikh fakul'tetov. Pod red. N. A. Gvozdet'skogo. [Moskva] Izd-vo Mosk. univ., 1959. 106 p.

KOMPLEKSNAIA IUZHNAIA GEOLOGICHESKAIA EKSPEDITSIIA, 1956-. [Transactions of the General Southern Geological Expedition] Trudy. Pod red. I. O. Broda. Leningrad, Gos. nauchno-tekhn. izd-vo neft. i gorno-toplivnoi lit-ry. Leningr. otd-nie. No. 4. [Geology and oil and gas potentials of the southern U. S. S. R. ; Daghestan] Geologia i neftegazonosnost' IUGA SSSR; Dagestan. 1959. 431 p.

MORDVILKO, T. A. [Lower Cretaceous sediments in Ciscaucasia and the Northern Caucasus] Nizhnemelovye otlozheniia Severnogo Kavkaza i Predkavkaz'ia. Moskva, Izd-vo Akad. nauk SSSR, 1960. 238 p.

RYZHKOV, O. A. [Tectonics of Cretaceous and Cenozoic sediments in the Fergana Valley] Tektonika melovykh i kainozoiskikh otlozhenii Ferganskoi depressii. Tashkent, Izd-vo Akad. nauk Uzbekskoi SSR, 1959. 199 p.

SUKHAREV, G. M. [Hydrogeology and waters of oil and gas fields] Gidrogeologia i vody nef'tian'nykh i gazovykh mestorozhdenii. Leningrad, Gos. nauchno-tekhn. izd-vo neft. i gorno-toplivnoi lit-ry. Leningr. otd-nie, 1959. 342 p.

TIKHOMIROV, V. V. [Geology in Russia in the first half of the 19th century] Geologia v Rossii pervoi poloviny 19 veka. Moskva, Izd-vo Akad. nauk SSSR. Pt. 1. 1960. 227 p.

TTTOV, A. G. [Mineralogy and fundamentals of geology; manual for pedagogical schools] Mineralogiia s osnovnymi svedeniami iz geologii; uchebnoe posobie dlia pedagogicheskikh uchilishch. Izd. 2., dop. Moskva, uchebno-pedagog. izd-vo M-va prosv. RSFSR, 1959. 126 p.

TKACHUK, V. G., and E. V. PINNEKER. [Underground waters of Irkutsk Province and their significance for the national economy] Podzemnye vody Irkutskoi oblasti i ikh narodnokhosiaistvennoe znachenie. Irkutsk, Irkutskoe knizhnoe izd-vo, 1959. 109 p.

VLASOV, K. A., and E. I. KUTUKOVA. [Emerald deposits] Izumrudnye kopi. Moskva, Izd-vo Akad. nauk SSSR, 1960. 249 p.

ZOLOTUKHIN, V. V. [Geological and petrographic studies of Chernaya Gora and adjacent regions in Transcarpathia] Geologo-petrografichni doslidzhennia chornoj gory ta pryleglykh raloniv Zakarpattia. Kyiv, Vyd-vo Akad. nauk URSS, 1960. 175 p.

13. SCIENCE

BAKHMAN, V. I., S. S. KRAPIVINA, and K. P. FLORENSKII. [Analysis of mineral waters] Analiz mineral'nykh vod. Izd. 2. Moskva, Gos. nauchno-issl. in-t kurortologii i fizioterapii, 1960. 223 p.

MALYSHEV, S. I. [Hymenopterans, their origin and evolution] Pereponchatokrylye, ikh proiskhozhdenie i evoliutsiia. Moskva, Gos. izd-vo "Sovetskaiia nauka, 1959. 290 p.

MATIAGIN, V. S. [Meteors, fireballs, meteorites] Me-teory, bolidy i meteority. Alma-Ata, Izd-vo Akad. nauk Kazakhskoi SSR, 1959. 67 p.

NOVOKSHANOVA, Z. K. [Ieronim Ivanovich Stebnitskii - military geodesist, geographer, scientist] Ieronim Ivanovich Stebnitskii - voennii geodezist, geograf, uche-nyi. Moskva, Izd-vo geodez. lit-ry, 1960. 91 p.

SHOKIN, P. F. [Gravimetry; apparatus and methods for gravity measurements] Gravimetriia; pribory i metody izmereniia sily tiazhesti. Moskva, Izd-vo geodez. lit-ry, 1960. 315 p.

16. TECHNOLOGY

ASSONOV, V. A., M. M. DOKUCHAEV, and I. M. KUKUNOV. [Boring and blasting operations] Burovzryvnye raboty. Moskva, Gos. izd-vo lit-ry po stroit., arkh. i stroit. materialam, 1960. 406 p.

FORISENKO, S. G., and F. A. KOPITSA. [Chamber and pillar system of ore mining] Kamernaia sistema razrabotki v gornorudnoi promyshlennosti. Moskva, Gos. nauchno-tekhn. izd-vo lit-ry po gornomu delu, 1960. 399 p.

CHUPRUNOV, G. D. [Mining and mine timbering] Pro-vedenie i kreplenie gornykh vyrabotok. Moskva, Gos. nauchno-tekhn. izd-vo lit-ry po gornomu delu, 1960. 532 p.

DAVYDOV, V. V. [Baring operations in open-pit mines under winter conditions] Vskryshnye raboty na ugol'nykh kar'erakh v zimnee vremia. Moskva, Gos. nauchno-tekhn. izd-vo lit-ry po gornomu delu, 1960. 49 p.

ERGALIEV, A. E. [Development of vine type deposits] Razrabotka mestorozhdenii zhil'nogo tipa. Alma-Ata, Izd-vo Akad. nauk Kazakhskoi SSR, 1960. 305 p.

IUROVSKII, A. Z. [Sulfur in coal] Sera kamennykh uglei. Moskva, Izd-vo Akad. nauk SSSR, 1960. 294 p.

KHOKHRIN, N. K. [Cellular concretes made with local materials] Iacheistyie betony na mestnykh materialakh. [Kuibyshev] Kuibyshevskoe knizhnoe izd-vo, 1959. 31 p. (Novoe v tekhnike)

KRUTOV, G. A. [Cobalt deposits] Mestorozhdenia kobal'ta. Moskva, Gos. nauchno-tekhn. izd-vo lit-ry po geologii i okhrane nedr, 1959. 231 p.

MASLOV, N. N., and Z. V. PIL'GUNOVA. [Dams of North Africa; from the design and construction practice] Plotiny Severnoi Afriki; iz praktiki proektirovaniia i stroitel'stva. Moskva, Gos. energ. izd-vo, 1960. 133 p.

MENKOVSKII, M. A. [Chemistry in coal mining] Khimiia v ugol'noi promyshlennosti. Moskva, Gos. nauchno-tekhn. izd-vo lit-ry po gornomu delu, 1960. 151 p.

MURAV'EV, I. M., ed. [Reference book on petroleum production] Spravochnik po dobyche nefli. Moskva, Gos. nauchno-tekhn. izd-vo nefi i gorno-toplivnoi lit-ry. Vol. 3. 1960. 712 p.

MUSIN, A. CH. [Mining flat ore deposits by the open stope system as applicable to conditions prevailing in Dzhezhgaskan] Razrabotka pologopadaushchikh rudnykh mestorozhdenii sistemoi s otkrytym ochistnym prostranstvom primenitel'no k usloviyam Dzhezhgaska. Alma-Ata, Izd-vo Akad. nauk Kazakhskoi SSR, 1959. 344 p.

POPOV, I. V. [Aerial photographic surveying and the study of inland waters] Aerofotos'emka i izuchenie vod sush. Leningrad, Gidrometeor. izd-vo, 1960. 166 p.

ROINISHVILI, N. M. [Structures to protect railroads from earth slides] Protivoobval'nye sooruzheniia na zheleznykh dorogakh. Moskva, Vses. izdatel'sko-poligr. ob'edinenie M-va puti soobshcheniia, 1960. 227 p.

RUSSIA (1923- U. S. S. R.) Ministerstvo geologii i okhrany nedr. [Origin of oil and gas and the formation of pools; transactions of the all-Union conference, Moscow, October 20-27, 1958] Problema proiskhozhdeniia nefli i gaza i uslovia formirovaniia ikh zalezhei; trudy Vsesoiuznogo soveshchaniia, Moskva, 20-27 oktiabria, 1958 g. Moskva, Gos. nauchno-tekhn. izd-vo nefi i gorno-toplivnoi lit-ry, 1960. 547 p.

RYBIN, A. A., and S. L. SHTIGLITS. [Soft rocks, their properties, and use] Miagkie kamni, ikh svoistva, obrabotka i primenie. Moskva, Vses. koop. izd-vo, 1959. 152 p.

RYSKIN, M. V. [Asbestos; market of capitalist countries] Asbest; rynek kapitalisticheskikh stran. Moskva, Vneshtorgizdat, 1960. 185 p.

SAVINOV, O. A., and A. IA. LUSKIN. [Vibration method of pile driving and its use in construction] Vibratsionnyi metod pogruzheniia svai i ego primenie. v stroitel'stve. Leningrad, Gos. izd-vo lit-ry po stroit., arkh. i stroit. materialam, 1960. 250 p.

TROFIMOV, G. T. [Highway construction on permafrost] Stroitel'stvo avtomobil'nykh dorog v usloviakh mnogoletnei merzloty. Moskva, Nauchno-tekhn. izd-vo M-va avtomobil'nogo transporta i shosseinykh dorog RSFSR, 1960. 43 p.

TSLAPKO, N. F., and A. M. CHAPKA. [Hydraulic coal breaking in underground coal mining] Gidrootolka uгля na podzemnykh rabotakh. Moskva, Gos. nauchno-tekhn. izd-vo lit-ry po gornomu delu, 1960. 312 p.

REFERENCE SECTION

TSYTOVICH, N. A., and others. [Foundation engineering] Osnovaniia i fundamenty. Pod red. N. A. Tsytoicha. Moskva, Gos. izd-vo lit-ry po stroit., arkhitekt. i stroit. materialam, 1959. 452 p.

No. 2. [Chemistry, refining, transporting, and storing oil and gas] Khimiia, pererabotka, transport i khranenie nefiti i gaza. Ekonomika, 1959. 40 p.

RESOUZNOE OB'EDINENIE KNIZHNOI TORGOVLI [Catalog of books on petroleum and gas to be published in 1960] Prospekt knig po nefiti i gazu izdavaemykh v 1960 godu. Moskva, Gos. nauchno-tekhn. izd-vo nef. i gorno-toplivnoi lit-ry.

No. 1. [Drilling wells and producing oil and gas] Burenie skvazhin i dobycha nefiti i gaza. 1959. 24 p.

ZENKIS, I. A. S. [Coal fields for coking; technical and economic factors determining the selection of coal fields for coking] Ugol'nye bazy dlia koksovania; tekhniko-ekonomicheskie osnovy vybora ugol'nykh baz dlia koksovania. Moskva, Gos. nauchno-tekhn. izd-vo lit-ry po gornomu delu, 1960. 132 p.

EDITOR'S NOTE

The Reference Section is extremely short this issue for two reasons: The August issue of the East European Accessions Index had not been received by deadline time and the Library of Congress has discontinued publication, in their Monthly Index of Russian Accessions, of translated tables of content of periodicals. For the past four months it has been possible to screen tables of content of periodicals in the several fields most likely to contain material of geologic relevance. The required information is now available only in the comprehensive subject index of all accessions for the month. Sheer mass of material and duplication of entries inherent to indexes makes screening of this part impracticable. An alternative means of effectively screening the literature is being sought.--M.R.

LED IN STACK